ANALYSIS OF POWER SYSTEM NETWORK STABILITY IN RWANDA

SILAS BIZIMUNGU

MASTER OF SCIENCE IN ENERGY TECHNOLOGY

JOMO KENYATTA UNIVERSITY OF AGRICULTURE AND TECHNOLOGY

2026

Analysis of Power System Network Stability In Rwanda

Silas Bizimungu

A Thesis Submitted in Partial Fulfilment of the Requirements for the Degree of Master of Science in Energy Technology of the Jomo Kenyatta University of Agriculture and Technology

2026

DECLARATION

This thesis is my original work and has not been presented for a degree in any other University

Signature……..Date …….

Silas Bizimungu

This thesis has been submitted for examination with our approval as the University Supervisors

Signature……..Date …….

Dr. Francis Njoka, PhD

KU, Kenya

Signature……..Date …….

Dr. Churchill Saoke, PhD

JKUAT, Kenya

DEDICATION

I dedicate this dissertation to my beloved family and Dr. Francis Njoka (My principal supervisor) and Dr Saoke Churchill that supported me in the entire period. I owe you more than you can imagine.

ACKNOWLEDGEMENT

When preparing this thesis, I was guided by the expertise of various people who reviewed and advised accordingly. Among them, I would like to express my heartfelt appreciation to Dr. Francis NJOKA, my first supervisor. His guidance, timely comments, objective criticisms, regular follow-up and various helpful suggestions made the completion of this work possible. May the Almighty GOD give you abundant blessing. I am also thankful to Dr. Churchill SAOKE, my second supervisor, for his patience, understanding and logistical support throughout the work. I am forever indebted to you Sir. I owe gratitude to the lecturers of the Institute of Energy and Environmental Technology for the knowledge gained from them.

Special appreciation to Rwanda's Energy Utility Cooperation Ltd for granting me access to the utility facilities and data used throughout this thesis, and fellow students for their constant encouragement, kindness and material support. I express my appreciation to Mr. Clement SIAME for his constructive contributions towards accomplishment of this thesis.

TABLE OF CONTENTS

LIST OF TABLES

LIST OF FIGURES

LIST OF APPENDICES

ACRONYMS AND ABBREVIATIONS

AGC	Automatic Generator Control
CIGRE	International Council on Large Electrical Systems
EUCL	Energy Utility Corporation Ltd
HPP	Hydro Power Plant
IEEE	Institute of Electrical and Electronics Engineers
kV	Kilo Volts
MW	Mega Watt
PP	Power Plant
PSS®E	Power System Simulator for Engineering
PV	Power-Voltage
REG	Rwanda Energy Group
SIL	Surge Impedance Loading
SS	Substation
TPP	Thermal Power Plant
TSO	Transmission System Operator
UFLS	Under Frequency Load Shedding
V	Voltage
GDP	Gross Domestic Product

ABSTRACT

Power system stability is a critical requirement for ensuring reliable and secure electricity supply, particularly in developing power systems experiencing rapid demand growth and increasing penetration of renewable energy sources. This study evaluates the stability of Rwanda's electricity grid with a focus on transient, voltage, and frequency performance under realistic operating and disturbance conditions. A detailed model of Rwanda's national power system was developed using Power System Simulator for Engineering (PSS®E), incorporating actual network parameters for generation, transmission, substations, and load centres. The model was verified and validated against available SCADA measurements before being subjected to steady-state power flow analysis and time-domain dynamic simulations. Stability performance was assessed under peak and off-peak loading conditions, generator and line outages, and renewable generation disturbances. The results show that the transmission network is generally lightly loaded, with maximum line loading of approximately 25% during off-peak and 46% during peak conditions; however, localised infrastructure constraints exist at critical substations, where transformer loading reaches up to 96% under normal operation and exceeds 130% under N-1 contingencies. Voltage stability analysis reveals widespread off-peak overvoltage, with several 110 kV busbars exceeding 120 kV, while dynamic simulations indicate slow voltage recovery following disturbances. Transient stability assessment demonstrates adequate stability margins, with critical clearing times ranging from approximately 200 ms to over 1000 ms, exceeding typical protection clearing times. Frequency stability analysis identifies limited spinning reserve as a major vulnerability: system frequency drops to 48.83 Hz following loss of 6.5 MW of solar generation when only 4 MW of reserve is available, necessitating under-frequency load shedding for recovery. The study further demonstrates that targeted mitigation measures significantly improve stability. The installation of shunt reactive power compensation reduces overvoltage and improves post-fault voltage recovery, while increased local generation or reserve capacity mitigates frequency excursions and reduces dependence on load shedding. Overall, the findings confirm that while Rwanda's electricity grid possesses adequate transient stability, its operational performance is constrained by reactive power management challenges, low reserve margins, and topology sensitivity. The study provides practical insights for system operators and planners on improving voltage and frequency stability through targeted network reinforcement and operational strategies

CHAPTER ONE

INTRODUCTION

1.1 Background to the Study

According to the IEEE/CIGRE Task Force, power system stability is "the capacity of an electric power system, for a given initial operating condition, to recover a state of operational balance after being confronted with an electrical disturbance with most system variables bounded, so that essentially every component remains intact." (Hatziargyriou et al., 2021). System stability concerns energy balance and its ability to generate sufficient restoring forces to counter system disturbances (Hatziargyriou et al., 2021). Such a disturbance may be small or big, and the system may become unstable in either event, depending on the operating conditions at a given time. When the disturbances are large, the non-linearity inherent in the power system can no longer be ignored, and the study of stability under such circumstances is of much importance in system stability (Adeleke et al., 2022). As power systems have evolved over time, through expansion, interconnections, the use of modern technologies and advanced control systems has improved power system ability to withstand instability conditions (Yao et al., 2023). However, different forms of system instability have emerged. For example, voltage stability, frequency stability and inter-area oscillations that become of greater concerns than in the past with changes in power supply characteristic requirement in modern loads (Yao et al., 2023).

The development of power system networks and operation brings new type power system stability problems, for example, the impact of renewable energy on interconnected power system (Safdarian et al., 2024). Frequency fluctuation and Voltage instability in modern power systems have become more common than in the past (Ur Rehman et al., 2023).

As per the Rwanda Energy Group database (Rwanda Energy Group, 2023), Rwanda's electricity network energy source is based on generation from Peat, Hydro, Methane gas, solar and thermal (Heavy and Light Fuel Oil). The nation power system grid comprises of voltage levels from 0.4 kV, 6.6 kV, 11 kV, 15 kV, 30 kV and 110 kV

which are used currently and as presented in Figure 1.1. The completed 220 kV Transmission Line is currently being used to evacuate power at 110 kV level.

Due to the increased load in the country resulting from industries, real estates and rural electrification programs, generation increased from 120 MW in 2012 to 216 MW in 2020. The Transmission network has grown from 409.4 km in 2014 to 744.7 km as of March 2019 with High Voltage substations increase from 18 in 2014 to 29 in early 2023 and expected to be 34 by end 2024 (Rwanda Energy Group, 2023).

In order to improve system stability through improving system strength with respect to generation, Rwanda's network was connected to a 36 MW power plant with generation equally shared with the Democratic Republic of Congo and Burundi. However, this further introduces external disturbances into the national grid.

Due to changes in the network setup, its operational behaviour has drastically changed. This has increased stability, operational and control challenges that have often resulted in total system collapse. The negative consequences have called for a detailed system study and analysis of network operation to understand the adjustments required to stabilize the network while ensuring quality of power supplied. Due to the need to optimize the usage of the national grid, looking at the grid behaviour changes, and considering the need to provide high quality of supply, power system stability study analysis for the Rwanda network is imperative.

Figure 1.1 shows the current 110 kV Transmission Network and main power plants connected to the 110 kV bus bars. Some micro hydro and thermal power plants are connected on the distribution system (at 30 kV and 15 kV network level) as embedded generators which also have its own effect on system stability (Rwanda Energy Group, 2023).

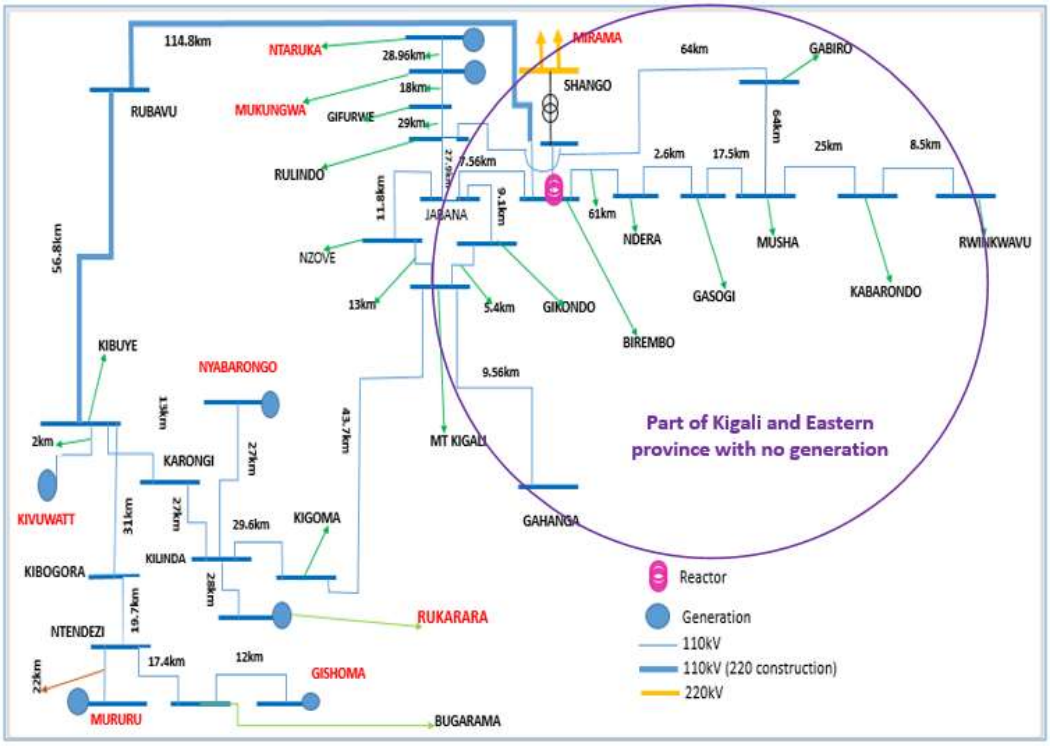

Figure 1.1: 110 kV Transmission System Scheme for Rwanda

1.2 Statement of the Problem

Rwanda's sustained economic growth and rapid urbanisation have led to a significant increase in electricity demand. However, investments in generation and transmission infrastructure have not consistently matched this growth, resulting in increasing stress on the existing power system. As demand rises, power flows on transmission lines frequently operate outside optimal ranges, either exceeding or falling below their surge impedance loading limits. This operating condition exposes the power system to various forms of instability, including rotor angle instability, frequency deviations, voltage instability, and overall system insecurity.

These challenges are further compounded by the geographical separation between major generation centres and key load centres, as well as the increasing integration of renewable energy sources such as solar power, whose intermittent nature introduces additional dynamic disturbances into the grid. Moreover, regional interconnections intended to improve system adequacy also introduce external disturbances that can propagate across the national network.

As a result, the Rwandan electricity grid continues to experience operational challenges such as unexpected outages, frequency excursions, voltage fluctuations, and reliance on corrective actions such as under-frequency load shedding. These events negatively affect system reliability, increase operational risk, and impose economic costs on both the utility and end-users. Despite these challenges, a comprehensive, system-wide assessment of Rwanda's power system stability covering transient, voltage, and frequency stability under realistic operating conditions has remained limited. This gap constrains informed planning, operational decision-making, and the development of effective mitigation measures.

1.3 Research Objectives

1.3.1 Main Objective

The main objective of the study is to comprehensively analyse the stability of the current Rwandan electricity grid by creating artificial fault conditions arising from current stability challenges.

1.3.2 Specific Objectives

The specific objectives of the study are:

i. To conduct an assessment of the current infrastructure of the electricity grid in Rwanda, encompassing generation, transmission, and distribution systems.
ii. To assess the Rwandan electrical grid's performance under different loading scenarios using voltage, frequency, and transient stability studies.
iii. To identify and evaluate appropriate operational and network reinforcement measures for improving power system stability based on the results of transient, voltage, and frequency stability analyses.

1.4 Justification

The necessity of this study is rooted in the critical requirement for a stable, secure, and reliable grid to support Rwanda's sustained economic development and annual GDP growth, which averaged 7.4% between 2000 and 2023 (The World Bank Group, 2024).

As the energy utility embarks on rapid expansion to meet surging demand, the technical complexities of the grid, such as the geographic concentration of generation far from load centres, as shown in Figure 1.2 and the increasing penetration of intermittent solar energy, have heightened the risk of system-wide instability.

By utilizing PSS®E to create a high-fidelity model of the national network, this research provides a vital technological framework for identifying system vulnerabilities and validating modern stabilization strategies, including dynamic reactive power supports (SVCs) and optimized under-frequency load shedding schemes. Beyond the immediate operational benefits of reducing unpredictable blackouts and preventing financial losses for end-users, this work serves a significant academic purpose. It bridges a persistent gap in existing literature by providing a unified analysis of voltage, frequency, and transient stability specifically tailored to the unique operational challenges of an African power system.

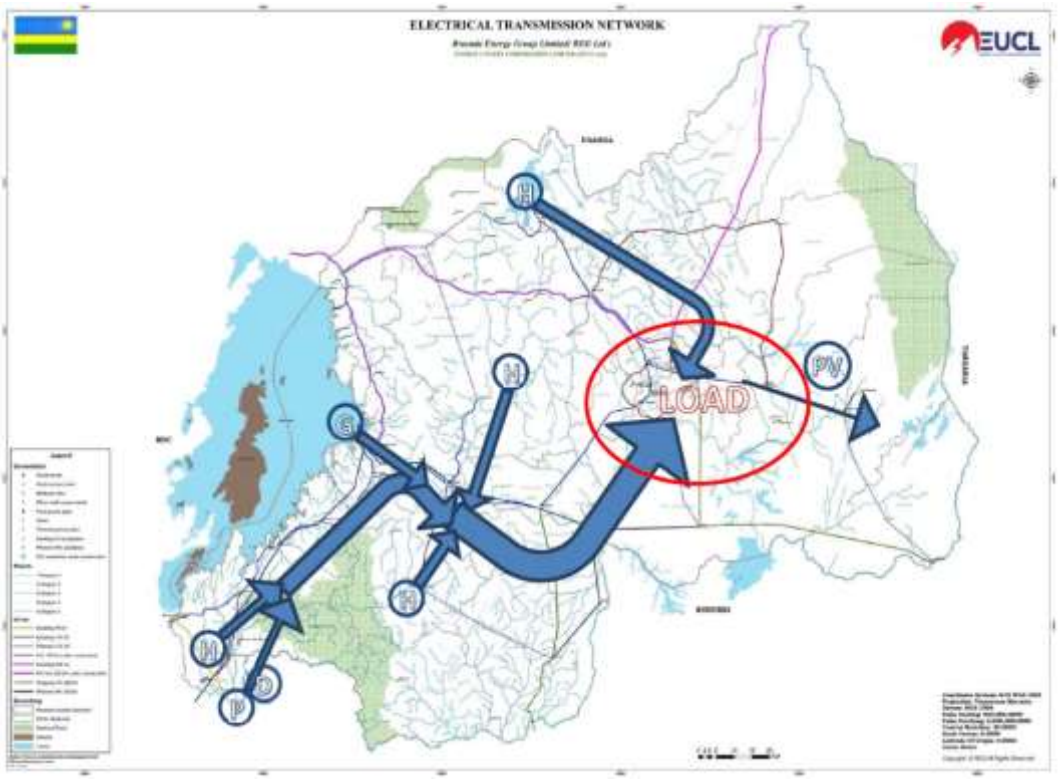

Figure 1.2: Rwanda's Generation and Load Concentration Centres

1.5 Research Questions

i. What are the strong and weak points of Rwanda's grid, and which aspects present the highest probability of failure?
ii. What are the unique challenges associated with the various components of the Rwanda's grid?
iii. What solutions are available to improve the stability of the grid?

1.6 Scope of the Study

This research commences with an overview of the entire Rwanda's electricity network status and the detailed description of static and dynamic stability, a function of the operation conditions and disturbances. This is followed by a literature review presenting findings and useful theoretical definitions and conventions hinged on components of power system stability such as voltage, frequency. With the understanding of the background and theory, a description of the adopted methodology is provided. The study is based on desk top studies, modelling and simulations of the entire Rwanda's grid network. The data is obtained from the National Utility and hence a replica of the exact system. The results from the performed studies and simulations are discussed in detail. Finally, the project concludes with the summary findings and provide relevant recommendation for future development in this area of research.

1.7 Study Limitations

Availability of utility technical personnel was a daunting challenge. The same employees are assigned with network control, maintenance that includes regular interventions hence hindering timely response to data acquisition and queries. As most power plants in Rwanda are owned by Independent Power Producers, it took much time to get all necessary data as they were not always readily available to facilitate and provide data. Most power plants and substations are located in remote areas with a poor road network and limited in terms of phone and internet connectivity, making data collection complicated.

CHAPTER TWO

LITERATURE SURVEY

2.1 Theoretical Principles

2.1.1 System Stability

Power system stability denotes the capacity of an electric power system to maintain balance during standard operating conditions and to restore an acceptable operational state after a disturbance (Saleh et al., 2024). Stability is often categorised as rotor angle stability, frequency stability, and voltage stability, based on the type of disturbance and the relevant system reaction characteristics.

Rotor angle stability refers to the ability of synchronous machines to maintain synchronism following disturbances, such as short circuits or sudden changes in load (Shrestha and Gonzalez-Longatt, 2021). Frequency stability relates to the system's ability to maintain nominal frequency following large imbalances between generation and demand, while voltage stability refers to the ability of the power system to maintain acceptable voltage levels at all buses under normal and disturbed operating conditions.

In interconnected and evolving power systems, these stability issues are highly interrelated. Frequency deviations resulting from generation loss can induce voltage instability due to inadequate reactive power support, whereas voltage collapse can worsen frequency drop by initiating load disconnections or generator tripping (Anderson and Moore, 2013). As power systems expand and incorporate new generation sources, especially renewable energy, stability assessment emerges as a vital planning and operational necessity.

There exist three states of stability (Bayliss and Hardy, 2007), (Hatziargyriou et al., 2021); *a)* The term "steady state stability" pertains to the ability of a system to sustain synchronization despite minor disturbances or progressive changes in the system, such as a slow increase in load as the maximum demand over a 24-hour period approaches. *b)* Transient stability refers to the response of a system following a sudden change in

loading conditions, such as a fault, the abrupt loss of generation or an interconnecting line, or the sudden addition of extra load. The transitional period has a maximum duration of around one second. The current behaviour of the system is crucial for the design of the power system. *c)* Dynamic stability refers to the behaviour of a system during the period between transient behaviour and the steady state region. Dynamic stability studies may investigate the operational characteristics of turbine governors, the flow rates of fuel and steam, load shedding mechanisms, and motor load recovery processes.

2.1.2 Categories of System Stability

Classification of stability is crucial in evaluation of the impact of disturbances on the electromechanical dynamic behaviour of the power system.

The classification of power system stability can be based on various considerations (Lindner et al., 2022), (Van Cutsem and Vournas, 2008); *a)* the main system variable that shows the tangible properties of the resulting state of instability., *b)* the stability forecast and calculation approach are affected by the magnitude of the disturbance being considered., and, *c)* the tools, methodologies, and time frame that must be taken into account in order to assess stability.

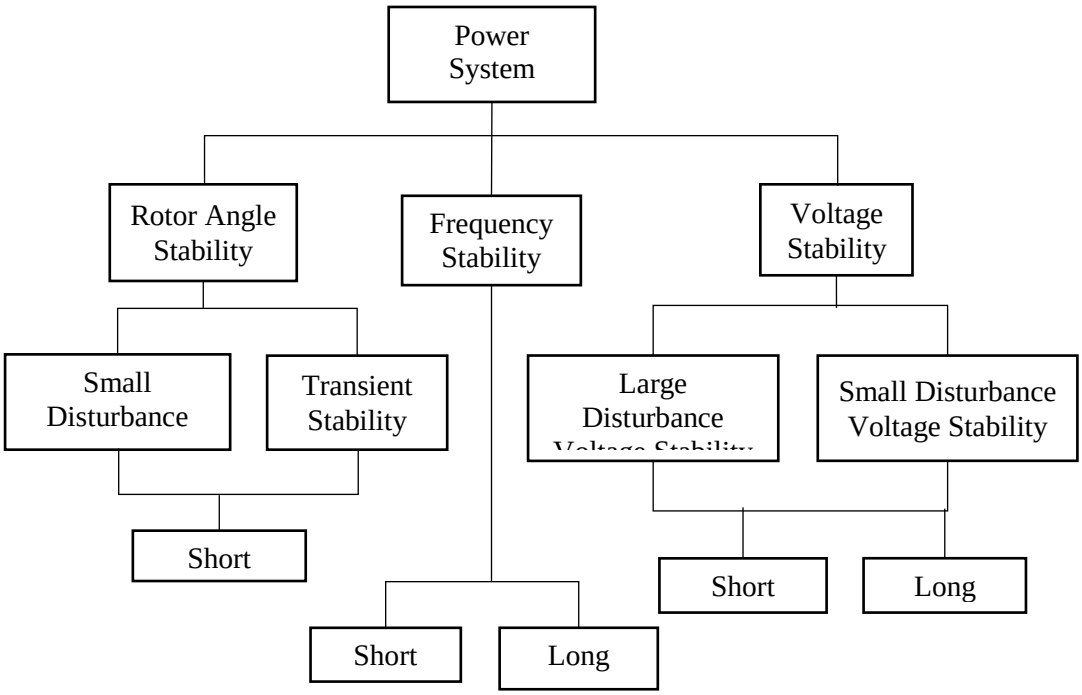

Figure 2.1: Classification of Power System Stability

Source: (Lindner et al., 2022)

2.1.2.1 Rotor Angle Stability

Rotor angle stability refers to the ability of synchronous machines in a connected power system to retain synchronization after a disruption. This will be determined by the capacity of each synchronous machine in the system to maintain or restore balance between electromagnetic torque and mechanical torque (Ojha and Simkhada, 2022).

Rotor angle stability can further be placed under the subcategories below (Transpower Newzealand, 2024), (Shrestha and Gonzalez-Longatt, 2021).

A. ***Small-disturbance rotor angle*** pertains to the power system's ability to maintain synchronism even when faced with slight disturbances. Small-disturbance stability is determined by the initial operational state of the system. There are two forms of instability that could occur:

    i. Increase in rotor angle through a non-oscillatory or aperiodic mode due to lack of synchronizing torque, or

ii. Rotor oscillations of increasing amplitude due to lack of sufficient damping torque.

B. ***Large-disturbance rotor angle stability or also known as transient stability***, refers to the ability of a power system to maintain synchronization in the presence of a major disturbance, such as a short circuit in a transmission line (Yao et al., 2023).

i. Both the initial operating condition of the system and the magnitude of the disturbance play crucial roles in determining transient stability. Inadequate synchronizing torque commonly leads to the occurrence of initial swing instability, which is characterized by discontinuous angular separation.

ii. During transient stability studies, the relevant time period usually occurs between three to five seconds following the disturbance. In the case of really large systems with significant inter-area oscillations, the duration can extend to a range of 10 to 20 seconds.

2.1.2.2 Voltage Stability

In an electrical grid, a system of transmission and distribution channels transports power from the generating plant to the end users. In order for motors, lights, and other loads to function properly, it is crucial for consumers to receive a voltage that is consistently stable. Consumer-owned appliances may experience inconsistent operation or malfunction as a result of severe voltage fluctuations (Glavic and Greene, 2022).

Voltage stability refers to a power system's ability to maintain consistent voltages at each bus following a disturbance from a particular initial operating condition (Gourav et al., 2020). It depends on the power system's ability to maintain or restore balance between the supply and demand of electricity (Dondariya and D.K.Sakravdia, 2021).

Increased load in a system result in voltage drop at the receiving end due to factors such as voltage loss in transmission lines, transformer impedance, alternator

synchronous impedance, and feeders. When the load decreases, the opposite happens. When an interruption increases the need for reactive power beyond the capacity of the existing reactive power sources, it jeopardizes voltage stability.

Voltage stability is further categorized into the following subcategories (Onyegbadue et al., 2024), (Glover et al., 2022):

A. ***Large-disturbance voltage stability*** pertains to the ability of a system to maintain consistent voltages despite major disturbances such as system faults, power outages, or circuit emergencies.
B. ***Small-disturbance voltage stability*** refers to the ability of a system to maintain consistent voltages when faced with modest disturbances, such as gradual changes in the system's load. The stability of this kind is influenced by the characteristics of loads, continuous controls, and discrete controls at a certain point in time (Baleboina and Mageshvaran, 2023).

Another aspect is the steady state voltage stability. In this case, it is optimal for the voltage across various buses in a power system to consistently match the nominal value. The importance of this is increasing as energy networks transition from being a publically subsidized service to a profit-driven commodity. The aspiration to optimize the utilization of systems arises from this alteration, and it significantly impacts the stability of the system. Voltage stability refers to the capacity of a power system to maintain consistent and appropriate voltage levels at all of its buses, both during regular operation and following a physical disruption (Kothari and Nagrath, 2022).

Further, voltage stability necessitates the examination of the correlation between the power transmitted (P) and the voltage at the receiving end (V) in terms pf power curves. During the voltage stability study method, the power, P, is moved throughout the system, and the resulting impact on the system voltages, V, is observed. This type of research is occasionally called PV studies (Kundur, 1994).

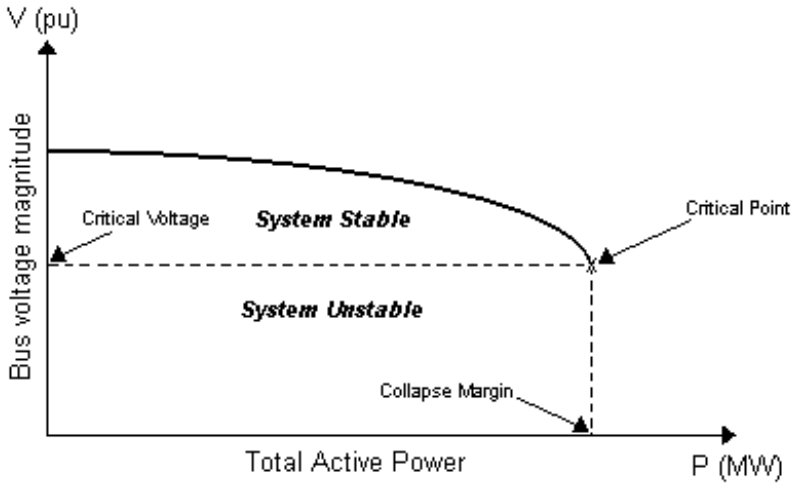

Figure 2.2: Typical Characteristic Curve for Power-Voltage (PV)

Figure 2.2 clearly demonstrates that there is a rapid decrease in voltage at the "knee" of the PV curve when the load demand increases. Once the load-flow reaches this point, any further convergence ceases, suggesting that the system has become unstable. This point is regarded as the pivotal point. This can be used to determine the critical operating voltage and collapse margin of the system (Kothari and Nagrath, 2022), (Stevenson, 1995). Operating points above the critical point often indicate that the system is functioning steadily. An unstable operating situation is declared for the system if the operating points fall below the critical point (Valuva et al., 2023), (Aikins and Amuzuv, 2020).

After examining the behaviour of real power against the voltage, it also becomes important to reflect on the relationship between reactive power and voltage. The way that fluctuations in Q and P impact the voltages at the load buses determines the voltage stability (Glavic and Greene, 2022). The Q-V relationship highlights the significant influence of the reactive power characteristics of the loads or compensating devices at the receiving end. The graphic shows the sensitivity and variation of bus voltages in response to injections or absorptions of reactive power. Figure 2.3 displays a typical QV curve, which is commonly generated by a series of load-flow solutions (Anderson and Moore, 2013).

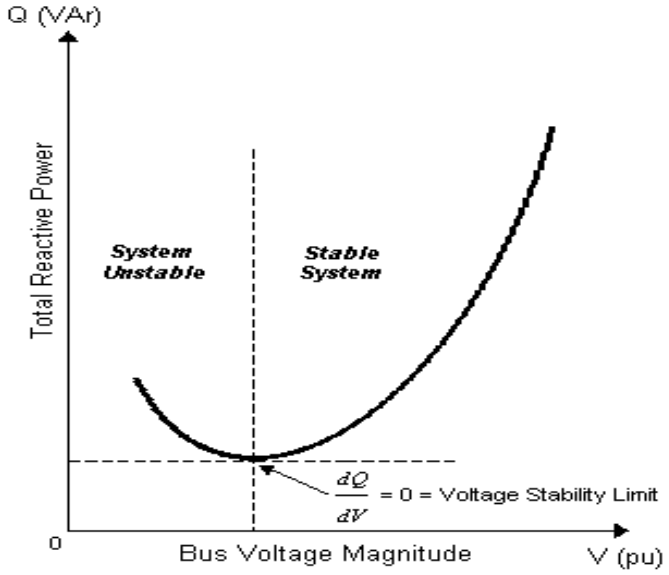

Figure 2.3: Characteristic Curve of the Typical Reactive Power-Voltage (QV)

It is evident from the figure that the derivative dQ/dV is zero at the voltage stability limit. This point also specifies the minimal amount of reactive power needed to maintain operation stability. Under typical operating conditions, a rise in Q will be accompanied by a rise in voltage (Gourav et al., 2020), (Kundur, 1994).

When the operating point falls on the right side of the curve, the system is said to be stable. On the other hand, the operations on the left side of the graph become unstable.

2.1.2.3 Frequency Stability

When a severe system upset occurs and there is a large imbalance between generation and load, the power system's capacity to maintain a stable frequency is referred to as frequency stability (Kroupa, 2012), (Al-Azzawi and Alturk, 2024).

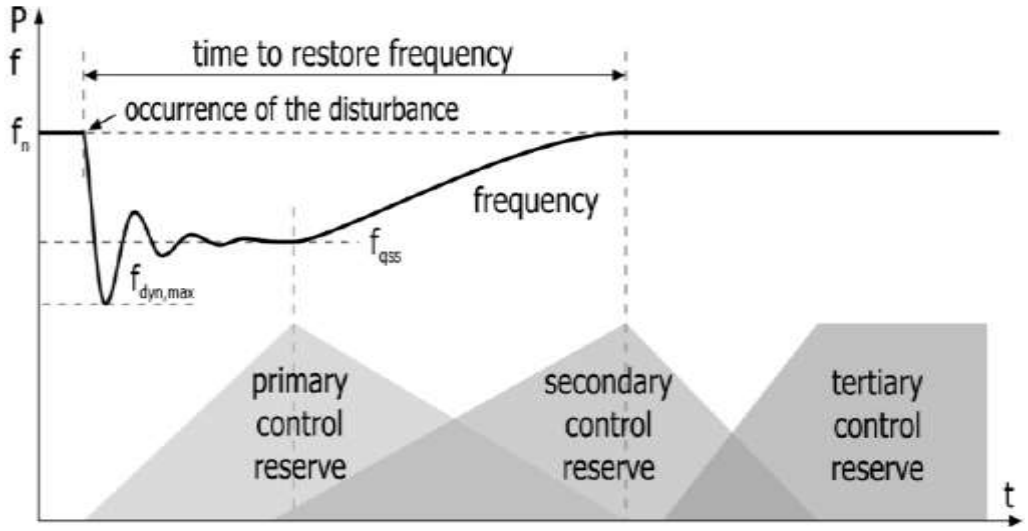

Figure 2.4: Creation of Reserves for Frequency Regulation

Source: (Lindner et al., 2022)

i. **Primary Control:** Keeping the generator unit synchronized through the use of governor controllers to uphold a balance between generation and demand within the synchronous area is the fundamental objective of primary frequency control. Adequate primary control performance requires the generation resources referred to as primary control reserve. Both the primary control speed and the total system inertia have an impact on the frequency deviation.

ii. **Secondary control:** The objective of secondary control is to maintain balance between generation and consumption (demand) in each control area/block and system frequency in the synchronous region while taking the control program into account. The active power set points of generation can be quickly changed by secondary control to time-to-restore-frequency (about 15 minutes) with a centralized AGC without affecting primary control.

iii. **Tertiary Control*:*** The TSOs typically manually engage tertiary reserve, also referred to as minute reserve, after secondary control activation in order for tertiary control to release secondary control reserves. Secondary control usually means using fast-acting generating units, but these are less important in terms of cost and effectiveness.

2.1.3 Relationship between Reliability, Security, and Stability

A power system's reliability is determined by how well its component parts work together to deliver power to customers in the appropriate quantity and within acceptable parameters.
A power system is said to be stable if it can continue to function normally after an interruption (Obio and Mutale, 2015), (Ur Rehman et al., 2023). The type of physical disturbance and the operational conditions determine the outcome.

A system's security is determined by its capacity to endure unexpected component losses or other abrupt disruptions like electric short circuits (Yao et al., 2023), (Bayliss and Hardy, 2007).

The key distinctions between the three facets of power system performance are as follows:

i. When designing and operating power systems, reliability is the main goal. The electricity system has to be mostly secure in order to be dependable. The system needs to be stable in order to be considered secure, but it also needs to be protected against other potential threats that aren't related to stability issues, like equipment damage from sabotage or explosive cable failure, or towers falling because of ice loading.
ii. It is possible to differentiate system security from stability based on the outcomes that follow. One system may be comparatively more secure than the other, for instance, even when both have comparable stability margins and are stable with less severe instability effects.
iii. Time-varying characteristics like security and stability can be assessed by looking at how the power system operates under a certain set of circumstances. Conversely, reliability is contingent upon the power system's time-averaged performance and can only be assessed by analysing the system's actions over an extended duration (Sauer and Pai, 2006), (Kazemi and Ansari, 2022).

2.1.4 Power Flow Study

Power flow studies are necessary for planning and constructing future network improvements as well as figuring out how to operate an existing grid as efficiently as possible (Abakar et al., 2020). The primary output information obtained from a power flow study includes actual and reactive power flowing in each line, as well as the voltage magnitude and angle at each bus. This makes it possible to analyse network resilience in relation to the different scenarios that a grid may encounter, which opens the door for wise operation practices and careful planning of upcoming grid expansions (Shahzad U. , 2021).

2.1.4.1 Bus Power Flow Formulation

A power flow study seeks to determine the entire behaviour of buses under various circumstances. A load bus is one that has no generators attached to it. A bus that has at least one generator attached to it is referred to as a generator bus, with one exception. The one bus with a generator that was chosen at random is the exception. People call this bus the Slack Bus. When addressing load flow issues, a single-phase model is used to depict the system and assume balance (Sauer and Pai, 2006), (Shahzad A. , 2022).

The system buses are generally classified into three types.

For the power flow calculations, one bus also referred to as the swing or slack bus—is used as a reference. There is specification for the voltage angle, δ, and voltage magnitude, |V|. Rather than being imposed as boundary conditions, the net real and reactive power input to a swing bus is a free variable that arises from the power flow solution. The power differential resulting from network losses between scheduled loads and generated power is made up by this bus. Therefore, the P and Q that the slack bus will produce are (Glover et al., 2022), (Kundur, 1994);

$$\Sigma P_{gen} = \Sigma P_{load} + \Sigma P_{loss} \quad (2.1)$$

$$\Sigma Q_{gen} = \Sigma Q_{load} + \Sigma Q_{loss} \quad (2.2)$$

Therefore, the scheduled active power, Psch and scheduled reactive power, Qsch is

$$P_{sch} = P_{gen} \quad (2.3)$$

$$Q_{sch} = Q_{gen} \quad (2.4)$$

This bus type is frequently referred to as a PQ bus. Loads are typically believed to have a steady power source. As a result, |V| and δ are typically unknown although P and Q are known. The planned power can be found out by:

$$P_{isch} = P_{igen} - P_{iload} \quad (2.5)$$

Where i is the bus number i and since the PQ bus is a non-generator bus,

$$P_{igen} = 0 \quad (2.6)$$

Thus,

$$P_{isch} = -P_{iload} \quad (2.7)$$

A similar relationship applies for the scheduled reactive power, Qsch.

Voltage control occurs when the magnitude of the voltage remains consistent. The parameters |V| and δ are given in this kind of bus. Furthermore, restrictions on Q (Qmin $< Q \leq$ Qmax) are stipulated based on the attributes of the specific devices.

Buses with generators, synchronous condensers, and static VAr compensators are a few examples (Bayliss and Hardy, 2007). Since this bus is not a load bus,

$$P_{jload} = 0 \quad (2.8)$$

Then scheduled power is determined by

$$P_{jsch} = P_{jgen} \quad (2.9)$$

2.1.4.2 Network Equation

Using Kirchoff's current and voltage rules, the relationship between network bus voltages and currents may be determined for each bus. After that, these can be

expressed as network equations for an n-bus system using a bus admittance matrix (Kothari and Nagrath, 2022), (Anderson and Moore, 2013).

$$\begin{bmatrix} I_1 \\ I_2 \\ \vdots \\ I_n \end{bmatrix} = \begin{bmatrix} Y_{11} & Y_{12} & \cdots & Y_{1n} \\ Y_{21} & Y_{22} & \cdots & Y_{2n} \\ \cdots & \cdots & \cdots & \cdots \\ Y_{n1} & Y_{n2} & \cdots & Y_{nn} \end{bmatrix} \begin{bmatrix} V_1 \\ V_2 \\ \vdots \\ V_n \end{bmatrix} \quad (2.10)$$

Where: n = total number of buses

Yii = the self-admittance of node i

Yij = the mutual admittance between node i and j

Vi = the phasor voltage to ground of node i

Ii = the phasor current flowing into the network at node i [12]

Or generally,

$$[I_{bus}] = [Y_{bus}]\,[V_{bus}] \quad (2.11)$$

I_{bus} is the injected bus currents. V_{bus} is the bus voltages measured from a reference bus.

Y_{bus} is the bus admittance matrix.

The self-admittance is the sum of admittance connected to a particular node and can be determined by (Power Technology International - Siemens, 2016)

$$Yii = \sum_{i=0}^{n} y_{ij} \quad j \neq I \quad (2.12)$$

The mutual admittance is the off-diagonal element of Ybus and is equal to the negative of the admittance between the nodes.

$$Yij = Yji = -yij \quad (2.13)$$

When the currents are known, equation (2.11) can be solved for the n bus voltages.

$$[V_{bus}] = [Y_{bus}]^{-1} [I_{bus}] \quad (2.14)$$

The inverse of the bus admittance matrix is the bus impedance matrix, Zbus, that is

$$[Z_{bus}] = [Y_{bus}]^{-1} \quad (2.14)$$

2.1.5 Per Unit System for Power Flow Study

With the use of this method, engineers can more easily analyze single-phase networks by simplifying calculations on systems with multiple voltages (Sajadi et al., 2023), (Sauer and Pai, 2006):

i. All P and Q quantities are three-phase.
ii. Voltage magnitudes are represented as a fractional part of their standard or "base" value.
iii. All phase angles are represented in the same units as normally used.

Actual Value Base /Value in the Same Units = P.U. of a Quantity Value.

The conversion of base unit and per unit values takes the following steps

i. Indicate the basic MVA. This usually has to do with a generator, transformer, or transmission line rating. Simply select the one that requires the least amount of computation. This basis will not change over the course of the system.
ii. Designate a voltage base at every point in the circuit. Usually, this is the nominal voltage at that specific spot.
iii. Whenever a transformer is encountered in the circuit, determine the voltage basis for all other locations by adjusting by the turns ratio.
iv. Having specified the voltage and MVA base throughout the system, current and impedance bases may be determined
v. For each value, the Per Unit quantity is the actual value divided by the base value (Van Cutsem and Vournas, 2008), (Stevenson, 1995).

$$\text{Per Unit Values} = \frac{\text{Actual Value}}{\text{Base Value}} \quad (2.15)$$

$$\text{Per Unit MVA} = \text{MVAp.u} = \frac{\text{MVAa}}{\text{MVAb}} \quad (2.16)$$

$$\text{Per Unit Voltage} = \text{kVp.u.} = \frac{\text{kVa}}{\text{kVb}} \quad (2.17)$$

$$\text{Per Unit Impedance} = \text{Zp.u} = \frac{\text{Za}}{\text{Zb}} = \text{Za.}\ \frac{\text{MVAb}}{(\text{kVb})2} \quad (2.18)$$

$$\text{Per Unit Current} = \text{Ip.u.} = \frac{\text{Ia}}{\text{Ib}} \quad (2.19)$$

Where a and b stand for actual and base values, respectively

2.1.6 Power System Simulator for Engineering

The PSS®E software comprises programs and structured data files that are intended to manage the fundamental tasks involved in power system performance simulation, specifically (Siemens, 2017) data handling, updating, and manipulation, power flow, fault analysis, dynamic simulation and extended term simulation, and equivalent construction.

PSS®E allows the user to choose from five different AC power flow iteration schemes:

1. Gauss-Seidel iteration.
2. Modified Gauss-Seidel iteration suitable for series capacitors.
3. Fully coupled Newton-Raphson iteration.
4. Decoupled Newton-Raphson iteration.
5. Fixed slope Decoupled Newton-Raphson iteration.

The PSS®E program is based on the engineering philosophy that all power system simulations should use the best possible modeling of all items of equipment (Siemens, 2017).

The governing factors in selecting equipment models are:

i. Understanding of the physical processes inherent in each item of equipment and their effect on behaviour as observed from the power system.
ii. Availability of adequately accurate data.

Because of this, modelling criteria drive the architecture of PSS®E; choices on how to represent equipment are made based on mathematical methodologies and database structure, not the other way around.

The steps in using PSS®E to simulate a power system and investigate its performance are (Colorado State University, 2016):

i. Determine the appropriate equations and parameter values to represent the physical components of the simulation, such as the transmission lines, generators, relays, governors, etc., by examining or designing the equipment.
ii. Convert the system's physical model into a PSS®E input data file by referencing linked models of the various busses, branches, generators, and other components. For equipment not covered by an explicit model in PSS®E, create equivalent circuits using equivalent branches and dummy buses as needed.
iii. Use the PSS®E programs to process the data, apply calculations, and print reports.
iv. Interpret the calculation results in terms of the indicated physical behaviour of the equipment with which the process was started in the first step.

2.2 Previous Works Related to the Study Area

This section examines prior stability studies on African and developing power systems utilising simulation-based methodologies, with a specific focus on research employing PSS®E and equivalent tools. The reliability of African power grids has garnered heightened scholarly attention, especially concerning the difficulties associated with long-distance transmission, low inertia, and the incorporation of renewable energy sources. The subsequent studies indicate the recent status of research within regional contexts:

A stability study of the Zambian Interconnected Power System investigated frequency response under severe generation loss contingencies using PSS®E and adaptive under-frequency load shedding (UFLS) schemes (Kanjelesa et al., 2023). This study addresses the lack of spinning reserve in the Zambian grid by proposing an adaptive

UFLS scheme, demonstrating that system inertia, rate-of-change-of-frequency (RoCoF), and UFLS configuration significantly influence post-disturbance frequency recovery. Simulation results showed that appropriate UFLS settings could improve frequency nadir and reduce overshoot under both islanded and interconnected conditions. It further identifies that conventional static load shedding is often insufficient for severe disturbances, leading to total system collapse. The strength of this work is its modelling of RoCoF to trigger faster shedding, a methodology relevant to the solar-induced frequency excursions observed in Rwanda. However, the study focused exclusively on frequency stability and did not consider voltage stability or the combined interaction of frequency and voltage dynamics.

In a study conducted on the Niger power grid, PSS®E was used to evaluate voltage and transient stability following the integration of a 30 MW photovoltaic power plant (Abdourahimoun et al., 2025). The authors modelled the national grid with and without PV integration and assessed system response under short-circuit disturbances. The research identifies that while the steady-state integration is feasible, three-phase faults at the connection bus significantly impact the voltage profile and frequency stability. The study further showed that PV integration led to transient overvoltage, voltage dips, and altered frequency response, highlighting the sensitivity of weak grids to renewable penetration. The primary strength of this work is the determination of Critical Fault Clearing Times (CCT) for PV integration, providing a benchmark for protection settings in similar solar-heavy grids like Rwanda's. Nevertheless, the study did not investigate frequency stability limits, inertia effects, or system-wide dynamic interactions involving conventional generators.

A comprehensive voltage stability study of Ghana's generation and transmission system employed Newton–Raphson load flow analysis and dynamic simulations to identify weak buses and voltage violations under contingency conditions (Aikins and Amuzuv, 2020). This study explores the use of Flexible AC Transmission Systems (FACTS), specifically SVCs and STATCOMs, to mitigate voltage violations on the Ghanaian 330 kV and 161 kV lines. Flexible AC Transmission System (FACTS) devices were optimally placed to improve voltage profiles and reduce system losses. The research identifies that SVCs are highly effective in absorbing excess reactive

power during light-load conditions (Ferranti effect) and injecting it during peak periods. This provides a strong technical justification for the SVC simulations conducted in this thesis. While the study successfully demonstrated voltage stability enhancement techniques, it did not examine frequency stability, swing bus behaviour, or the dynamic interaction between large hydropower plants and interconnected networks.

Voltage Stability Assessment of Nigeria 330 kV Power Grid (Onyegbadue et al., 2024) focuses on identifying critical buses and voltage collapse margins using P-V and Q-V curve analysis. The study identifies that the radial nature of the Nigerian grid leads to high susceptibility to voltage instability during peak loading. Its strength lies in the use of the "critical bus" perspective to prioritize where reactive power compensation should be placed, which is highly applicable to the Rwandan grid's star-like 110 kV topology.

These studies collectively affirm that African power systems are becoming progressively susceptible to frequency and voltage instability as a result of system expansion, renewable integration, and operational limitations. Nevertheless, the majority of current research emphasises either frequency stability or voltage stability independently, with insufficient consideration for a holistic network-wide stability evaluation that includes validated dynamic models of actual systems.

2.3 Existing Research Gaps

Despite the strengths of the existing recent literature on grid system stability, the subsequent research gaps have been identified:

- Most existing studies on African power systems assess either frequency stability or voltage stability independently, with limited integrated analysis of multiple stability modes within a single interconnected network.
- The existing research frequently assumes a strong electricity network interconnectivity when discussing swing bus dynamics. The dynamic performance of small power plants in small grids (such as Rwanda) with low-

inertia system when confronted with high PV penetration dips is not well understood.

- Few studies explicitly document the modelling, verification, and validation procedures used to ensure that simulation models accurately represent real physical power systems.
- The role of large hydropower plants operating as swing buses in maintaining frequency stability during severe disturbances is underexplored in most existing grid studies in Africa.
- There is insufficient research focusing on Rwanda's power system stability despite increasing interconnections, growing demand, and evolving generation mix.

This study addresses these gaps by developing, validating, and applying a detailed PSS®E-based dynamic model of Rwanda's high-voltage power system to assess voltage, frequency, and transient stability under credible disturbance scenarios.

CHAPTER THREE

METHODOLOGY

3.1 Overview

This study adopted a simulation-based research methodology to assess the stability of Rwanda's high-voltage power system under normal and disturbed operating conditions. The methodology involved data collection, network modelling, model verification and validation, steady-state power flow analysis, and time-domain dynamic simulations using Power System Simulator for Engineering (PSS®E) software.

The modelling and simulations were performed using actual network data to ensure that the developed model accurately represented the physical power system. Stability performance was evaluated in terms of voltage response, frequency behaviour, and transient dynamics following credible disturbance scenarios.

This chapter describes the systematic approach that was used to collect technical data, construct the Rwandan grid in PSS®E, and validate the model against real-world SCADA measurements. The study adopted an experimental simulation-based design, where network variables were controlled to evaluate the system's resilience under contingency scenarios.

3.2 Current and Relevant Conceptual Models

This study adopted a simulation-based research design aimed at assessing the stability of the entire Rwanda's high-voltage power system under normal and disturbed operating conditions. The research design followed a structured and sequential process, beginning with data collection and ending with stability performance assessment and interpretation of results. This formulated the needed framework used in answering the research questions. The research design followed a structured sequence of activities, as illustrated in Figure 3.1.

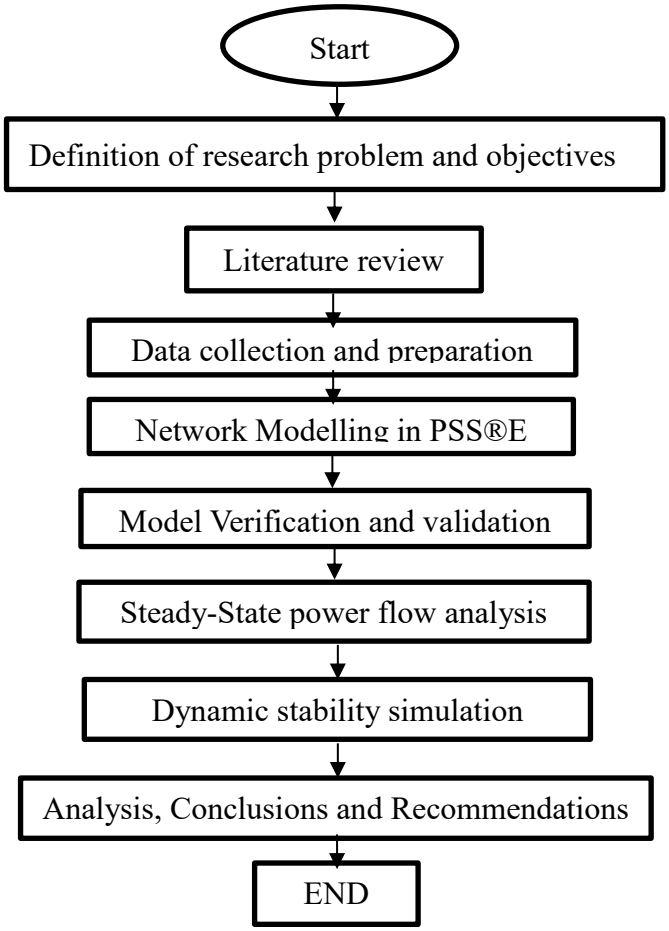

Figure 3.1: Research Design Flowchart

As shown in Figure 3.1, **t**he main stages included data collection, network modelling, model verification, model validation, steady-state analysis, dynamic simulation, and result interpretation.

Based on this framework, a simulation model is developed to help simulate stability scenarios of the power system. It is a fixed design study because the engineering simulation requires fixing some parameters before the simulations. Parameters such as swing bus voltage and the loading have to be fixed for any particular case. The simulations being carried out are taken as fixed designs because the assumptions taken are driven from the theoretical aspect, which gives the ability within marginal error to know in advance which variables need to be controlled.

The research design is simulation-based, utilizing PSS®E to model changes in network conditions such as varying load levels and fault locations. This approach allows for

the assessment of system responses, including voltage stability angle, reactive power network resilience and fault levels.

Network data to be used in assessing stability status was collected from the Rwanda's state-owned power utility company. Line and generator outages were applied to determine the system's ability to withstand disturbances. Results obtained through simulations were further validated using the existing grid parameters monitoring system.

3.3 Grid Study Procedures

3.3.1 Modelling Data Sources and Analysis

Based on the problem statement and literature review, the following propositions and hypotheses can be deduced.

Network modelling in this study was based on actual power system data obtained from Rwanda's national transmission planning and operational records. In order to simulate the network parameters, data from transmission line impedances and charging admittances, busbar voltages, transformer impedances and tap ratios, admittances of shunt-connected devices such as static capacitors and reactors, load-power consumption at each bus of the system, real power output of each generator or generating plant, either voltage magnitude at each generator bus or reactive power output of each generating plant, was collected. The maximum and minimum reactive power output capabilities of each generating plant, as well as single-line diagrams of the substations, were also used as inputs to the model. Important parameters specific for the simulation to have reference and accuracy respectively are: power system MVA base, and power mismatch accuracy, maximum iterations and correction factor.

Data used in modelling of the network was collected from line parameters of transmission lines using designs documents, loads obtained from the metered values at all major substations monitored over a year period, and transformer, generator, reactors name plate details, and during commissioning, were used. Since the generation sector has a lot of Independent Power Producers, data was collected from

different companies with a stake in grid connected generators. To ensure data acquisition and utilization of accurate data from these plants, on-site data, mainly from network equipment/devices, was used.

The Rwandan network is composed of several transmission lines interconnected by system buses. They transport power to reach various substations that are able to distribute power to various consumers. To obtain accurate simulation results, parameters of the entire network comprising of 121 busbars of which 29 make up the 110 kV transmission subsystem, 34 are 30 kV distribution subsystem, 8 form 15 kV distribution subsystem and 50 forming the generation level subsystem ranging from 0.4 kV to 11 kV (Rwanda Energy Group, 2023) are added into PSS®E Version 34 software, setting up a power system model in the working file. The 110 kV subsystem being the backbone of the Rwandan network, its stability was of main focus to fully comprehend the subsequent effect it would have on the entire grid. Most power system analysis uses a system of parameter normalization in which all voltages, currents, and power flows are expressed per unit of the designated base values (e.g., ohm/mile, ohm/kilometer). This system is convenient in connection with transmission lines and transformers, and virtually necessary for the dynamic simulation of generators and their controls. Transmission line operating voltages may range from 69 kV to 750 kV in a single network model, however, it is easier and more feasible to execute digital computations with a minimal range of numerical values. Hence, per unit values calculated using equations 2.15 to 2.19 were used for modelling. The data gathered was converted into Per Unit values using equations under the section “Base Quantities and Per Unit values conversion procedure” using these equations (2.15 to 2.19). This was achieved by using a base value of 100 MVA as is mainly used by PSS®E software version 34, 2018. The same software has the capability to handle very many buses and provide for static and dynamic simulation by doing a load flow simulation of the transmission systems under study. It utilizes Newton-Raphson load flow algorithm among others to analyse system voltage, frequency, machine angles, active and reactive power under any loading conditions as per data input. The network parameters compiled from substations, generators, transformers and transmission line converted into per unit values is presented in Tables 3.1 to 3.4.

Table 3.1: Key Model 110 kV Subsystem Parameters

FROM SUBSTATION	TO SUBSTATION	VOLTAGE (kV)	OHM/KM R1	OHM/KM X1	micF/KM C1	LINE LENGTH (KM)
MURURU I	MURURU II	110	0.231	0.437	0.008	0.4
MURURU II	KIBOGORA	110	0.123	0.427	0.009	41.7
MURURU II	NTENDEZI	110	0.123	0.427	0.009	22
NTENDEZI	BUGARAMA	110	0.123	0.427	0.009	17.4
BUGARAMA	GISHOMA	110	0.123	0.427	0.009	17
NTENDEZI	KARONGI	110	0.123	0.427	0.009	61.7
KIBOGORA	KARONGI	110	0.123	0.427	0.009	42
KARONGI	KILINDA	110	0.123	0.427	0.009	27
NYABARONGO	KILINDA	110	0.231	0.437	0.008	27
RUKARARA	KILINDA	110	0.231	0.437	0.008	23
KILINDA	KIGOMA	110	0.123	0.427	0.009	29.6
KIGOMA	MONT KIGALI	110	0.123	0.427	0.009	43.7
MONT KIGALI	GIKONDO	110	0.123	0.427	0.009	5.4
GIKONDO	JABANA I	110	0.123	0.427	0.009	9.1
JABANA I	RULINDO	110	0.231	0.437	0.008	27.9
RULINDO	GIFURWE	110	0.231	0.437	0.008	29
GIFURWE	MUKUNGWA	110	0.231	0.437	0.008	18
MUKUNGWA	NTARUKA	110	0.123	0.427	0.009	28.9
JABANA I	BIREMBO	110	0.231	0.437	0.008	7.5
KARONGI	KIBUYE	110	0.123	0.427	0.009	12.4
BIREMBO	GASOGI	110	0.231	0.437	0.008	16.5
GASOGI	MUSHA	110	0.231	0.437	0.008	16.5
MUSHA	KABARONDO	110	0.231	0.437	0.008	25
KABARONDO	RWINKWAVU	110	0.231	0.437	0.008	8.5
JABANA II	JABANA I	110	0.123	0.427	0.009	1.2
NYABARONGO	KILINDA	110	0.231	0.437	0.008	23
SHANGO	BIREMBO	110	0.13181	0.43215	0.00849	9.53
SHANGO	RUBAVU	110	0.06637	0.31235	0.01172	105.25
RUBAVU	KIBUYE	110	0.06637	0.31235	0.01172	56.81

Source: (Rwanda Energy Group, 2023)

AC transmission lines have resistance, reactance and capacitance that influence power flow across a specific line. These parameters are provided per km and were calculated depending on the length of a particular transmission line, for use in PSS®E.

Table 3.2: Substations and Respective Transformers Model Parameters

Substation	Voltage (kV)	Rating (MVA)	% Impedance	R	X/R	X0	R0
Gokondo	110/15	2*15	9.2	0.484	19	27.6	1.453
	110/15	15	8.93	0.47	19	26.79	1.41
Jabana i	110/15	2*10	8.6	0.662	13	25.8	1.985
	0.4/15	6*1.625	5.74	0.82	7	17.22	2.46
Jabana 2	110/6.6	3*15	12.11	0.637	19	36.33	1.912
Karongi	110/30	10	7	0.583	12	21	1.75
Kibogora	110/30	6	8.67	0.723	12	26.01	2.168
Kigoma	110/30	10	8.35	0.522	16	25.05	1.566
Kilinda	110/30	6	8.5	1.214	7	25.5	3.643
Ndera	110/15	2*20	10	0.484	20.652	30	1.453
Gabiro	110/30	2*10	8.25	0.637	12.943	24.75	1.912
Gahanga	110/15	20	10.08	0.521	19.314	30.24	1.566
Nzove	110/15	20	10.08	0.521	19.314	30.24	1.565
Mont kigali	110/30	20	8.25	0.515	16	24.75	1.546
	110/15	20	10.1	0.841	12	30.3	2.525
Mukungwa	110/6.6	2*15	12	0.631	19	36	1.894
	110/30	15	8.63	0.719	12	25.89	2.157
Mururu 2	110/70	15	10	0.526	19	30	1.578
Ntaruka	110/6.6	2*10	8.2	0.512	16	24.6	1.537
	110/30	15	6.47	0.539	12	19.41	1.617
Rulindo	110/30	2*10	10	1.428	7	30	4.285
Gihira	30/6.6	3	7.2	0.986	7.3	21.6	2.958
Gisenyi	0.4/6.6	0.8	5	-0.5	-10	15	-1.5
Gisenyi	30/6.6	5	6.6	-0.519	-12.7	19.8	-1.559
Rukarara	30/6.6	15	9.5	0.524	18.1	28.5	1.574
Gifurwe	110/30	10	10	1.428	7	30	4.285
Birembo	110/15	20	10.46	0.445	23.5	31.38	1.335
Gasogi	110/15	10	9.32	0.776	12	27.96	2.33
Musha	110/15	10	10	1.111	9	30	3.333
Kabarondo	110/30	10	6.77	0.564	12	20.31	1.693
Rwinkwavu	110/15	6	10.36	1.151	9	31.08	3.453
Kibuye	110/11	2*20	10.5	0.552	19	31.5	1.657
Nyabarongo	6.6/110	2*13.2	8.4	0.381	22	25.2	1.145
Keya	3.3/30	2.5	6.6	0.55	12	19.8	1.65
Cyimbili	0.4/30	0.4	5	0.7415	4	15	2.224
Nkora	0.4/30	0.8	5	0.513	6	15	1.539
Rugezi	0.69/30	1.6	6	1.142	7	18	3.426
Nshiri	0.4/30	0.5	5	0.832	4	15	2.497

Source: (Rwanda Energy Group, 2023)

To model a transformer in PSS®E, its vector group, HV and LV side voltages, MVA rating were required in addition to the reactance and resistance of windings. Such data was available from transformer name plates and manufacturers technical data sheets.

Table 3.3: Sub-Stations' Off Peak and Peak Loads

Substation	Off-peak Load		Peak load	
	MW	**MVAr**	**MW**	**MVAr**
Kigoma	3.353	1.834	9.86	5.8
Mt. Kigali	4.11	1.5	9.477	3.913
Gikondo	12.29	3.86	25.05	2.91
Jabana	6.46	2.76	19.07	6.07
Rulindo	2.536	0.746	3.758	1.069
Birembo	16.7	2.6	26.6	7.2
Gasogi	3.27	0.729	7.932	1.529
Musha	5.92	3.11	7.62	3.385
Kabarondo	2.37	0.6	3.73	1.97
Gabiro	3.4	0.5	2.4	2.6
Ndera	1.8	0.3	3.6	0.9
Gifurwe	1.163	0.314	2.816	1.183
Kibogora	0.9	0.1	1.3	0.6
Karongi	2.8	0.66	7.8	1.19
Rwinkwavu	0.68	0.9	1.18	1.53
Bugarama	5.41	2.78	8.04	3.38
Ntendezi	1.6	0.3	1.3	0.9
Kirinda	0.098	0.183	0.178	0.257
Rukarara	2.54	0.9	4.53	1.82
Total	**77.4**	**24.676**	**146.241**	**48.206**

Source: (Rwanda Energy Group, 2023)

The Rwandan grid load variation behaviour pattern was observed to be the same throughout the year with off-peak regimes occurring at night from midnight to 7am and during the weekend (Saturday and Sunday), while peak regimes occur between 6pm and 11pm. This data was obtained from the national dispatch center of Rwanda.

Table 3.4: Power Plants' Model Parameters

Plant name	Type	Installed capacity (MW)	MVAr	Reactance (pu)	Resistance (pu)
Ntaruka	Hydro	11.25	6.75	0.32	0.01
Mukungwa 1	Hydro	12	7.2	0.197	0.01
Nyabarongo	Hydro	28	16.8	0.14	0.023
Gisenyi	Hydro	1.2	0.72	0.2	0.01
Gihira	Hydro	1.8	1.08	0.4	0.01
Murunda	Hydro	0.1	0.06	0.21	0.013
Rukarara 1	Hydro	9.5	5.7	0.138	0.01
Rugezi	Hydro	2.2	1.32	0.145	0.01
Keya	Hydro	2.2	1.32	0.23	0.01
Nyamyotsi I	Hydro	0.1	0.06	0.21	0.013
Nyamyotsi II	Hydro	0.1	0.06	0.21	0.013
Agatobwe	Hydro	0.2	0.12	0.11	0.0031
Mutobo	Hydro	0.2	0.12	0.11	0.0031
Nkora	Hydro	0.68	0.408	0.23	0.01
Cyimbili	Hydro	0.3	0.18	0.23	0.01
Gaseke	Hydro	0.582	0.3492	0.081	0.002
Mazimeru	Hydro	0.5	0.3	0.0142	0.0018
Janja	Hydro	0.2	0.12	0.11	0.0031
Gashashi	Hydro	0.2	0.12	0.11	0.0031
Nyabahanga I	Hydro	0.2	0.12	0.11	0.0031
Nshili1	Hydro	0.4	0.24	0.043	0.0051
Musarara	Hydro	0.45	0.27	0.135	0.0012
Mukungwa 2	Hydro	2.5	1.5	0.145	0.01
Rukarara 2	Hydro	2.2	1.32	0.138	0.01
Giciye1	Hydro	4	2.4	0.243	0.01
Ruzizi 2	Hyrdo	12	7.2	0.204	0.01
Giciye2	Hydro	4	2.4	0.243	0.01
GigaWatt	Solar	8.5	5.1	999999	0
Nasho Solar PP	Solar	3.3	1.98	999999	0
Jabana 1	Diesel	7.8	4.68	0.093	0.005
Jabana 2	Heavy fuel Oil	20	12	0.15	0.0035
Mukungwa Thermal	Heavy fuel Oil	10	6	0.0929	0.001
SO Energy	Heavy fuel Oil	10	6	0.0929	0.001
Birembo	Heavy fuel Oil	10	6	0.0929	0.001
Gishoma	Peat	15	9	0.15	0.0021
Kivuwatt	Methane	26.4	15.84	0.15	0.0035
Rukarara 5	Hydro	1.6	0.96	0.093	0.005

Source: (Rwanda Energy Group, 2023)

3.3.2 Modelling of the Grid

The Rwanda power system network was developed in PSS®E by modelling all high-voltage buses, transmission lines, transformers, generators, and loads corresponding to the actual transmission network. Hydro power plants were represented as synchronous machines with appropriate governor and excitation system models.

For modelling purposes, the raw data calculated using the Per-Unit data system equations 2.15 to 2.19 were entered in PSS®E to create a network data file (.sav file). This file was then used to create a single line diagram of the network (.sld file). The numbering of busbars was based on the principle of voltage level to ensure they are easily differentiated in the model. Transmission lines, transformers and generator units were then affiliated to the respective busbars defined. PSS®E then uses these parameters to determine the power flow and behaviour of the system being modelled (Olaogun et al., 2024), (Abdourahimoun et al., 2025).

The modelling process involved converting physical parameters into a mathematical framework. The network of transmission lines and transformers is described by the linear algebraic equation

$$[I_n] = [Y_{nn}]\,[Vn] \tag{3.1}$$

Where; I_n is the vector of positive-sequence currents flowing into the network at its nodes (buses), V_n is the Vector of positive-sequence voltages at the network nodes (buses), Y_{nn} is the Network admittance matrix (Ur Rehman et al., 2023).

It is simple to calculate the power flow if one knows either In or Vn. Since neither In nor Vn are known in practice, the power flow program's job is to create successive trials of both In and Vn that meet all of the load and generation requirements listed in the data presentation as well as equation 3.1 (Stevenson, 1995). After After V_n has been determined, to handle the diverse voltage levels (0.4 kV to 110 kV), all parameters were normalised using the Per-Unit (p.u.) system with a base of 100 MVA. The following equations 3.2, 3.3 and 3.4 were applied to calculate line and transformer loading (Glover et al., 2022), (Shahzad U. , 2021).

$$I_{flow}\ (A) = \frac{MVA_{flow}}{kV_{actual} \times \sqrt{3}} \times 1000 \quad (3.2)$$

$$\text{Percentage line loading} = \frac{I_{flow}}{I_{rating}} \times 100 \quad (3.3)$$

$$\text{Percentage transformer "MVA loading"} = \frac{MVA_{flow}}{MVA_{rating}} \times 100 \quad (3.4)$$

One effective iterative scheme requires making an initial estimate of the voltage at each bus, building an estimated current inflow vector (In) at each bus from a boundary condition using equation 3.5.

$$V_k = Pk + jQ_k \quad (3.5)$$

Where $P_k + jQ_k$ is the net load and generation demand at bus k, and V_k is the present estimate of voltage at bus k. Use equation 3.1 to obtain a new estimate of the bus voltage vector (Vn). Return to equation 3.2 and repeat the cycle until it converges on an unchanging estimate of Vn.

Although this scheme is not very effective for calculating general power flow, where the terminal voltage magnitude is specified for many generators instead of the reactive power output, PSS®E gives the user the option to select from a variety of AC power flow iteration schemes, including fully coupled, decoupled, and fixed slope Newton-Raphson iterations, as well as modified Gauss-Seidel iteration that is appropriate for series capacitors. According to equations 3.6 to 3.8, system performance indexes are calculated (Salami, 2017).

$$\text{Thermal ratings limit testing} = \frac{P_{max} - P_{ilineflow}}{MVA_{\text{system base Value}}} \quad (3.6)$$

Where P_{max} = Maximum real power ratings of the system branches, P_{iline} flow = Power flow on line i after contingency, MVA as system base is 100 MVA, as widely used by PSS®E (Bayliss and Hardy, 2007).

$$PI_{av} = \frac{\sum_{i=1}^{n} f(x)}{t} \quad (3.7)$$

Where PI_{av} is average value performance index for thermal ratings encountered when more than one lines are overloaded due to branch outage, f(x) is post line outage thermal rating overload for each transmission line, t is total number of lines overloaded due to a certain single line outage (Bayliss and Hardy, 2007), (Kundur, 1994).

$$PI_V = \sum_{i=1}^{N_{PQ}} \left[\frac{2(V_i - V_{i\,norm})}{V_{i\,max} - V_{i\,norm}}\right] \quad (3.8)$$

Where Vi is the voltage at bus i after a contingency, Vi_{max} is the maximum voltage limit of bus i, Vi_{min} is the minimum voltage limit of bus i, Vi_{norm} is the average of the voltage maximum and minimum limits of bus i, and Npq is the total number of load buses in the system. PIv stands for voltage performance index. Consequently, the PSS®E model design necessitates the following actions (Siemens, 2017), (Colorado State University, 2016).

i. Convert the system's physical model into a PSS®E input data file by referencing linked models of the load, generators, individual buses, and branches. For equipment that is not covered by an explicit model in PSS®E, create equivalent circuits using equivalent branches and dummy buses as needed.
ii. Use the PSS®E programs to process the data, apply calculations, and generate reports.
iii. Interpret the computation findings in light of the equipment's stated physical characteristics, which were used to initiate the procedure in the first place.

Steady-state operating conditions were assessed using the Newton–Raphson load flow simulation approach, implemented in PSS®E. This algorithm was selected due to its superior convergence characteristics and suitability for small networks and large interconnected power systems. To enhance understanding, the Newton–Raphson load flow procedure used for modelling data analysis is presented as a block diagram in Figure 3.2 (Siemens, 2017)

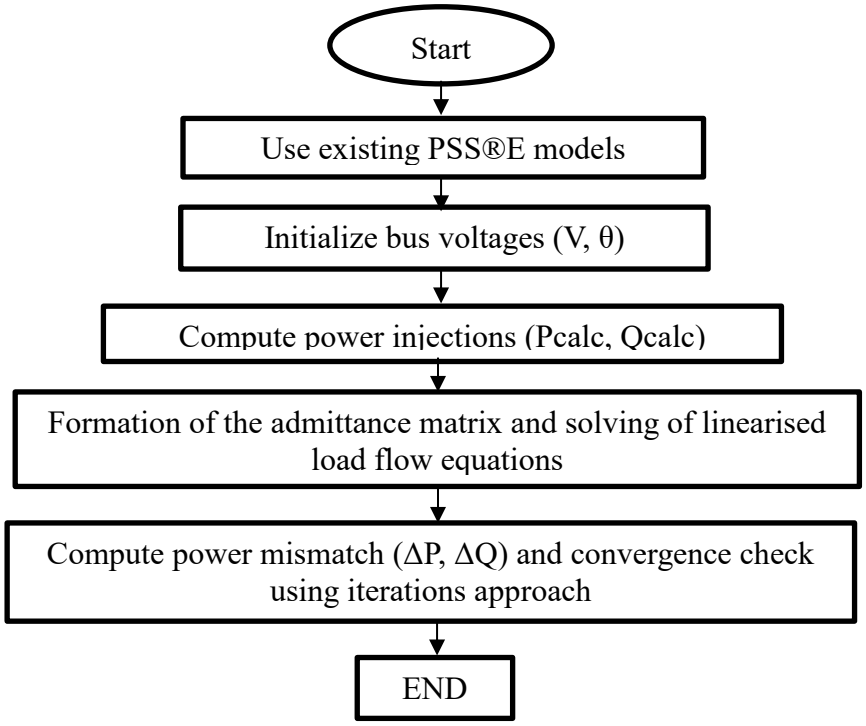

Figure 3.2: Newton–Raphson Load Flow Algorithm Block Diagram

Figure 3.2 illustrates how modelling data were analysed and processed using the Newton–Raphson method to establish the steady-state solution that served as the foundation for all subsequent stability simulations. The flowchart summarizes how modelling data were processed to obtain converged bus voltages and power flows prior to dynamic simulation.The Newton–Raphson method was applied to iteratively solve the nonlinear power flow equations governing the system by updating bus voltage magnitudes and phase angles until convergence was achieved (Van Cutsem and Vournas, 2008), (Stevenson, 1995).

Active power balance at bus *I*:

$$P_i = V_i \sum V_j(G_{ij} \, Cos\theta_{ij} + B_{ij} \, Sin\theta_{ij}) \qquad (3.9)$$

Reactive power balance at bus *i*:

$$Q_i = V_i \sum V_j(G_{ij} \, Sin\theta_{ij} - B_{ij} \, Cos\theta_{ij}) \qquad (3.10)$$

Where V_i and V_j are bus voltage magnitudes, G_{ij} and B_{ij} are elements of the bus admittance matrix, and θ_{ij} is the voltage angle difference between buses *i* and *j*.

The Newton–Raphson algorithm iteratively linearised these nonlinear equations 3.9, 3.10 and the admittance matrix equation 2.10 and solved for voltage magnitude and angle corrections until power mismatches were reduced below specified tolerances.

Nyabarongo Hydropower plant was designated as the swing bus, providing the system reference for voltage angle and absorbing the real and reactive power mismatches during load flow calculations.

3.3.3 Creating a New PSS®E Case

To develop and validate a model by comparing simulated results with actual system data obtained from the utility, a new PSS®E case was created. The validation involved comparing steady-state voltage profiles, power flows, and frequency under known operating conditions. Figure 3.3 shows how a new case of the any network is created in PSS®E.

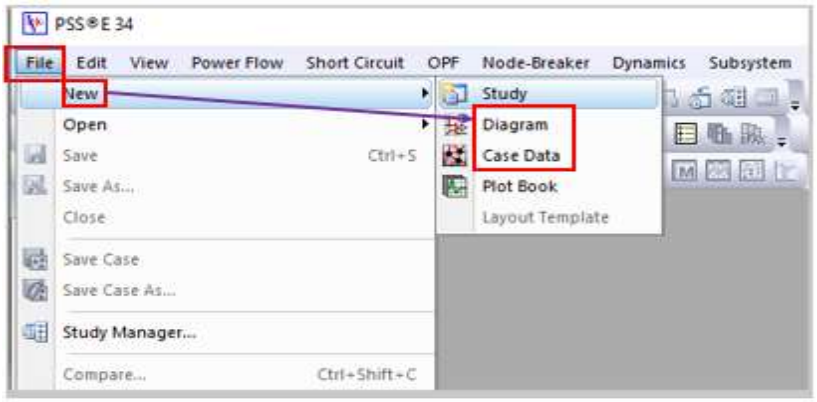

Figure 3.3: Creating a New Case in PSSE (Siemens, 2017)

Figure 3.3 shows how a new case is created using the menu bar file, opened by selecting the new network case via the toolbar button, and the base MVA, system frequency, and rating choices are entered, as per the instructions in the PSS®E 34.1 manual. Subsequently, the bus data (bus ID, code, and voltage), load data (zone, bus connected, active and reactive power capacity), machine data (base MVA, Impedance

in P.U., Gentap at high voltage side), and transformer data (voltage, off-nominal turns ratio in pu of bus base voltage, Impedance in terms of R and X, load loss R in watts and X in pu) are entered. All this data is entered in the spreadsheet data of PSS®E by entering data of all busbars first, followed by branches, transformer data, plants, machines and loads. System swing bus (type code 3) is defined since it is needed by power flow solution algorithm to provide a fixed reference bus voltage and angle and to "make up" the balance of total system generation such that: Generation – load – Losses = 0.

Once a new case has been created, the same data is utilized to generate a related single-line diagram utilizing the file and new diagram options, the subsystem selector to identify the subsystem, edit - preferences, and, if desired, only "Grow" network elements in the current bus subsystem. Click every bus in the subsystem in the tree view, then click the auto draw button. In diagram view, select the area where the diagram can "begin to grow". To solve the power flow model, open the created case, power flow solution (select from options of Newton-Raphson, Fixed slope decoupled Newton-Raphson, Full Newton-Raphson, Decoupled Newton-Raphson), then solve the system with taps locked, and VAr limits applied automatically. Check in the output bar whether the system converged; otherwise, check all modelling data, correct data, and re-solve the case (Siemens, 2017).

Using the PSS®E model, different scenarios reflecting the actual operating points across the grid (peak load and off-peak) are developed. Power flows are simulated to identify and analyze potential bottlenecks or overloaded sections in the transmission and distribution systems. Figure 3.4 shows the power flow simulation for steady state analysis.

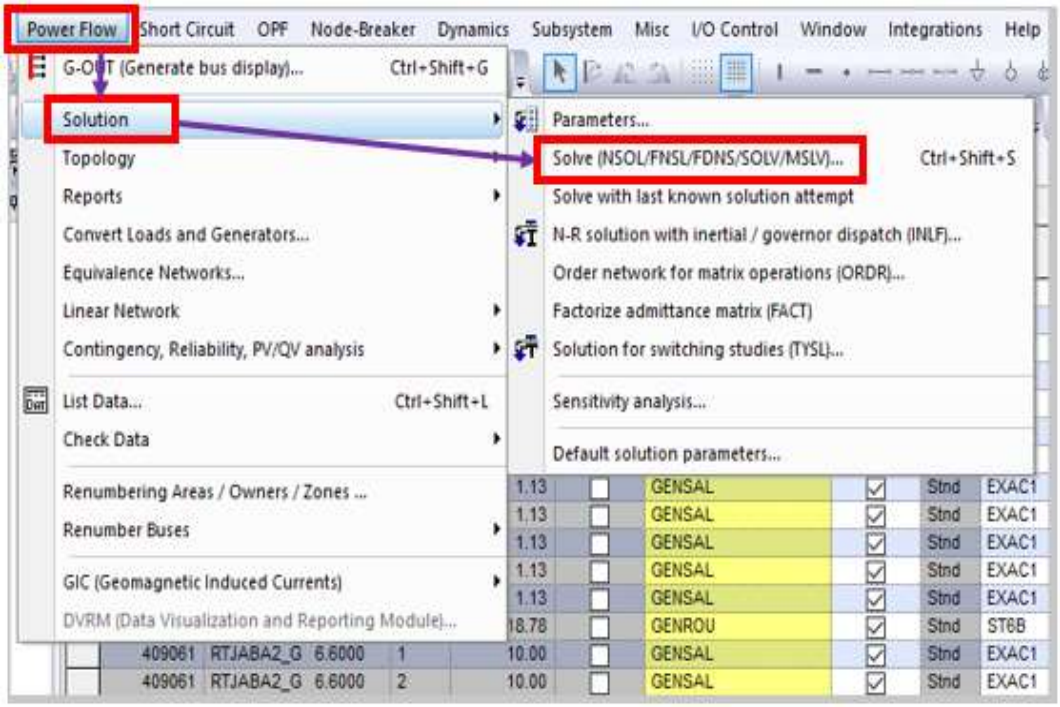

Figure 3.4: Steady State Analysis Simulation in PSS®E

Source: (Siemens, 2017)

3.3.4 Model Verification and Validation

The Rwandan power system was modelled based on the snapshot data obtained from the national electricity utility. The Rwandan power system was modelled based on the snapshot data obtained from the national electricity utility, model verification was performed to confirm that the network model was correctly implemented in PSS®E. This involved checking data consistency, confirming successful load flow convergence, and ensuring that power mismatches at all buses were within acceptable tolerances. Figure 3.5 shows the verification steps for a steady-state model to check whether there are no mismatches in active power flow on the swing bus.

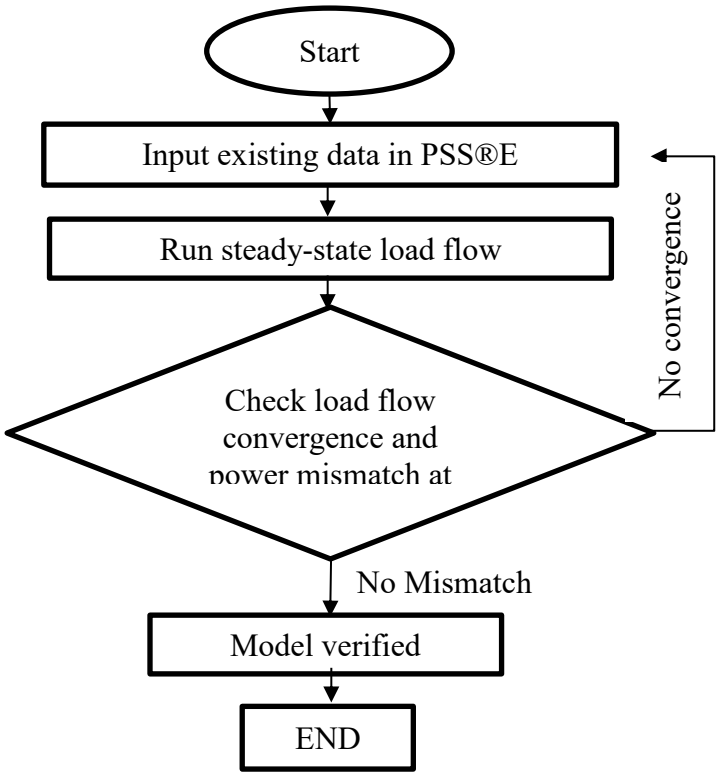

Figure 3.5: Model Verification Block Diagram

After updating all relevant parameters, the off-peak model was verified to have a system model that converges with no power flow mismatches. The Newton-Raphson iterative process was applied in PSS®E to solve for the mismatch until the system converged at the swing bus. The algorithm iteratively adjusted bus voltage magnitudes and phase angles until power mismatches were minimised.

Convergence with zero mismatch at the swing bus confirmed correct model formulation as shown in Figure 3.6.

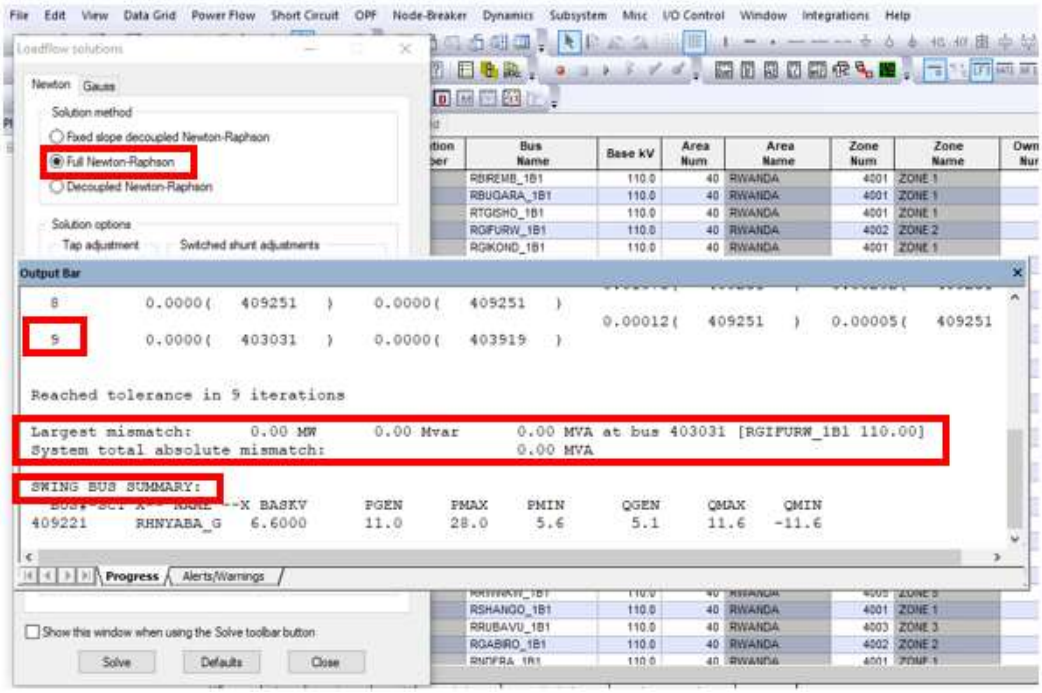

Figure 3.6: Model Mismatch Verification in PSS®E

The swing bus has 0 MW mismatch as shown in Figure 3.6, a scenario achieved after nine “full Newton-Raphson” iterations. This shows that the network model developed and run in PSS®E converges.

Model validation was conducted to ensure that the developed model accurately represented the real physical power system. Validation was achieved by comparing simulation outputs, including voltage profiles and system frequency, with actual operational data and known system behaviour following the steps in Figure 3.7.

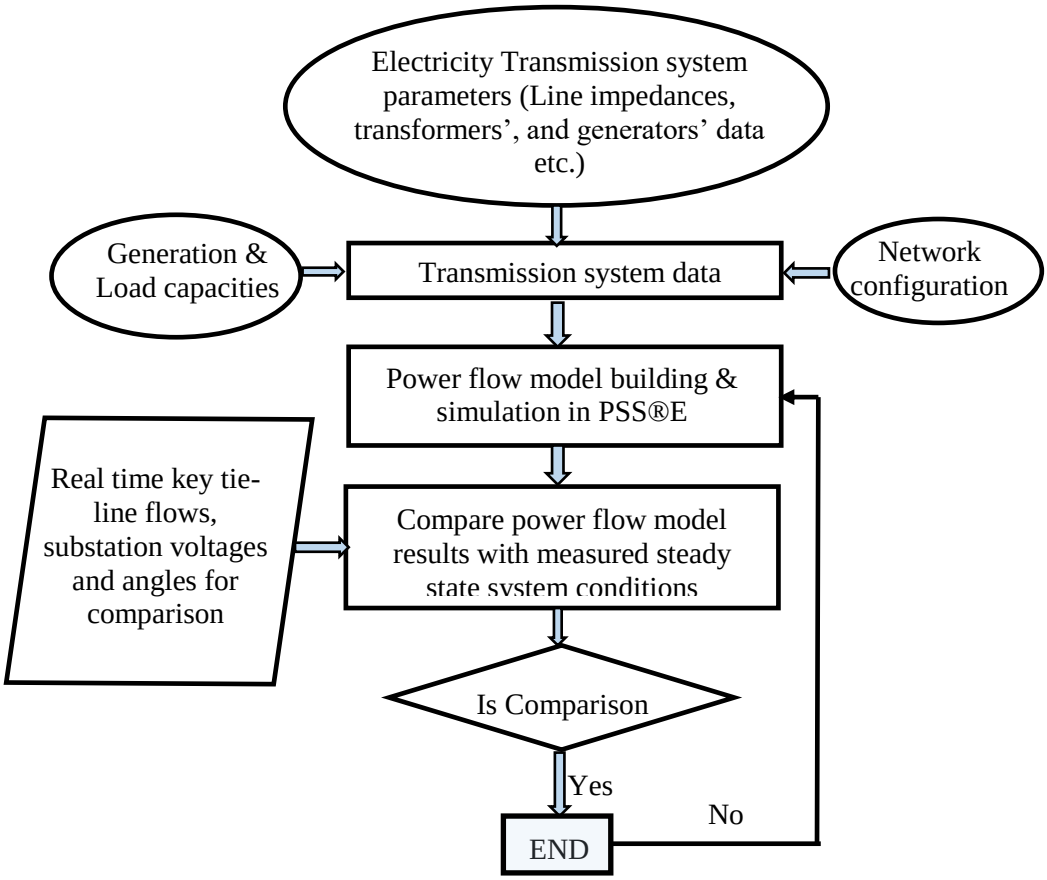

Figure 3.7: Model Validation Block Diagram

The model validation steps in Figure 3.7 were followed to obtain the results described in Section 3.3.5.

Following model verification and validation, detailed power flow and stability (steady state and dynamic) simulations were performed using a structured simulation sequence shown in Figure 3.8.

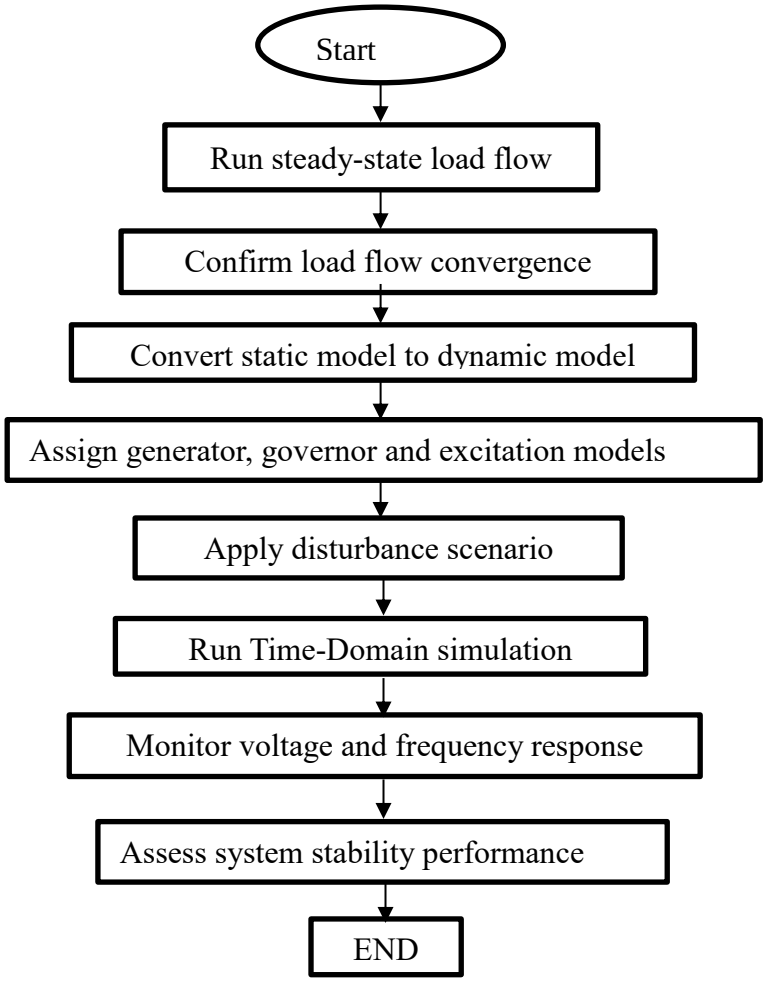

Figure 3.8: Power Flow and Stability Simulation Sequence

3.3.5 Study Simulations

3.3.5.1 Creating a Dynamic Model File

Transient stability analysis, frequency stability and voltage stability studies were conducted using a dynamic grid model that is created in PSS®E.

For dynamic stability analysis, a dynamic model is created. The dynamic file consists of data from generators, excitation systems, stabilizers, turbines, governors and all other equipment. Parameters should be in the right range of operation as out-of-range values are automatically highlighted. When highlighted in yellow, it is a warning that out of typical range and should therefore be checked but this doesn't mean that data are not good, while the red highlight means that the data is critically out of range and

must be checked and updated to avoid giving incorrect results and abnormal terminations the generator must be loaded within allowed bounds, and the node numbers and IDs in the network data file (.sav file) and dynamic file (.dyr) must match (Siemens, 2017), (Onyegbadue et al., 2024).

3.3.5.2 Assumptions

For simulation purposes, the following assumptions were made to reduce the number of variables in the power system to enable modelling of the network

i. Simultaneous loading on all buses.
ii. Constant loads during simulations
iii. Lumping loads at respective busbars.

3.3.5.3 System Dynamic Behaviour Simulation Steps

In order to do dynamic simulation, the network data file and the dynamic data file (.dyr file) must be loaded simultaneously, and the PSS®E dynamic simulation functionalities are shown in Figure 3.9.

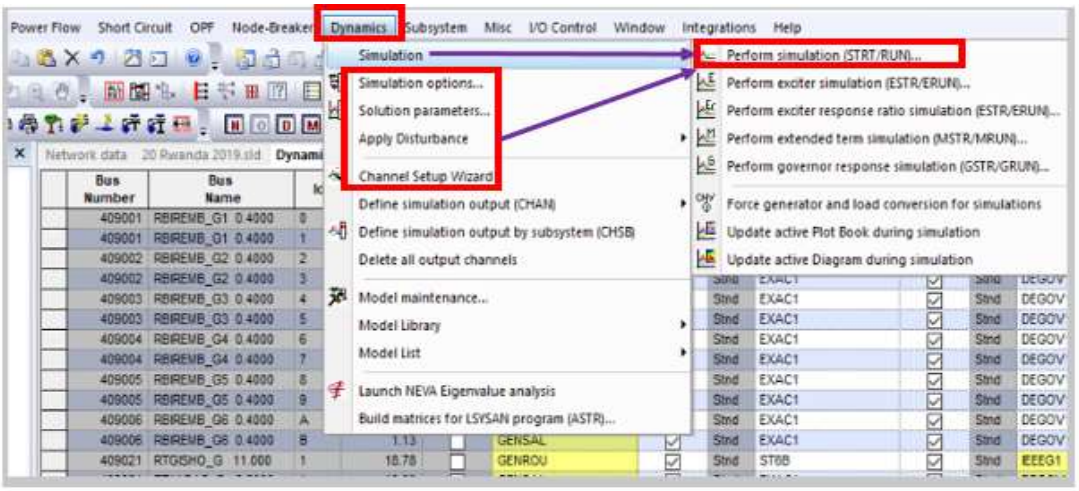

Figure 3.9: Dynamic Simulation in PSS®E

As shown in Figure 3.9, solution parameters from the dynamic option menu are selected, then adjusting the tolerance, integration step, and frequency filter before selecting the location for the channel output file. Configure the network frequency dependence, observe out-of-step conditions, relative machine angle, and generators exceeding machine angles within the simulation options. Continue from the menu bar and choose the load, bus, machine, and line quantities to be monitored and simulated under the Channel Selection Wizard. Then, initialize the simulation to make sure the initial conditions are correct (Siemens, 2017).

A standard simulation involves starting the model in a state of no disturbance, applying a disturbance, running the model during the disturbance for a certain amount of time, clearing the disturbance, changing the topology as needed, and continuing the simulation until the monitoring time is up (Abdourahimoun et al., 2025). After that, the simulation output results are shown graphically by loading the output file, displaying the Plot Tree View, expanding the tree, and then dragging and dropping the desired simulated output and channels onto the PlotBook.

PSS®E's dynamic simulation capabilities allow for the examination of the system's response to disturbances over time (system stability), identifying critical points of instability and potential cascading failures.

Through dynamic simulations, the frequency response of the grid under different operating conditions is analysed. PSS®E facilitates the study of frequency deviations resulting from load fluctuations, generation changes, or system contingencies, enabling the evaluation of grid stability concerning frequency control mechanisms.

Voltage stability analysis is also conducted to assess the grid's ability to maintain acceptable voltage levels under varying operating conditions. PSS®E's modelling features enable the investigation of voltage profiles, reactive power flows, and voltage stability margins, helping identify voltage collapse phenomena and voltage control strategies.

By leveraging the comprehensive capabilities of PSS®E, the study simulation will provide valuable insights into the current state and future needs of the Rwandan grid,

ultimately assisting policymakers and utilities in fostering a robust and resilient energy infrastructure.

CHAPTER FOUR

RESULTS AND DISCUSSIONS

4.1 Introduction

Under this chapter, findings from the network model simulation and related explanation are presented. In line with the results obtained, the results analysis and discussion based on the tabulation made up on the case study model with respect to system stability are displayed. Simulated results and collected real-time data associated with power system stability under normal operational status and contingency implications on transmission lines and voltage variation on system buses are of major focus in this chapter. Deliberate tripping of lines, generators and load is done to fully understand the effect this will have on system voltage and frequency. The response also reflects system stiffness, hence its ability to recover from disturbances.

4.2 Model Validation Results

In order to validate that the PSS®E model developed using collected data is accurate, two models representing day time and night time regimes were used and steady state simulation results of voltages were compared to real time voltage measurements taken from the utility SCADA.

Figure 4.1 shows model comparison for 7th April 2023 at 8 am. This was selected as a representative for two reasons:

i. All measured voltages (from SCADA) were higher than 121 kV, which is voltage limit set in the grid code, a condition that is typical in the system during off-peak conditions.
ii. Rwandan National Grid normally experiences over voltages on such a date, being a national commemoration day, the industries and offices are closed, annually, so developed model can be used as a base for appropriate simulation.

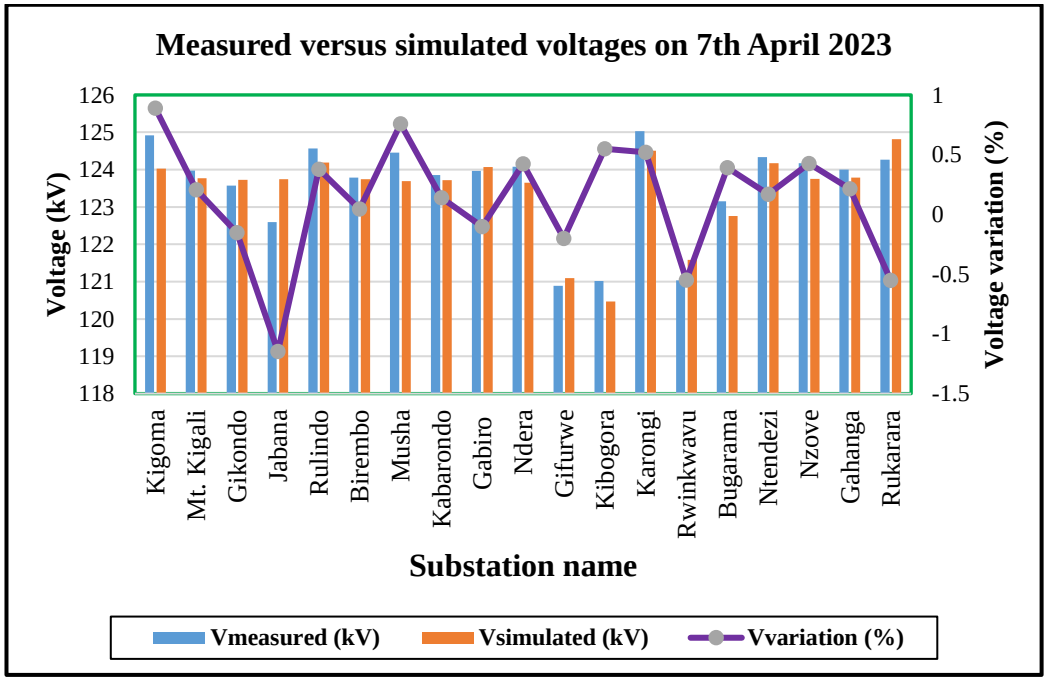

Figure 4.1: Measured and Simulated Voltages for the 110 kV Sub-System Busbars

The simulation and measured values of voltage on April 7th 2023 shows that the error between grid operating voltage and SCADA measured values on all 110 kV busbars is below 1% as per Figure 4.1. This implies that the model is accurate enough to be used for the simulation of steady-state and dynamic situations.

Figure 4.2 Shows model comparison for 28th August 2023 at 2 PM, which was selected as a representative one based on the following reasons:

i. All measured voltages (from SCADA) were below 115 kV, which is typical of daytime and peak regimes in the Rwandan grid.
ii. Generation of solar power plant Gigawatt was at the highest level; this model was used for the simulation of Solar Power Plant outage.

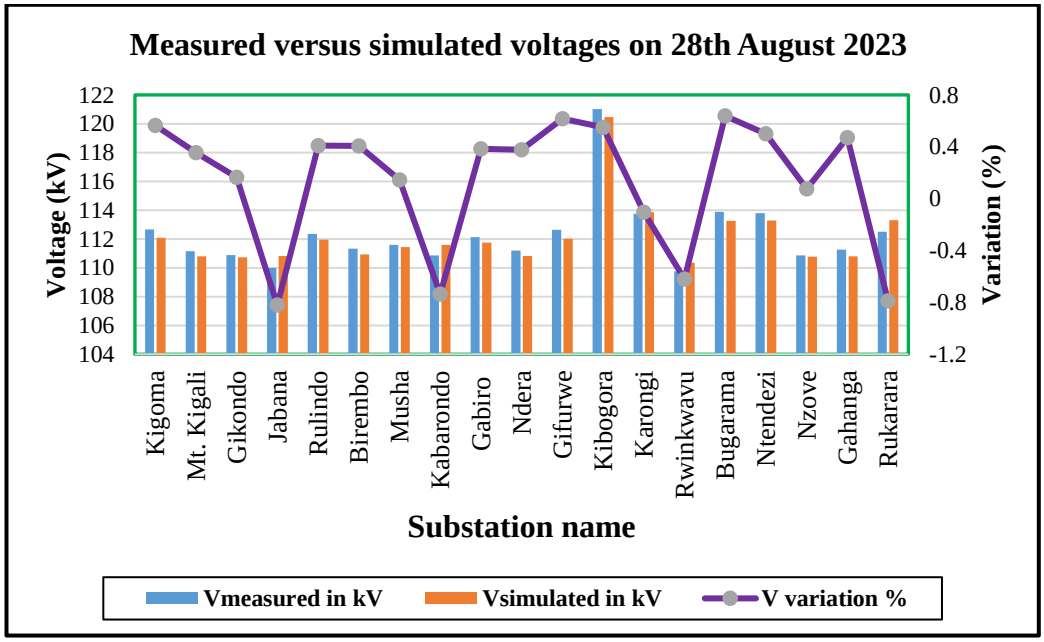

Figure 4.2: Comparison of Voltage Flow Simulation Results and Available Recordings

The comparison of power flow simulation results with available recordings of nodal voltages from SCADA for day time model shows a variation of less than 1%. The model can therefore be used for further simulations.

4.3 Steady-State Assessment of the Current Electricity Grid

The steady-state assessment of Rwanda's electricity grid involved the examination of various components and parameters in a static or balanced operating condition (normal operating conditions), where the system is in a stable equilibrium without significant transient disturbances. By performing a comprehensive steady-state assessment, the research established a baseline understanding of Rwanda's current electricity grid infrastructure performance across generation, transmission, and distribution systems. This information served as a foundation for further stability analyses (transient, frequency, voltage) which explored the grid's behaviour under dynamic conditions and potential disturbances.

This section hence describes results of steady state analyses using developed network simulation models of Rwandan power system. Load flow and contingency analysis are

performed for current system state for both peak and off – peak regimes. The steady-state load flows and contingency (n-1) will be performed for the defined scenarios based on the following planning criteria:

i. Loading of network elements: Under normal conditions and at steady state following single contingencies loading of all transmission equipment should not exceed 100% of the continuous rating. During contingency conditions loading should not increase up to the level of settings of overload protection which is a threshold justified by the fact that the equipment can stand this level for certain period (defined by protection engineers), in which the operator applies remedial actions for bringing the system back to a normal state.
ii. A contingency event is the unexpected failure or outage of a system component which includes; a) Single transmission line, b) Single transformer and, c) Single generator unit.
iii. Voltage profile analyses criteria based on defined voltage limits set in national grid code which is ± 10% voltage change at the steady state for full network topology and after a single contingency for 110 kV voltage level.

Rwanda power network has a "star"-like 110 kV grid although part of the network forms a ring from Jabana substation to Karongi substation via Birembo, Shango and Kibuye substations as well as via substations Gikondo, Kigoma and Kilinda, as can be seen in Figure 1.1. There are radial branches that are connected to Jabana 1 and Birembo substations. As a consequence, many of the 110 kV line outages lead to the formation of islands and power supply interruptions. In these cases, the load demand of one island can only be supplied from the generators in the same island, in case that formed island is dynamically stable. Any deviation in power system balance is covered by regulating the generation in accordance with available reserves. If that is not achievable (not enough generation reserves), all demand is shed and complete island collapse.

Summary of the steady state analysis of network element loadings in Figures 4.1 and 4.2 shows that in the peak regime, there is no overloading of network elements and no voltages outside allowed limits for N-0 situations. For N-1 analysis, only one insecure

event occurred. The outage of one step-up transformer in Jabana2 TPP leads to overloading of the second parallel step-up transformer (136 % of rated capacity). The Transformer at Musha substation is loaded by 96% during the peak regime, which is so close to the limit. Steady state analysis for the Off-Peak shows that in the Off-Peak regime (N-0 situation) there were no overloading of network elements while there were voltage violations on almost all 110 kV busbars and a few 30 kV busbars.

4.3.1 Element Loading

By analysing the loading status of transmission lines and transformers during peak and off-peak regimes, the study assesses the capacity utilization and adequacy of grid components.

Loading of a system is critical for system stability. Assessments of the load flow results for peak and off-peak loading is shown in Figure 4.1 for transmission system and Figure 4.2 for transformers.

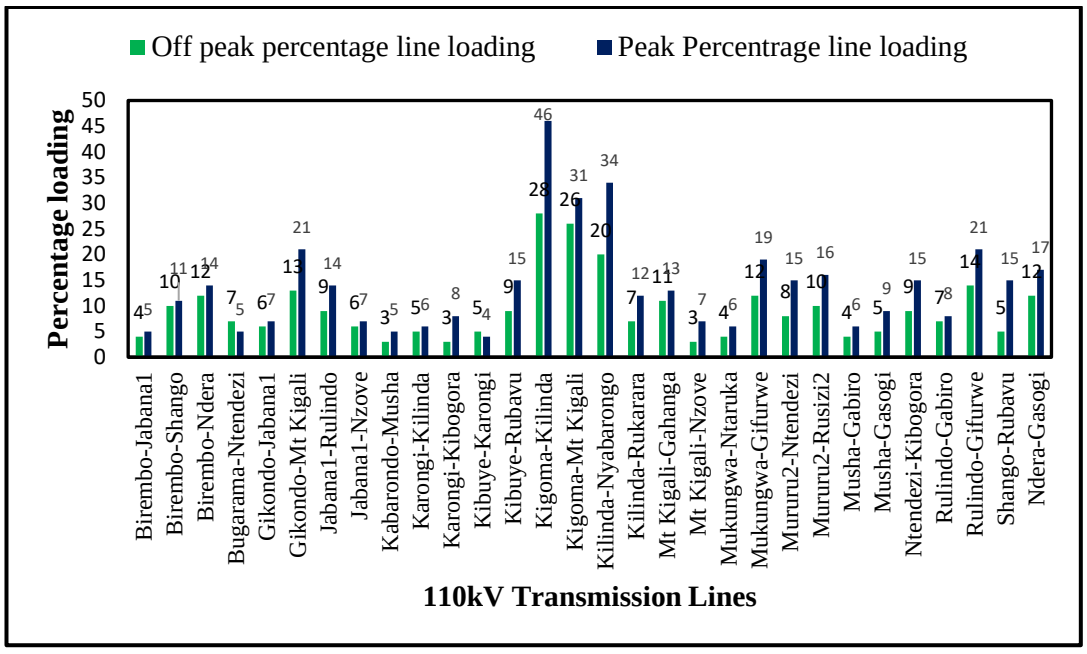

Figure 4.3: Peak and Off-Peak Loading of 110 kV Transmission Lines

Figure 4.3 shows that during off-peak regime, 110 kV lines in the system are lightly loaded, with a maximum loading of 25% on Kigoma – Kirinda line. This suggests

potential overcapacity in certain parts of the transmission network. During the peak regime, the system is loaded to almost two times the off-peak load with the highest being 46% of line capacity.

To further analyse the loading status of the network at different scenarios, the peak and off-peak loading of transformers at different substations is investigated as shown in Figure 4.3.

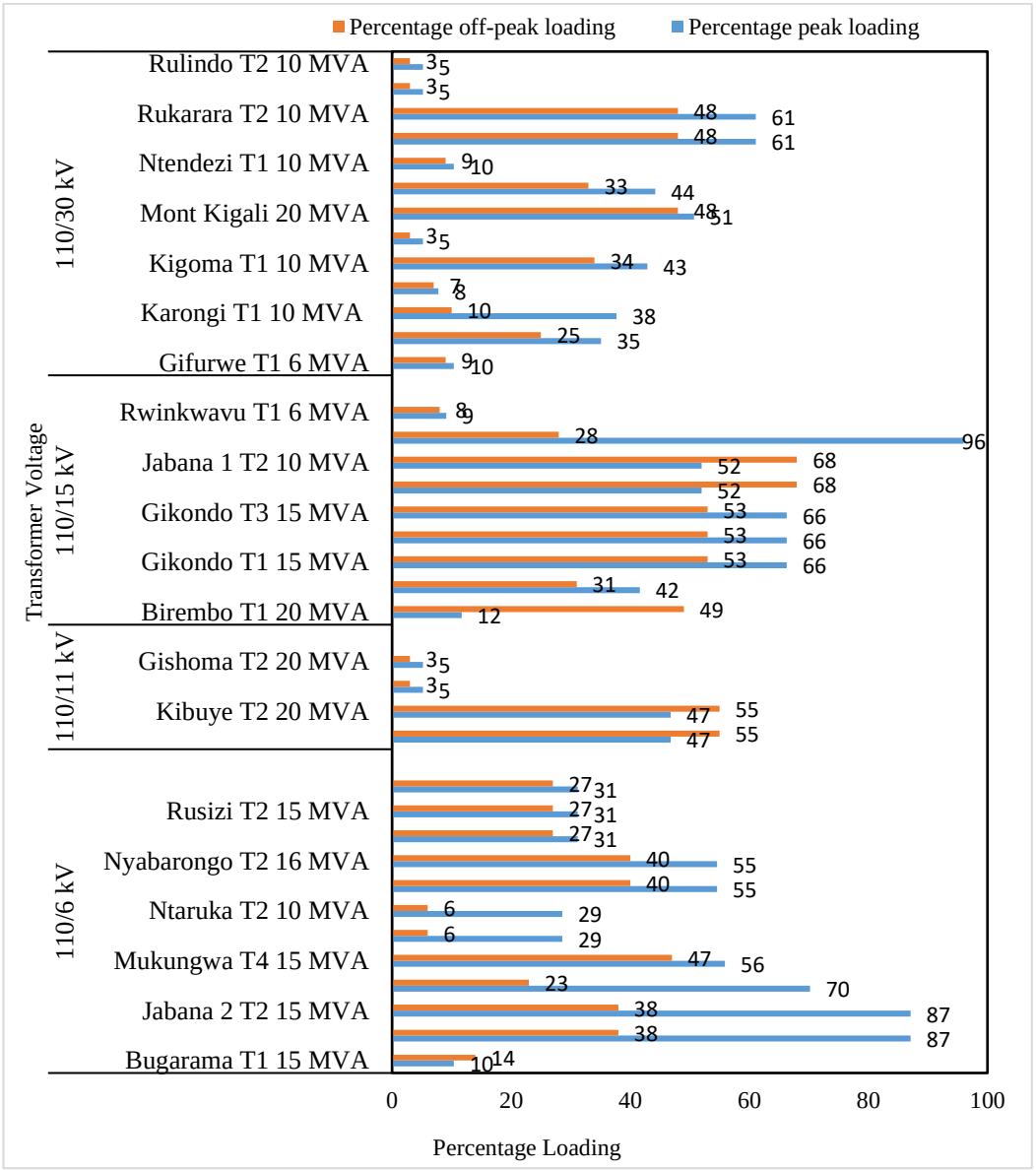

Figure 4.4: Loading of 110/X kV Transformers in Peak and Off-Peak Regimes

Figure 4.4 shows that for 110/X kV transformer loadings, there is lack of transformer capacity reserve in Jabana 1 TPP and Jabana 2 TPP which implies that one transformer gets overloaded when the second one trips or fails. At Musha substation, the single transformer operates very closer to the limit at 96% of the nominal transformer rating in normal operation state, respectively.

The loading results indicate that Rwanda's 110 kV transmission backbone is generally not thermally constrained under the analysed N-0 conditions, since the highest line utilisation remains relatively low (46% at peak and 25% off-peak). This pattern is typical of "capacity-adequate but operationally constrained" networks where instability is driven more by voltage/reactive power balance and topology sensitivity than by thermal overloads. However, the N-1 outcome revealing overloading of the remaining Jabana step-up transformer (136% when its parallel transformer is out) indicates a localised adequacy weakness at critical injection points, where redundancy is insufficient and a single outage forces abnormal power transfer through the remaining unit. The Musha transformer operating at 96% in peak conditions further signals limited margin, meaning even moderate load growth or contingency-driven power re-routing can push this node into sustained overloading. From a planning perspective, these findings justify prioritising (i) improved transformer redundancy at key generation injection substations (e.g., Jabana) and (ii) targeted reinforcement or operational constraints at high-utilisation transformers (e.g., Musha), rather than broad transmission re-conductoring, which is not supported by the observed low line loading levels.

The observed maximum loading on transmission lines and transformers indicates the extent to which these elements are being utilized, highlighting potential areas of overloading due to limited transformer reserves. This assessment provides crucial information for identifying investment needs and optimizing grid infrastructure to ensure reliable and efficient operation.

4.3.2 Voltage Profile

Figure 4.5 and Figure 4.6 show 110 kV and 30 kV system voltage at the different busbars, respectively. An examination of the voltage profiles at peak and off-peak

times provides information about the voltage stability of the grid and the effectiveness of its voltage regulation systems. This assessment guides the identification of voltage control strategies and the deployment of voltage compensation devices to mitigate voltage violations and ensure grid reliability.

During peak normal system operation state, voltages are within normal operating range as shown in Figure 4.5. Voltages are out of limits during off – peak regime due to light system loading. This is due to capacitive behaviour of the network (Ferranti effect) coupled with under-excitation limiters preventing generators and/or synchronous compensators from absorbing the excess reactive power (Dondariya and D.K.Sakravdia, 2021), (Obio and Mutale, 2015). In Rwanda's case, the instability is affiliated to the persistent inability of both generation and transmission system to operate below some load level. As a result, transformer tap changers cause long-term voltage instability due to various attempts to regulate system voltages.

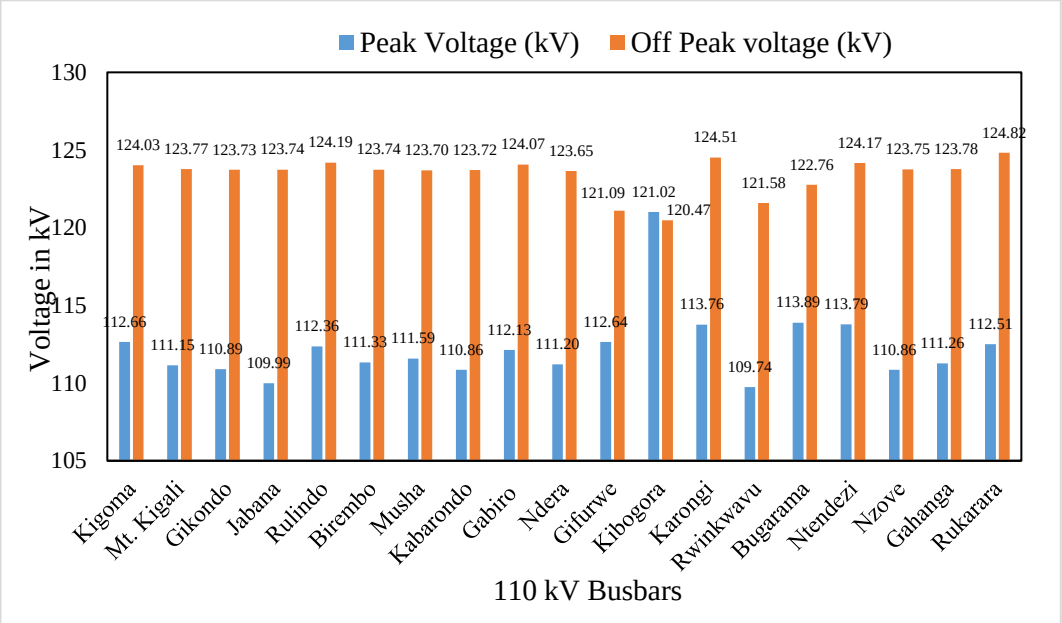

Figure 4.5: Voltage Profile of 110kV Bus Bars in Peak and Off-Peak Regimes

Figure 4.5 shows the voltages on all the 110 kV busbars, and it can be deduced that during off-peak, the system experiences high voltages above 120 kV. The observed off-peak overvoltage behaviour (voltages exceeding 120 kV on a nominal 110 kV network) is consistent with long, lightly loaded transmission corridors where shunt

capacitance becomes dominant (Ferranti effect), especially when the system lacks sufficient controllable reactive power absorption (e.g., generator under-excitation limits) (Dondariya and D.K.Sakravdia, 2021), (Yao et al., 2023). Importantly, this is not merely a "voltage quality" issue: persistent overvoltage increases insulation stress, accelerates equipment ageing, and can reduce protection coordination margins. Similar voltage-stability focused studies on large African transmission networks emphasise that weak reactive power management and poor VAr controllability are key drivers of voltage insecurity; (Olaogun et al., 2024), (Shahzad A. , 2022) report that introducing VAr compensation at defective/critical buses improves voltage magnitude and stabilises generator rotor-angle behaviour after faults.

In the Rwanda case, the implication is that mitigation should prioritise controllable shunt compensation (absorption during off-peak, injection during stressed periods), coordinated tap-changer control (to avoid long-term voltage instability loops), and operational rules that enforce minimum reactive absorption capability during low demand periods.

Figure 4.6 shows the voltage profile for the peak and off-peak scenarios in the 30kV distribution system.

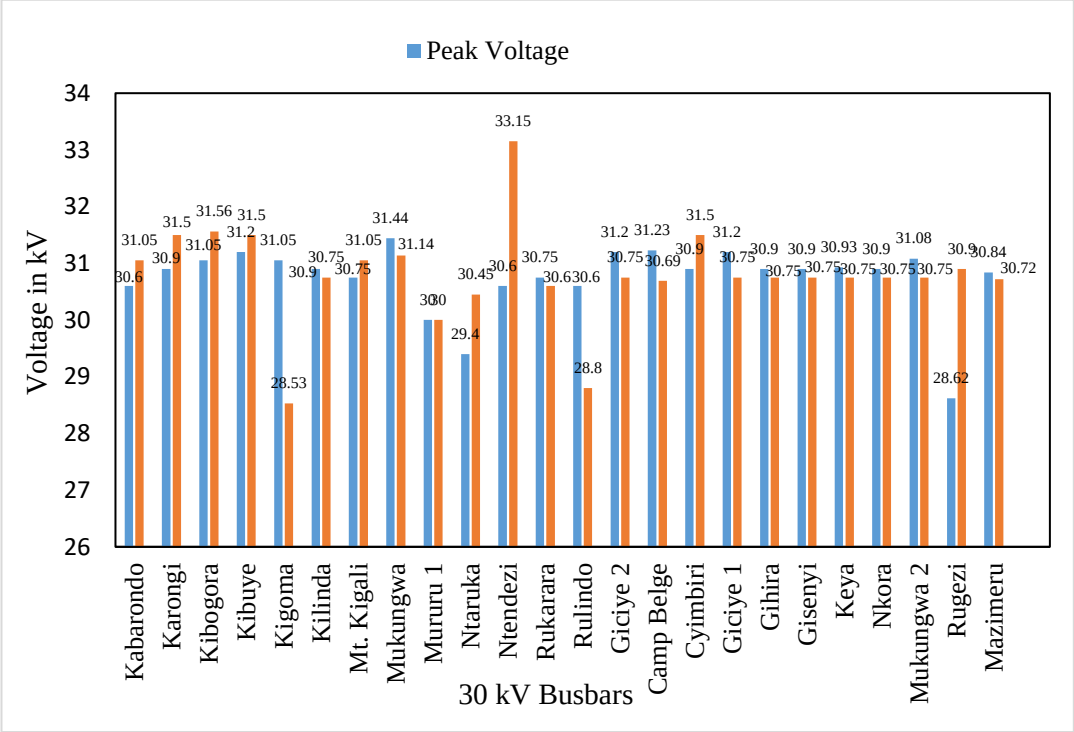

Figure 4.6: Voltage Profile of 30kV Peak and Off-Peak Regime

Figure 4.6 shows that for base case (N-0), voltage violation is observed on the 30 kV bus in SS Ntendezi – voltage in base case being 1.1037 pu, which shows that the transformer at these substations does not sufficiently regulate the voltage. The other voltages are below 32 kV and considered to be in operating ranges of ±10% on the buses.

The observed voltage violations exceeding 1.1 p.u (over 121 kV) indicate potential voltage instability issues, especially during off-peak periods when the system experiences high voltages.

Voltage contours for the 110 kV base case system simulated in PSS®E simulation are shown in Figures 4.7 and 4.8. It is observed that the 110 kV transmission system for both peak and off-peak regimes the voltages vary between 0.9 pu to 1.1 pu. This suggests a lack of reactive power compensation, leading to excessively high voltages across the grid.

In Rwanda's case, the instability is affiliated to the persistent inability of both generation and transmission system to operate below some load level. As a result, transformer tap changers cause long-term voltage instability due to various attempts to regulate system voltages.

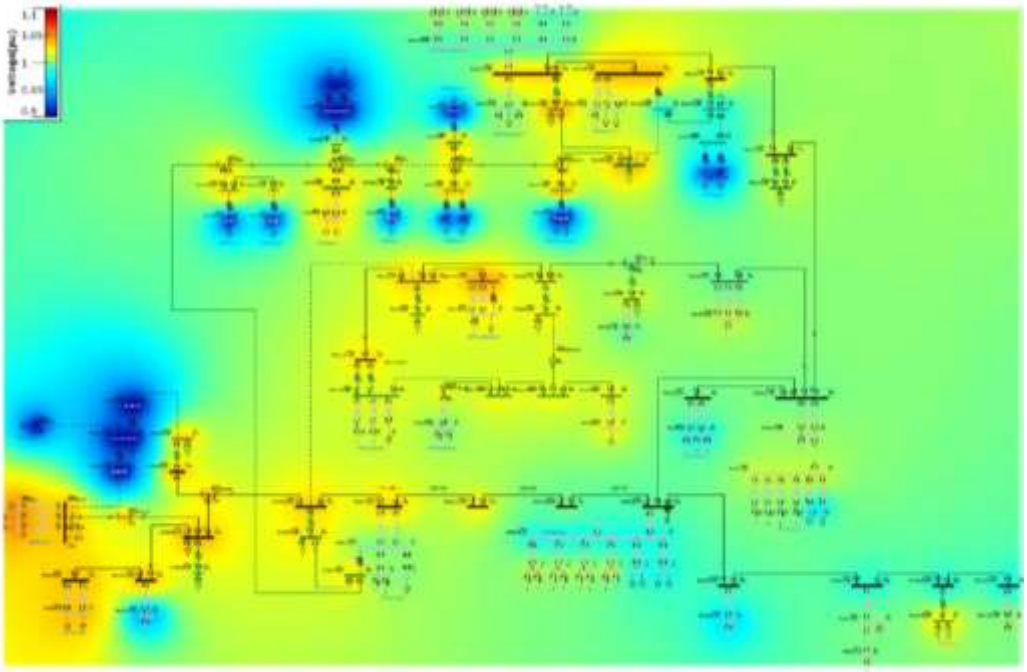

Figure 4.7: Voltage Contour Diagram in Peak Regime

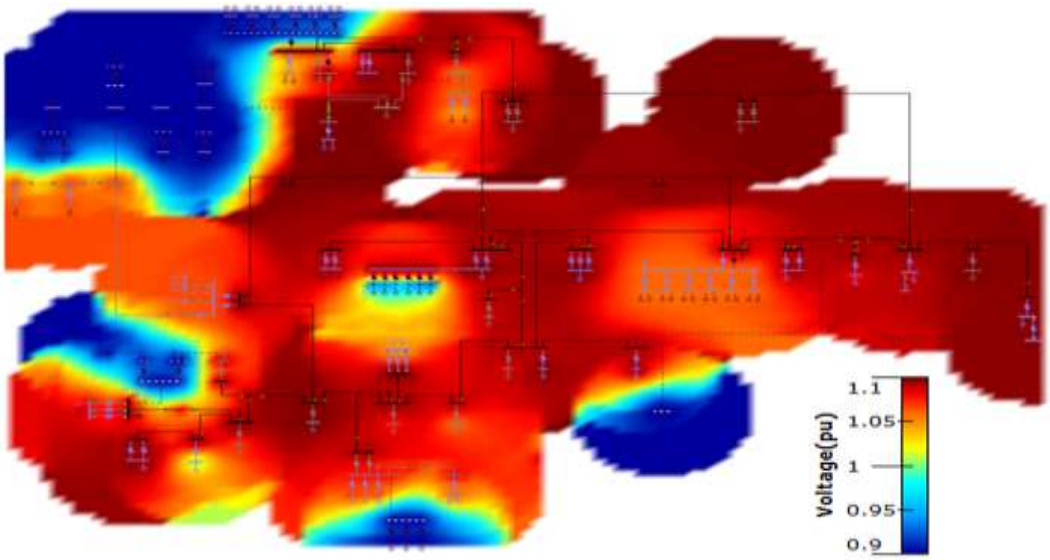

Figure 4.8: Voltage Contour Diagram in Off-Peak Regime

Figure 4.8 shows the contour diagram where most sections of the 110 kV transmission lines, with voltage exceeding 1 p.u (the normal 110kV operating voltage) as shown in the red sections of the figure. This is mainly due to the fact that the system is lightly loaded as shown in the figure without sufficient voltage compensation devices to absorb the excessive reactive power.

Taking voltage measurements from EUCL's SCADA for the period of February to April 2023 in a 15-minute interval at all 110 kV substations, it is observed that voltage violations are consistent in most areas as shown in Figure 4.9 with the highest being at Mukungwa substation.

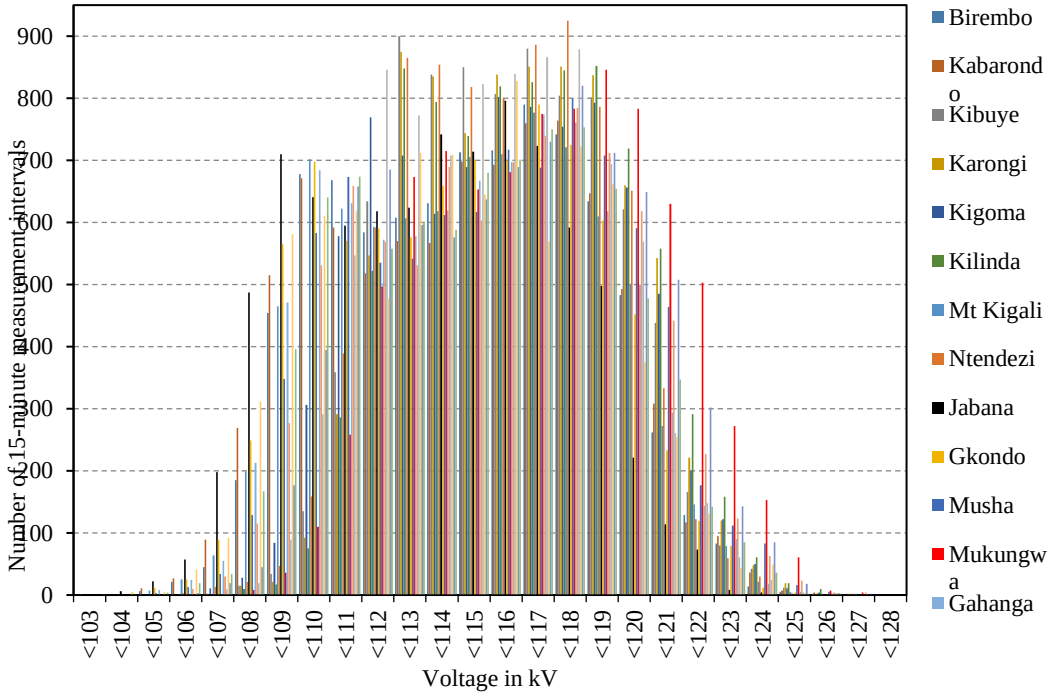

Figure 4.9: SCADA Voltage Measurements from Feb to April 2023

This 15-minute interval at all 110 kV substations, shows that the system is prone to rampart voltage violations.

These findings point to a possible vulnerability in the infrastructure of voltage control. Insufficient reactive power correction devices may result in equipment damage and voltage instability.

4.3.3 N-1 Security Assessment

The grid's resilience to single component outages, such as those involving transformers, generators, and transmission lines, is assessed by the N-1 security assessment. Understanding the major outages that cause network islanding or overloading of crucial components sheds light on the general security and dependability of the grid.

Contingency (N-1) analysis was additionally performed to assess the overall system security. As contingency events (outages) following cases were considered: single line outage, single transformer outage and single generator outage analysed for the peak

regime. The most severe outages are outages in 110 kV network that leads to islanded operation of Rwandan system and interruption of power supply due to radial structure of 110 kV network.

In the analysed cases, there is separation of one or more buses, and in some cases, islands are formed in such way that demand can be supplied from the local generation capacities in the island in case that frequency stability of the island is preserved. In order to assess the stability of the formed islands after the disturbances, additional dynamic analysis has to be conducted. These would take into consideration the type of generators which remain in individual islands, as well as the characteristics of the supplied load.

Beside outages that lead to network islanding, the lack of transformer capacity reserve in TPP Jabana 2 was noticed. One transformer in Jabana 2 TPP is loaded more than 87% of transformer rating in the normal system state. Outage of one transformer in Jabana 2 substation will cause overloading (loading above 100% of thermal rating) of the parallel transformer.

In addition, step-up transformers in Jabana 1 TPP have a lower rating than the corresponding generators and are overloaded in case of increased generation.

These findings highlight the grid's limited redundancy and potential cascading failures during outages. The radial structure and lack of transformer reserves leave the system susceptible to islanding and overloading under certain contingencies. The study, hence, evaluates the resilience of the grid's infrastructure by taking into account multiple contingency scenarios, which helps prioritize desired enhancements to increase grid redundancy and resilience.

4.4 Grid Dynamic Analysis

The analysis of the electricity grid's response to sudden disturbances and fluctuations in real operating conditions was made possible by the grid's dynamic behaviour, which dug deeper into the resilience and performance of Rwanda's electrical system under different operating settings. The grid's response to transient disturbances, frequency

variations, and voltage variations was thoroughly evaluated using dynamic modelling approaches, which shed light on the grid's resilience to unanticipated events and stable operation.

Through dynamic simulations, the frequency response of the grid under different operating conditions was analysed. Voltage stability analysis was also conducted to assess the grid's ability to maintain acceptable voltage levels under varying operating conditions.

4.4.1 Transient Stability Assessment

This dynamic simulation component evaluates the grid's resilience to significant disruptions, like short circuits or abrupt shifts in generation or load. By modelling the system's transient response using PSS®E, critical events can be analysed to determine the effectiveness of protective schemes, control strategies in preventing cascading failures.

Large-disturbance rotor angle stability, or transient stability, refers to the power system's capacity to sustain synchronism in the face of a severe disturbance, like a transmission line short circuit (Shahzad A. , 2022), (Ur Rehman et al., 2023). Large rotor angle excursions in the resultant system response are caused by the nonlinear power-angle relationship. If, following a significant disturbance, at least one generating unit fails (as in the case of a three phase short circuit), the system is deemed unstable. This criterion does not apply to generators or plants that continue to operate as an island because a faulty element has tripped (e.g., a single line that connects the generator/plant to the rest of the system is malfunctioning and has been disconnected), (Abakar et al., 2020).

The time frame of interest in transient stability studies is usually 3 to 5 seconds following the disturbance (Abakar et al., 2020), (Hatziargyriou et al., 2021). Critical Clearing Time (CCT) or Critical Fault Clearing Time (CFCT) is one of the indicators of the transient stability margin. It provides information on adequacy of switching equipment in faulted substations and dynamic stability system reserves. Calculations of CCTs are performed in order to determine influence of dynamic parameters used to

transient stability margin for the peak and off-peak regimes for 2023. Typically, CCTs are calculated at the start and finish of each HV line under consideration by simulating a three-phase failure with zero fault impedance (Glover et al., 2022).

The CCT value indicates the maximum time a fault can persist on the system before a generator loses synchronism and cascading failures occur. Higher CCT signifies greater transient stability margin, meaning the grid has more time to clear the fault before instability sets in.

Having in mind that outage of most transmission lines in Rwanda separates power system in two, approach for CCT calculation will be determined for the temporary faults at each 110 kV busbar. CCT is calculated for selected substations that are electrically close to connection spots of the HV line, i.e. HV bus bars which are the first order neighbours of connection spots of analysed lines.

The corresponding values of CCT obtained after various simulations in PSS®E while observing the critical generating unit that would be affected when a fault lasts for a specified duration are shown in the Table 4.1.

Table 4.1: Critical Clearing Time Values

110 kV busbar	Peak regime CCT and critical machine		off peak regime CCT and critical machine	
	CCT (ms)	**Critical machine**	**CCT (ms)**	**Critical machine**
Birembo	340	BIREMBO_G1	630	MUKUNGWA_G
Bugarama	400	RUSIZI2_G	240	RUSIZI2_G
Gasogi	700	JABANA2_G	1000	
Gifurwe	220	SOENERGY_G1	290	SOENERGY_G1
Gikondo	440	JABANA2_G	700	MUKUNGWA_G
Jabana 1	380	JABANA2_G	580	MUKUNGWA_G
Kabarondo	>1000		>1000	
Karongi	350	KIVUWATT_G	200	RUSIZI2_G
Kibogora	360	RUSIZI2_G	210	RUSIZI2_G
Kibuye	310	KIVUWATT_G	200	RUSIZI2_G
Kigoma	300	RUKARARA2_G	410	RUKARARA2_G
Kilinda	240	RUKARARA2_G	310	RUKARARA2_G
Mukungwa	190	SOENERGY_G2	250	SOENERGY_G1
Mururu 2	320	RUSIZI1_G	200	RUSIZI2_G
Ntendezi	340	RUSIZI1_G	210	RUSIZI2_G
Shango	530	JABANA2_G	480	RUSIZI2_G

110 kV busbar	Peak regime CCT and critical machine		off peak regime CCT and critical machine	
	CCT (ms)	**Critical machine**	**CCT (ms)**	**Critical machine**
Gishoma	450	RUSIZI2_G	260	RUSIZI2_G
Musha	>1000		>1000	
Rulindo	290	SOENERGY_G2	380	MUKUNGWA_G
Mt. Kigali	480	JABANA2_G	780	MUKUNGWA_G
Jabana 2	380	JABANA2_G	590	MUKUNWA_G
Rwinkwavu	>1000	-	>1000	-
Kibogora	360	RUSIZI2_G	210	RUSIZI2_G
Rubavu	420	KIVUWATT_G	230	RUSIZI2_G
Nyabarongo	320	RUKARARA2_G	340	NYABARONGO_G
Rukara	220	RUKARARA2_G	280	RUKARARA2_G
Ntaruka	240	NTARUKA_G	350	MUKUNGWA_G

The calculated CCT values for the Rwandan grid in Table 4.1, ranging from 190 ms at Mukungwa to over 1000 ms at Musha, are significantly higher than the 100 ms typical relay clearing time. A key interpretation of the CCT values is that Rwanda's grid shows a "protection-feasible" transient stability margin under the simulated operating conditions: even the lowest CCTs (e.g., 220 ms at Gifurwe in peak regime and 200–240 ms on several buses in off-peak regime) remain above typical first-zone protection relay clearing times (~100 ms), meaning that properly coordinated protection should clear most temporary faults before synchronism is lost. However, the dispersion in CCTs across busbars (≈200 ms to >1000 ms) also indicates that transient stability is spatially non-uniform and depends strongly on which generating units dominate the local electromechanical response (notably units around Rusizi 2 and other hydro/thermal plants listed as "critical machines"). This aligns with findings in transient-stability enhancement literature where weak/critical areas are those electrically close to major generation or constrained corridors.

This finding aligns with the study by (Abdourahimoun et al., 2025) on the Niger power grid, which established that maintaining CCTs above protection trigger thresholds is vital for weak grids integrating renewable energy. Similar to the findings of (Olaogun et al., 2024) on the Nigerian 330 kV grid, the critical machines (like those at Rusizi 2) exhibit the lowest stability margins, emphasizing that localized faults near low-inertia generation zones are the primary threats to synchronism.

The Rwanda model yields significantly larger CCTs (hundreds of milliseconds), which suggests that under the studied scenarios, the grid is not “fast unstable” but rather exhibits a transient stability margin compatible with conventional protection performance. The difference in absolute CCT magnitude across studies is expected because CCT depends on system strength, inertia distribution, network impedance, generator controls, and fault locations; therefore, the more important comparison is qualitative: both this study and (Olaogun et al., 2024) show that (i) there exists a critical clearing threshold beyond which synchronism is lost, and (ii) reactive power/FACTS-type support can increase the stability margin by improving voltage during and after faults.

4.4.2 System Voltage Response

Voltage stability is another key aspect addressed through dynamic simulation, focusing on the grid's ability to maintain acceptable voltage levels under changing operating conditions and contingencies. Voltage stability is threatened when a disturbance results into increase or decrease in the reactive power demand beyond the sustainable capacity of the available reactive power resources and load. It is therefore necessary to analyse the extent to which a system disturbance affects voltage limits and to understand the mitigation mechanisms (Anderson and Moore, 2013), (Valuva et al., 2023).

By modelling voltage profiles, reactive power flows, and system constraints, voltage stability analysis helps identify potential voltage collapse phenomena, voltage control strategies, and measures to enhance grid resilience. PSS®E's modelling features enable the investigation of voltage profiles, reactive power flows, and voltage stability margins, helping identify voltage collapse phenomena and voltage control strategies. In Figure 4.10 (a) and (b), loads consuming reactive power are automatically disconnected at Mururu 2, Bugarama and Nzove busbars while monitoring voltage at Mukungwa and Bugarama 110 kV busbars.

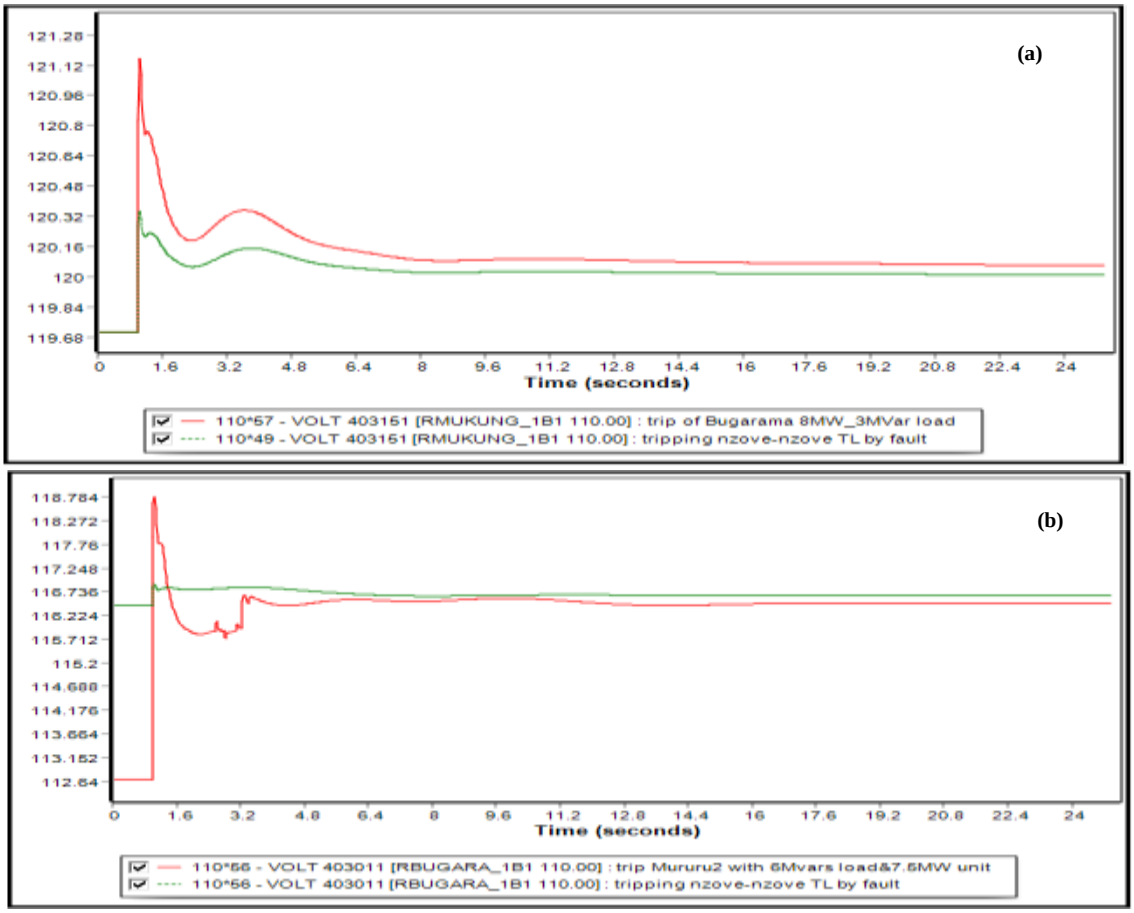

Figure 4.10: Voltage at (a) Mukungwa during Off Peak and (b) Bugarama during Peak after Tripping of Bugarama, Nzove and Mururu2 Loads

As per Figure 4.10 (a), outage of Bugarama load absorbing 3 MVAr pushes the voltage at Mukungwa busbar from 119.7 kV to over 121 kV for a system of nominal voltage as 110 kV. The simulated voltage rise at Mukungwa to 120.1 kV following a 3 MVAr load trip confirms a critical lack of reactive power support. This vulnerability mirrors the "critical bus" perspective discussed by (Onyegbadue et al., 2024), who found that radial, star-like topologies—much like Rwanda's 110 kV network—are highly susceptible to voltage instability during load fluctuations.

On the other hand, the voltage at the same busbar increases to 120.35 kV for a fault and tripping at Nzove – Nzove line. In either case the already high voltage further rises that it settles to 120.1 kV after 8 seconds. In Figure 4.10 (b), outage of Mururu 2 load absorbing 6 MVAr pushes the voltage at Bugarama 110 kV busbar from 112.7 kV to

over 118.8 kV for a system of nominal voltage of 110 kV whereas voltage on the same busbar increases to 116.8 kV for a fault and tripping at Nzove – Nzove line. The outage of Mururu 2 unit and affiliated load leads to a delay in voltage stabilization as more loads trip due to drop in frequency. The slow voltage recovery observed at Bugarama is consistent with (Ur Rehman et al., 2023), who demonstrated that without dynamic compensation, contingencies on an IEEE 39-bus system lead to prolonged settling times and potential voltage collapse.

The dynamic voltage responses show that the system's main challenge is not undervoltage collapse but rather overvoltage sensitivity under load/generation disturbances, especially during lightly loaded conditions. The rise of Mukungwa from 119.7 kV to above 121 kV and the prolonged settling time (~8 seconds to ~120.1 kV) indicates insufficient controllable reactive power absorption and slow effective damping of voltage excursions.

In operational terms, prolonged overvoltage can drive automatic disconnections, trigger protective trips, and increase the probability of cascading events when combined with frequency disturbances (as noted by the delayed stabilisation at Bugarama when Mururu 2 trips).

These voltage response results from the PSS®E simulations directly contribute to evaluating the voltage stability of the Rwandan electricity grid under various operating conditions, by bringing out the following aspects:

Voltage rise: Both figures depict voltage increases at the busbars following load tripping or line faults. This indicates a potential for voltage instability, especially considering the system's nominal voltage is 110 kV. The higher the voltage rise, the closer the grid is to exceeding safe operating limits.

Impact of reactive power consumption: Figure 4.10 (a) demonstrates a clearer voltage rise when a larger reactive power consuming load (Bugarama, 3 MVAr) trips compared to the Nzove-Nzove line fault. This suggests the grid might be deficient in reactive power support, causing voltage to rise upon the loss of a reactive power consuming element.

Voltage recovery time: Figure 4.10 (b) highlights the delayed voltage stabilisation at Bugarama busbar after tripping the Mururu 2 load. This indicates potential weaknesses in voltage regulation mechanisms. A longer recovery time suggests the grid might struggle to maintain voltage within acceptable limits during significant load changes.

Analysing these voltage responses, helps assess the Rwandan grid's ability to handle reactive power imbalances and voltage fluctuations under various operating conditions, including: load shedding, line faults and varying load conditions.

4.4.3 Frequency Stability Assessment

Dynamic simulation enables the evaluation of the grid's frequency response under varying operating conditions, including load variations, generation fluctuations, and disturbances (Saleh et al., 2024). Through detailed frequency stability analysis, the impact of these factors on grid frequency, frequency deviation, and stability margins can be assessed, providing insights into the effectiveness of frequency control mechanisms and grid synchronization techniques. The results provide insights into the grid's ability (or inability) to maintain frequency within acceptable limits under various operating conditions (peak vs. off-peak) and during disturbances (faults).

To ensure frequency stability in any transmission system, primary, secondary and tertiary control are relied on (Kroupa, 2012). Any electrical system must be able to handle instantly both changes in demand and outages in generation (as well as variations in renewable energy) and transmission, which preferably should not become noticeable to network users. Hence the amount of primary control reserve should be sufficient to buffer such load variations (Bashar, S., 2016). A system with limited and varying active power reserve as the one shown in figure 4.11 ends with a low inertia which result in frequency deviation from its nominal value.

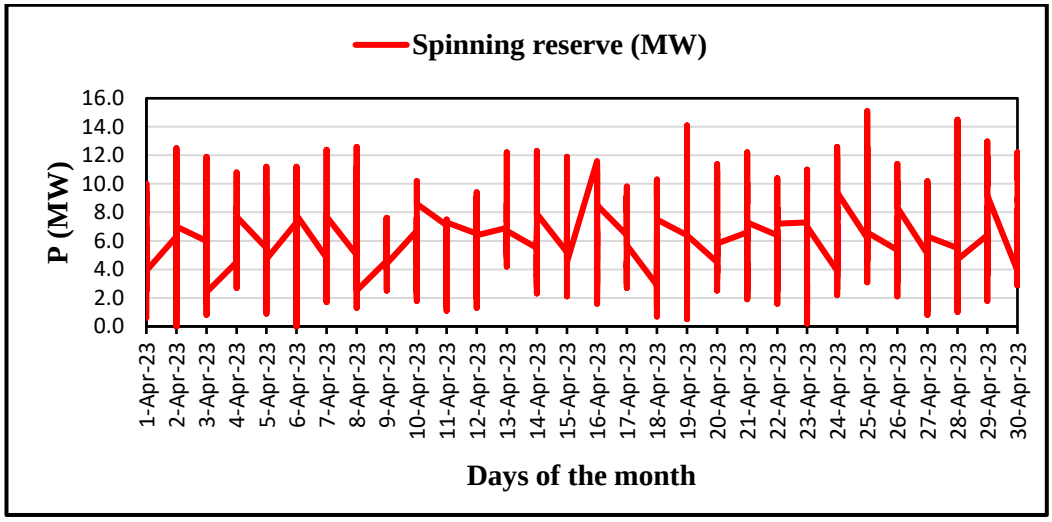

Figure 4.11: System Spinning Reserve in MW for the Month of April in the Rwandan Grid

Figure 4.11 shows that the amount of primary control reserve varies from 0 MW to 15 MW and for about 40% of analysed time, total system reserve was below 5 MW for an off-peak demand of 85.5 MW and peak demand of 232 MW. The variation of Rwandan system frequency between 49.1 Hz and 50.8 Hz indicates a severe lack of spinning reserve, which was found to be below 5 MW for 40% of the analysed period.

The inadequacy of system reserve, the rotating system inertia which counteracts large frequency excursions, is much smaller than in a large interconnected system. This indicates the grid's limited ability to respond to changes in power balance (generation vs. demand), making it susceptible to frequency deviations.

Furthermore, increasing penetration of non-dispatchable renewable energy sources in such systems, usually connected to the system by a stage of power converters, further reduces rotating inertia by substituting conventional generators. The dependence on non-dispatchable renewables further reduces inertia, worsening frequency response.

System frequency (hourly resolution) for the same period is shown in Figure 4.12 in the Rwandan grid obtained from SCADA. This month is taken into consideration since it’s a month the Rwandan system experienced a total blackout.

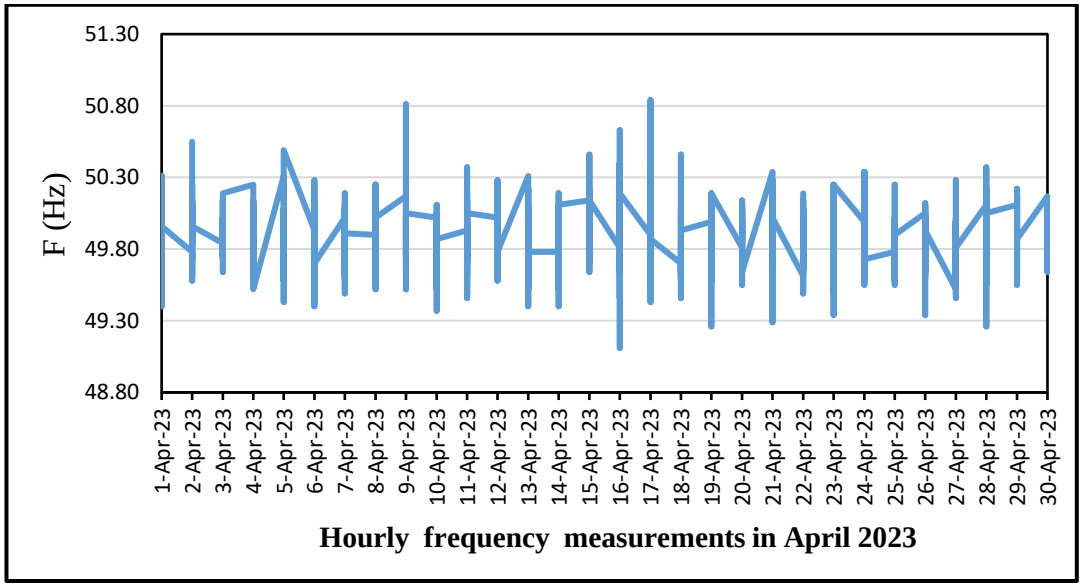

Figure 4.12: Hourly Frequency Measurements in April 2023

Figure 4.12 shows that the system frequency varies significantly throughout the analysed operational regimes between 49.1 Hz and 50.8 Hz due to low overall system inertia and lack of spinning system reserve. The variation of Rwandan system frequency between 49.1 Hz and 50.8 Hz indicates a severe lack of spinning reserve, which was found to be below 5 MW for 40% of the analysed period. This instability is directly comparable to the Zambian scenario studied by (Kanjelesa et al., 2023), where low system inertia and inadequate primary control led to total system collapse during generation loss. Kanjelesa et al. (2023) argued that static load shedding is often insufficient.

To further investigate the extent of system frequency response towards disturbances that occur, PSS®E simulation by applying faults on the transmission system and/or tripping of generators is done. Figure 4.13 (a) and (b) shows simulated frequency response during peak and off-peak regimes, respectively.

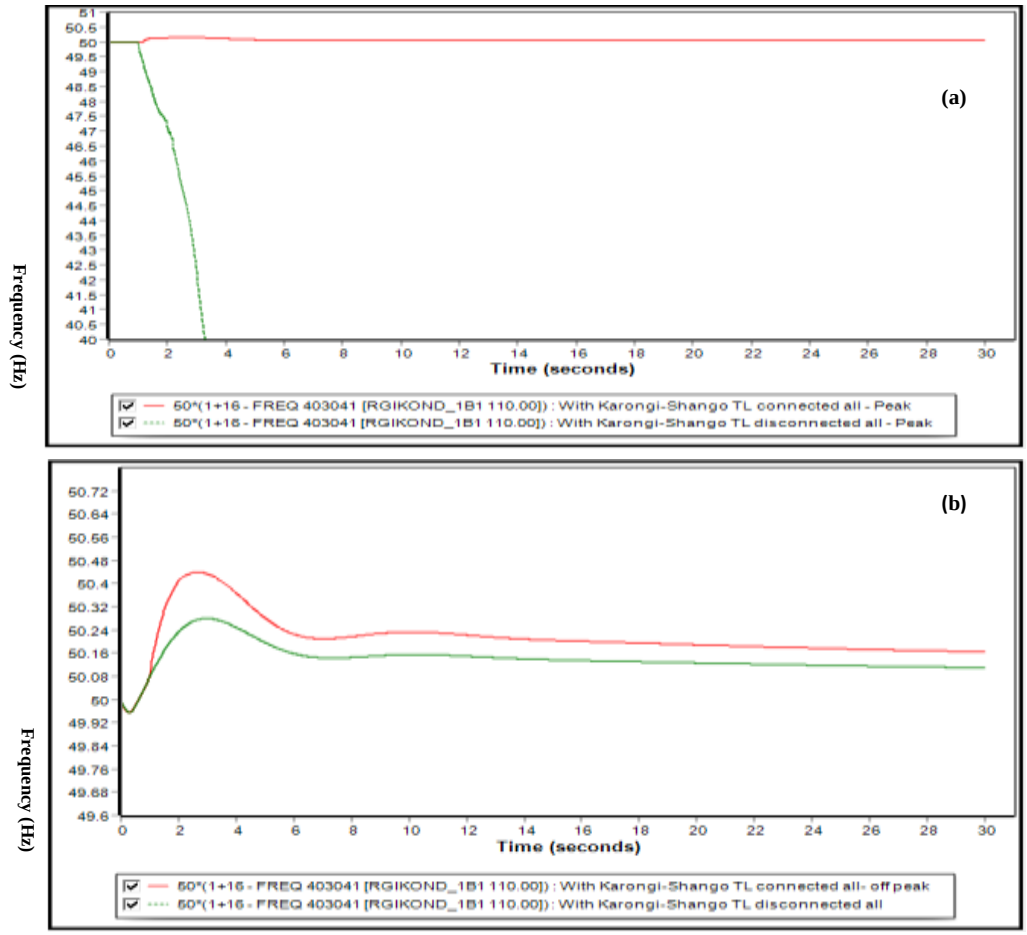

Figure 4.13: System Frequency for the Three-Phase Fault at the Beginning of the Line Kigoma - Kilinda, With and Without the 110 kV Line Karongi – Shango (a) Peak Load and (b) Off-Peak Load Regimes

Figure 4.13 (a) shows that during peak hours, when a fault is applied on Kigoma – Kilinda transmission lines while Karongi – Shango line is closed, frequency remains stable but when this section of the transmission system is open, the system frequency collapses. During off peak hours, occurrence of the same line tripping shown in Figure 4.11 (b), the system frequency rises and indication that some load trips hence generation exceeds demand but later stabilizers as governors of the other generators on grid regulate generation to balance with load requirements.

Peak hours as per Figure 4.13 (a) shows that when a fault occurs on Kigoma – Kilinda lines with the Karongi – Shango line closed, frequency remains stable. This suggests

sufficient capacity in the remaining lines to maintain power balance during peak demand. However, with the Karongi – Shango line open, the system collapses. This highlights the critical role of specific transmission lines in maintaining frequency stability during peak conditions.

Off-Peak Hours as per Figure 4.13 (b) shows that when a fault on the same line results in a frequency rise, indicating excess generation compared to demand. The subsequent stabilization suggests governor action on other generators to reduce generation and match demand. However, this response might be slow, leading to temporary frequency excursions.

The frequency results indicate a system operating with limited frequency containment capability, which is consistent with small-to-medium grids with low inertia and highly variable reserves. In April, the spinning reserve distribution (0–15 MW, with ~40% of the time below 5 MW) implies that credible contingencies (loss of a medium generator, PV ramp-down, or topology-driven islanding) can exceed primary reserve, causing frequency excursions outside a narrow operational band. The wide observed frequency range (49.1–50.8 Hz) further suggests that regulation and reserve scheduling are not consistently sufficient to maintain tight control.

Importantly, the simulated collapse when the Karongi–Shango line is open during a Kigoma–Kilinda disturbance demonstrates that frequency stability is tightly coupled to network topology and the risk of islanding, consistent with the thesis' earlier observation that many 110 kV line outages can form islands that may collapse if generation-reserve balance cannot be maintained.

The analysis demonstrates the grid's susceptibility to frequency deviations due to limited reserves, low inertia, and dependence on renewables. Specific vulnerabilities like critical transmission lines are also identified.

4.4.4 Impact of the Solar Plant to System Frequency

As solar energy is part of the generation sources in the Rwandan grid, assessment on the influence of variation of solar to the system frequency is simulated by considering the 8 MW plant in PSS®E and real time behaviour of this plant in SCADA is considered. Regime from 22nd August 2023 at 12 O'clock is selected as a representative since generation of solar power plant Gigawatt was at the highest level. This model is used for simulation of the solar power plant outage. According to operational experience, sudden drop in generation of the Solar Power Plant can initiate activation of the UFLS (Rwanda Energy Group, 2023). One blackout was initiated by sudden drop of the 8 MW Solar Power Plant and sudden increase of load at a 7 MW steel factory which both happened at the same time. Figure 4.14 shows active power generation trend of the solar plant during a clear day whereas Figure 4.15 shows active power variation during a cloudy day.

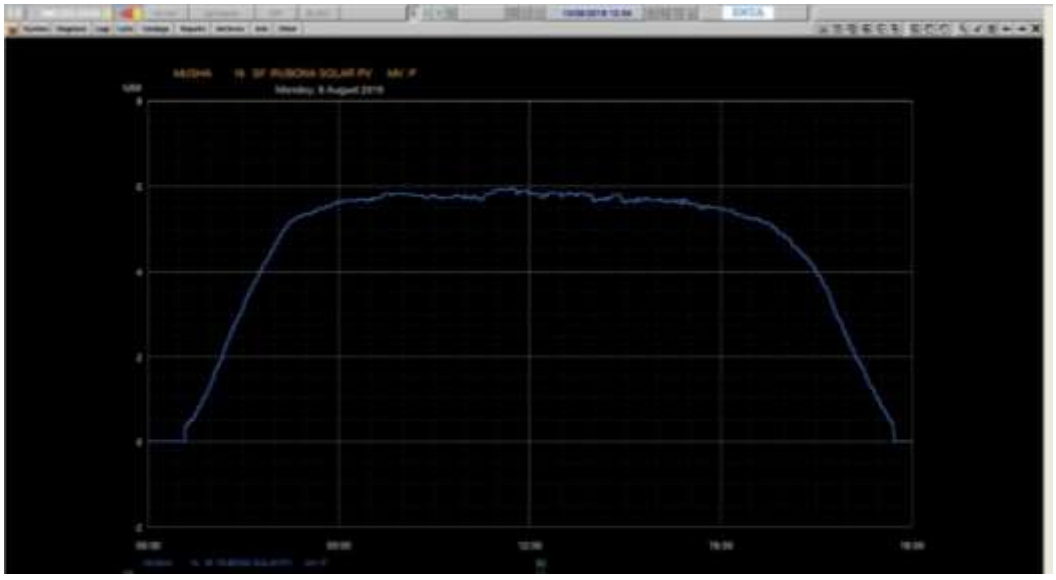

Figure 4.14: Generation Profile by 8 MW Solar Plant on a Clear Day

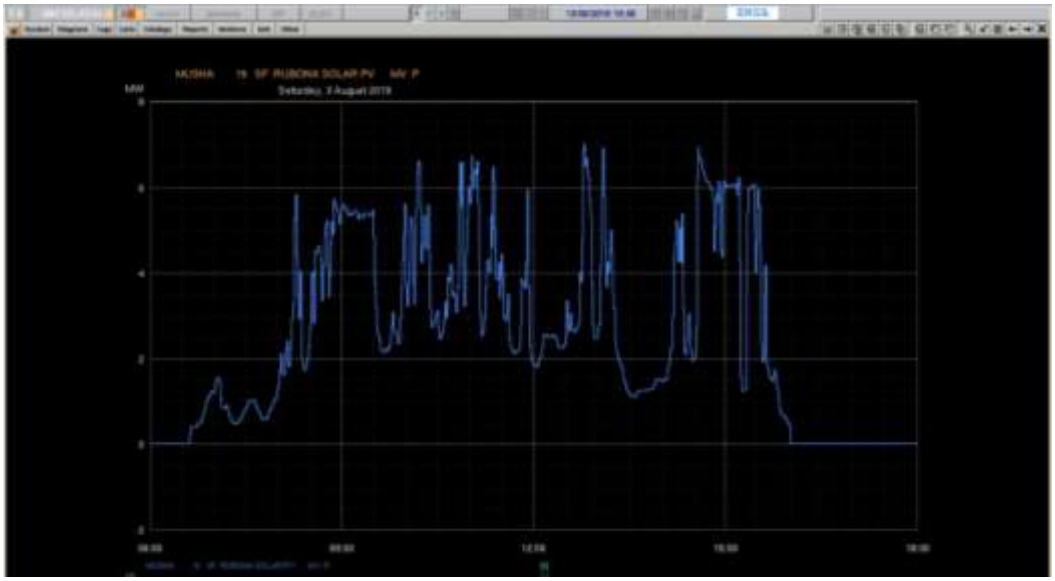

Figure 4.15: Generation Profile by 8 MW Solar Plant on a Clear Day

For selected date, total generation was 135.6 MW, total spinning reserve was 4 MW, while the solar power plant was generating 6.5 MW. As a disturbance, outage of 15 kV line connecting this plant to the grid at Musha substation is simulated and results shown in Figure 4.16.

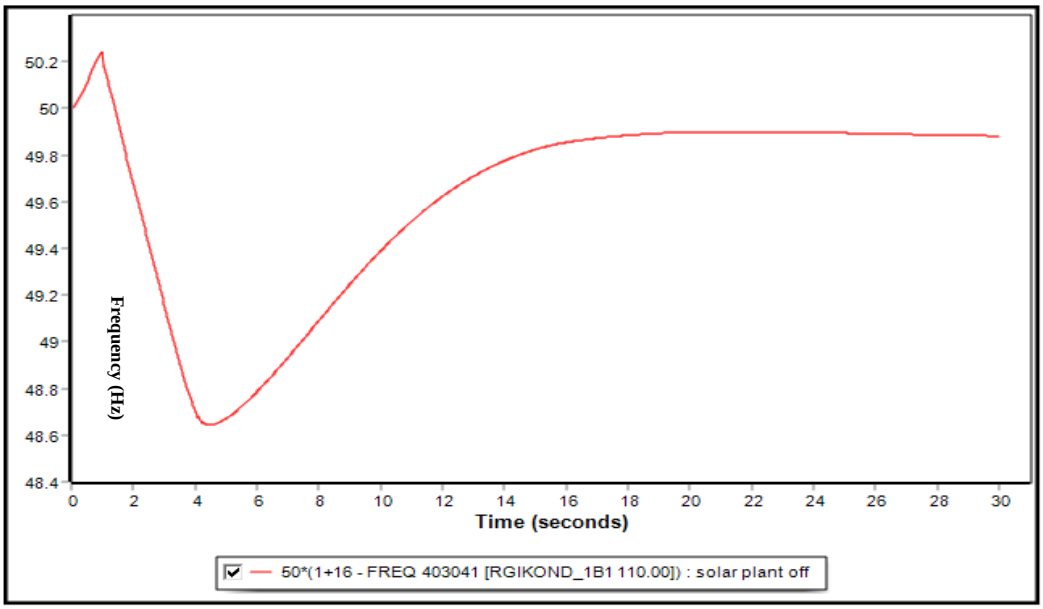

Figure 4.16: System Frequency after Outage Solar Power Plant

In Figure 4.16, due to the outage of the 15 kV line (evacuating power from the solar plant) and sudden loss of the solar power plant generating 6.5 MW, the system frequency declines, reaching 48.83 Hz. After activation of UFLS and shedding 2 MW of load, the system reaches new quasi-steady, and the frequency reaches 49.82 Hz. This shows that the Rwandan power system is able to cope with a sudden loss of the solar plant (which normally occurs as clouds cover the sun) generating 6.5 MW only if automatic load shading is done.

The solar-plant disturbance case quantifies the operational fragility created by low reserves relative to renewable variability. With total generation of 135.6 MW and spinning reserve of only 4 MW, the loss of 6.5 MW PV power exceeds available spinning margin, making UFLS necessary to arrest frequency decline (nadir 48.83 Hz) and restore a quasi-steady value (49.82 Hz after 2 MW shedding). The Rwandan grid's reliance on UFLS to stabilize at 49.82 Hz after a 6.5 MW solar drop highlights that current reserves cannot manage disturbances without customer interruptions. This indicates that the present reserve policy is not robust against credible PV contingencies during selected operating regimes, especially when the grid is already experiencing low inertia and constrained dispatchable headroom. Comparison to recent UFLS-focused work supports both the mechanism and the need for adaptive settings. (Kanjelesa et al., 2023), in the Zambian scenario, show that for large generation-loss contingencies, UFLS selection significantly affects frequency nadir and overshoot; their results indicate that 10% UFLS provided acceptable nadirs (about 48.3 Hz and 47.3 Hz for severe events) while improving recovery behaviour.

In Rwanda's case, the achieved nadir (48.83 Hz) is comparable in the sense that it remains above extreme collapse thresholds, but it is attained only after load shedding, implying that UFLS is acting as a primary containment substitute rather than a last resort. The practical implication is that Rwanda would benefit from (i) increasing spinning/fast reserves above the largest credible renewable drop, (ii) adding fast frequency response (battery/inverter-based response) where feasible, and (iii) reviewing UFLS settings toward more adaptive logic (e.g., ROCOF- or contingency-sensitive schemes), as recommended in UFLS literature.

This frequency response assessment provides valuable information for evaluating the Rwandan grid's resilience and performance concerning frequency stability. This is crucial for:

Enhancing system reserves: The analysis emphasizes the need for increasing active power reserves and exploring options like storage solutions to improve frequency regulation.

Optimizing generation mix: Considering the impact of renewables on inertia, strategies for balancing dispatchable and non-dispatchable generation sources can be explored.

Strengthening transmission system: Identifying critical transmission lines for frequency stability highlights the importance of grid upgrades or alternative line configurations.

Improving control mechanisms: The response time of governor controls can be optimized to ensure faster frequency regulation during disturbances.

4.5 Feasible Solutions to Counter Instability

4.5.1 Voltage Profile Stabilization

Based on the observations from the PSSE simulations, there are persistent overvoltage at various busbars that affects grid stability in that regard. A possible approach to stabilize voltage in the Rwandan grid, particularly the issues of overvoltage and delayed voltage stabilization following disturbances, several strategies can be implemented and validated through PSSE simulations. One effective approach can be the implementation of dynamic reactive power support using devices such as Static VAR Compensators (SVCs). The SVCs provide dynamic reactive power support by either absorbing or injecting reactive power into the grid as needed.

The SVCs are installed at busbars experiencing the highest voltages to ensure placement is optimal in maximizing effectiveness of the devices. Figures 4.17 and 4.18 show the impact of installing SVCs of different ratings at specific busbars

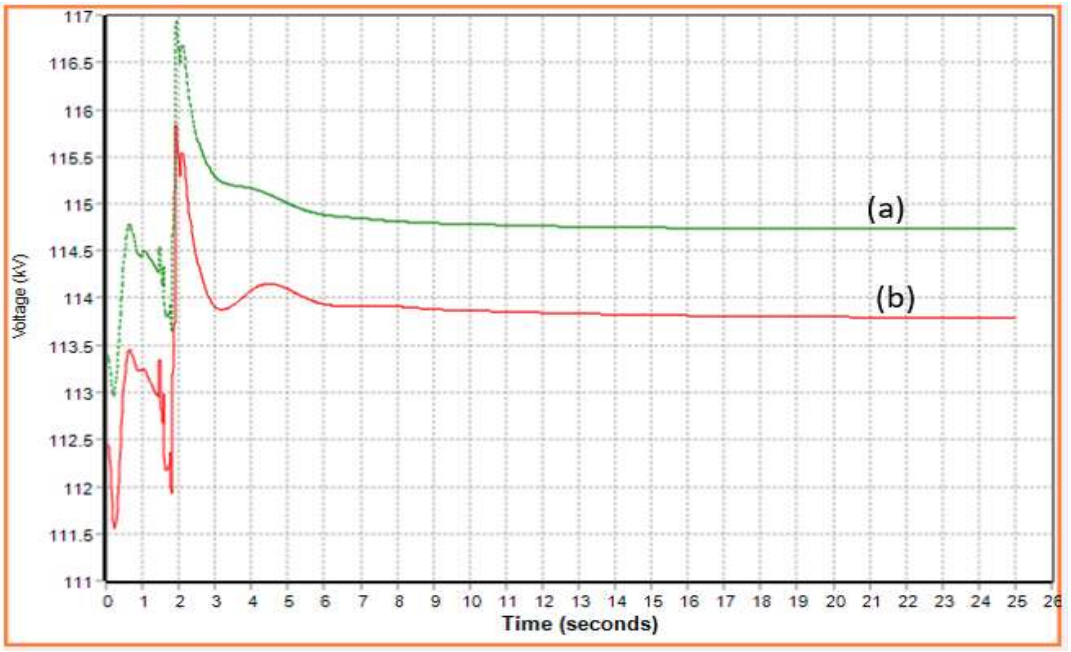

Figure 4.17: Voltage at (a) Bugarama and (b) Mukungwa 110 kV Busbars after Tripping of Bugarama Load, with -9 MVArs SVC Installed at Mukungwa Substation and -4.5 MVArs SVC at Ntendezi Substation

Figure 4.17 shows that the installation of a -9 MVARs SVC at Mukungwa substation and -4.5 MVARs SVC at Ntendezi substation, would reduce the voltage at Mukungwa and Ntendezi substations from 119.7 kV and 116.4 kV to 110.4 kV and 112 kV, respectively. These values, though closer to the Rwandan Transmission System operating voltage (110 kV), need further stabilization. Upon occurrence of a fault that trips a load consuming 3 MW and 1.6 MVArs, the voltage at both substations shoots up and eventually settles at values higher than (114.8 kV at Bugarama and 113.7 kV at Mukungwa) the pre-fault values, and takes 6 seconds to stabilize. However, the stabilization of the voltage at these busbars even after a fault indicates the positive role of the SVCs introduced in the network.

To test the appropriate SVC rating required, the one installed at Mukungwa is increased from -9 MVArs to -15 MVArs and the one at Bugarama from -4.5 MVArs to -5 MVArs as simulated in Figure 4.18.

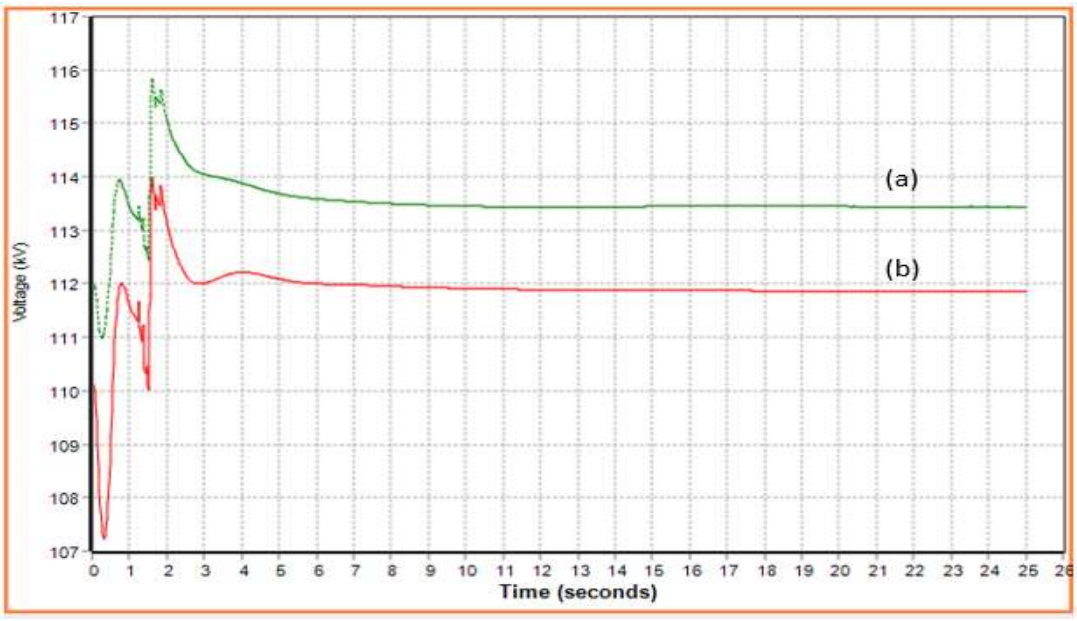

Figure 4.18: Voltage at (a) Bugarama and (b) Mukungwa 110 kV Busbars after Tripping of Bugarama Load, with -15 MVArs SVC Installed at Mukungwa Substation and -5 MVArs SVC at Ntendezi Substation

Figure 4.18 shows that with a -15 MVArs SVC installed at Mukungwa and a -5 MVArs SVC at Ntendezi, the post-fault voltages at both bars stabilizes faster (by 3rd second compared to 6 seconds earlier) and at lower values compared to the voltage results in Figure 4.17.

The implementation of a -15 MVAr SVC at Mukungwa reduced over-voltages from 119.7 kV to a stabilized 110.4 kV. This technical solution is supported by (Aikins and Amuzuv, 2020), whose research on the Ghanaian grid proved that SVCs are the most effective FACTS devices for absorbing excess reactive power during light-load "Ferranti effect" conditions. The study by (Onyegbadue et al., 2024) show that introducing VAr compensation at critical buses improves voltage magnitude and stabilises generator rotor-angle oscillations after faults, reinforcing the argument that voltage control and transient stability are coupled through reactive power support.

Similarly, (Olaogun et al., 2024) report that STATCOM compensation improves voltage magnitudes into acceptable ranges and extends critical fault clearing time by reactive power injection near the disturbance location.

The Rwanda grid simulation results align with this mechanism: adding shunt VAr absorption (SVC) reduces the pre-fault overvoltage at Mukungwa/Ntendezi (119.7/116.4 kV down to 110.4/112 kV) and improves post-fault settling behaviour. A key engineering insight from Figures 4.17 and 4.18 is that SVC sizing affects both steady-state voltage positioning and dynamic recovery speed. Increasing the Mukungwa SVC from -9 MVAr to -15 MVAr and Ntendezi from -4.5 MVAr to -5 MVAr reduces settling time from about 6 seconds to about 3 seconds and yields lower post-fault voltages.

By optimizing SVC placement at Mukungwa and Ntendezi, the stabilization time was halved from 6 seconds to 3 seconds, validating the placement strategies suggested in regional literature. This demonstrates that feasible solutions for Rwanda should consider (i) appropriately sized shunt compensation at the most overvoltage-prone nodes, (ii) staged/controllable reactors or SVC/STATCOM for off-peak absorption, and (iii) coordinated voltage control settings (AVR set points, transformer tap control logic) to avoid reinforcing overvoltage during light-load regimes.

4.5.2 Frequency Stabilization

Review of the hourly frequency and the simulation in PSSE depict critical frequency variations during peak and off-peak hours to levels that cause total system blackout. This, highlights the need for improved frequency stability in the Rwandan grid.

One of the ways to keep frequency within limits during generation deficits and disturbances, without much investment in the network, is to utilize a well-coordinated (pre-defined) automatic load shedding scheme. However, this is normally a “last line of defence” in any power system, although the Rwandan grid falls back to this scheme whenever there’s loss of generation.

Considering the scenario of the 8 MW solar plant that frequently drops generation to zero, a generator unit of an equivalent capacity at a busbar in the same zone.

BY adding a generator unit and incorporating load shedding strategies in the model, we can analyse how this can strategically help maintain grid frequency within safe limits, preventing frequency collapse.

The response of system frequency and power at Nyabarongo HPP (the swing bus) is simulated to determine the extent to which the grid is affected by tripping of the solar plant (dropping to zero) with a 7 MW generator unit installed in the same zone. Figure 4.19 shows that with a generator unit installed, the drop in generating capacity of the solar plant doesn't cause load shedding or blackout, as explained in Figure 4.16, as the frequency is restored back to the desirable 50 Hz. The swing bus (main power plant) also stabilizes after 3 Seconds with unit 2 increasing generation by 0.4 MW only.

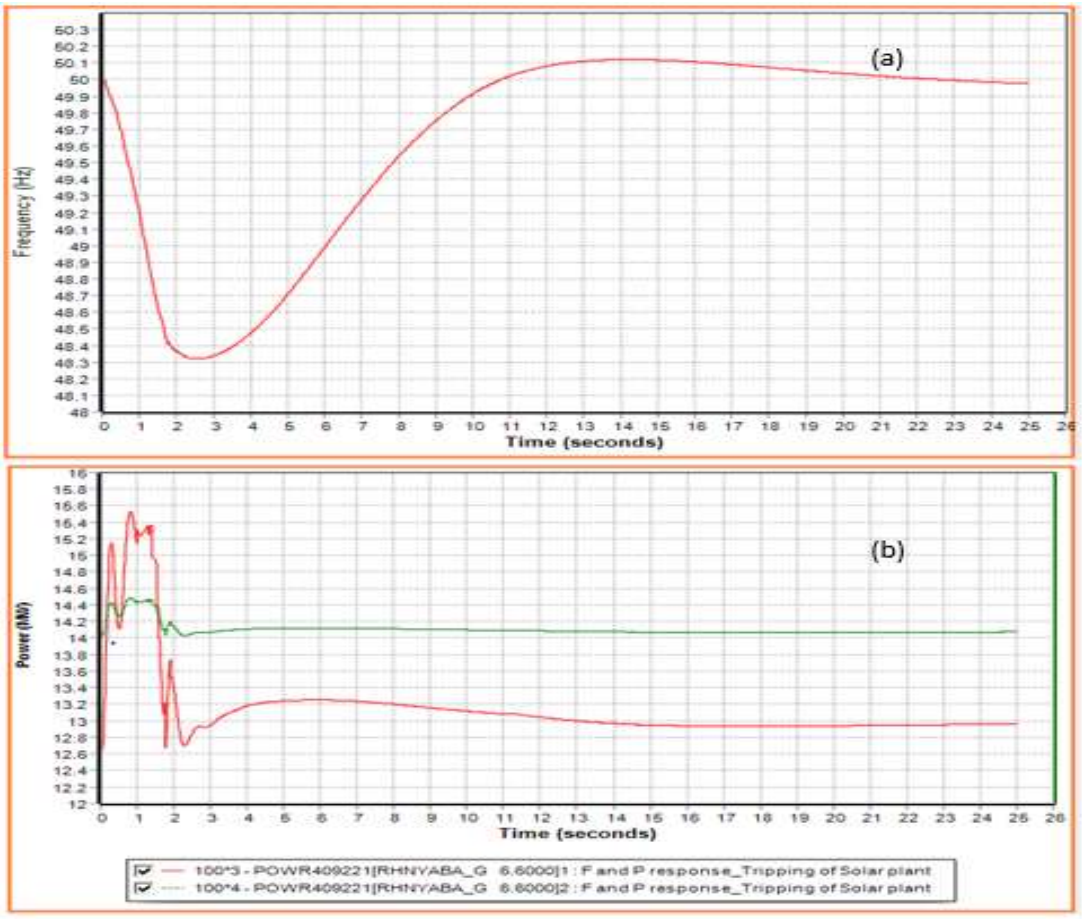

Figure 4.19: System Frequency Response (a) and Swing Bus Power (MW) Response (b) at Nyabarongo HPP

The frequency mitigation simulations demonstrate that reserve adequacy is the decisive factor for avoiding UFLS and blackout. In the PV-loss case, the system required UFLS to recover from a nadir of 48.83 Hz, confirming that existing spinning reserve (4 MW in the studied regime) is insufficient for a 6.5 MW contingency.

Installing a 7 MW generator unit in the solar zone restored frequency to 50 Hz without triggering UFLS, with the swing bus requiring only about 0.4 MW additional response and stabilising within ~3 seconds. This approach complements the findings of (Yao et al., 2023), who suggested that integrating localized demand response or distributed generation improves small-signal stability and frequency nadir. This supports a practical solution hierarchy: first, ensure minimum spinning/fast reserve coverage for the largest credible disturbance; second, deploy fast response resources (e.g., batteries/inverter controls) near renewable-rich areas; third, retain UFLS as a coordinated last defence but modernise it toward adaptive settings as recommended in recent UFLS research such as (Kanjelesa et al., 2023).

CHAPTER FIVE

CONCLUSIONS AND RECOMMENDATIONS

5.1 Conclusions

This study assessed the stability of Rwanda's electricity transmission network through steady-state and dynamic analysis in PSS®E, focusing on element loading, voltage performance, transient stability margins, frequency behaviour, and the impact of renewable variability. The conclusions are structured explicitly around the three specific objectives of the study to demonstrate how each objective has been addressed.

With respect to the first objective, which aimed to assess the current infrastructure of Rwanda's electricity grid encompassing generation, transmission, and distribution systems, the study established that the national grid is characterised by adequate transmission line capacity but exhibits localised infrastructure constraints at critical nodes. Steady-state power flow analysis shows that the 110 kV transmission network is generally lightly loaded, with maximum line utilisation of approximately 25% under off-peak conditions and 46% during peak demand, indicating that thermal limits of transmission lines do not presently constrain system operation. However, the infrastructure assessment revealed significant local weaknesses at key generation injection points and substations. Notably, the Musha transformer operates at approximately 96% of its rated capacity during peak conditions, and an N-1 contingency at the Jabana substation results in overloading of the remaining transformer to about 136% of its rated capacity. These findings indicate insufficient redundancy at critical transformer locations and highlight that infrastructure adequacy challenges in Rwanda's grid are concentrated at specific substations rather than across the transmission corridors.

In addressing the second objective, which sought to evaluate the performance of the Rwandan electricity grid under different loading scenarios using voltage, frequency, and transient stability studies, the study demonstrates that system performance varies significantly between peak and off-peak operating regimes and is strongly influenced by reserve availability and network topology. Voltage stability analysis reveals that,

while the system remains within acceptable voltage limits during peak loading, off-peak operation is characterised by widespread overvoltage, with several 110 kV busbars exceeding 120 kV. Dynamic simulations further show that voltage disturbances during off-peak conditions can persist for several seconds, with bus voltages such as Mukungwa rising from approximately 119.7 kV to above 121 kV and settling only after about 8 seconds. This indicates limited reactive power absorption capability and weak damping of voltage excursions under light-load conditions.

Transient stability analysis confirms that the grid possesses an acceptable transient stability margin under the simulated contingencies, with critical clearing times ranging from approximately 200 ms to over 1000 ms across different locations. All calculated critical clearing times exceed typical protection relay clearing times of around 100 ms, implying that temporary faults cleared by well-coordinated protection systems are unlikely to cause loss of synchronism. However, the wide variation in critical clearing times across the network indicates that transient stability strength is highly location-dependent and closely linked to the distribution of major generating units and network impedance.

Frequency stability assessment identifies frequency control as a key operational weakness of the grid. Analysis of spinning reserve availability shows that total reserve varies between 0 MW and 15 MW, with approximately 40% of the analysed period having less than 5 MW of reserve. This insufficient reserve margin leads to wide frequency excursions, with recorded and simulated values ranging from approximately 49.1 Hz to 50.8 Hz. Dynamic simulations further demonstrate that frequency stability is highly sensitive to network topology; disturbances that are survivable under intact network conditions can lead to system collapse when key transmission corridors are unavailable, indicating a strong coupling between topology, islanding risk, and frequency stability.

Regarding the third objective, which focused on identifying and evaluating appropriate operational and network reinforcement measures for improving power system stability, the study confirms that targeted interventions can significantly enhance both voltage and frequency stability. Reactive power compensation using shunt devices was

shown to be an effective solution for mitigating off-peak overvoltage and improving post-disturbance voltage recovery. The installation of static var compensators rated at −9 MVAr at Mukungwa and −4.5 MVAr at Ntendezi reduced steady-state voltages from approximately 119.7 kV and 116.4 kV to about 110.4 kV and 112 kV, respectively. Increasing the compensator ratings to −15 MVAr and −5 MVAr further improved dynamic performance by reducing voltage settling time from about 6 seconds to approximately 3 seconds following disturbances.

For frequency stability, the study demonstrates that improving reserve adequacy is critical to reducing reliance on under-frequency load shedding. In the case of solar generation loss, where a 6.5 MW photovoltaic output was lost while the system had only 4 MW of spinning reserve, system frequency dropped to 48.83 Hz and required the shedding of 2 MW of load to recover to approximately 49.82 Hz. In contrast, the introduction of a 7 MW generating unit in the affected zone eliminated the need for load shedding and restored frequency toward the nominal value of 50 Hz, with the swing bus stabilising within approximately 3 seconds using an additional response of about 0.4 MW. These results confirm that increasing fast-acting local generation or reserve capacity is an effective and feasible measure for improving frequency stability in Rwanda's grid.

In brief, the study concludes that Rwanda's electricity grid is structurally adequate at the transmission level but operationally constrained by localised infrastructure weaknesses, limited reactive power controllability, low reserve margins, and sensitivity to network topology. While the grid exhibits sufficient transient stability under the analysed contingencies, voltage and frequency stability challenges, particularly during off-peak operation and renewable generation variability pose significant operational risks. The evaluated mitigation measures demonstrate that targeted reactive power compensation, improved reserve management, and reinforcement at critical substations can substantially enhance system stability, thereby supporting reliable and secure operation of Rwanda's evolving power system.

5.2 Recommendations

Based on the study findings, the following recommendations are proposed to improve stability, prioritised according to the dominant issues identified (off-peak overvoltage, low reserves/frequency excursions, and local redundancy constraints):

- Deploy controllable reactive power absorption/support at critical buses (voltage control priority). Because off-peak voltages exceed 120 kV on the 110 kV network and dynamic events push Mukungwa above 121 kV with slow settling, Rwanda should prioritise controllable shunt compensation at buses with recurrent overvoltage signatures (e.g., Mukungwa/Ntendezi/Bugarama zones). The tested SVC ratings indicate that increasing compensation from -9 MVAr to -15 MVAr at Mukungwa and setting -5 MVAr at Ntendezi improves post-fault stabilisation time from ~6 s to ~3 s, therefore future planning should adopt compensation sizing studies as part of grid code compliance.
- Strengthen operating policy for reserves and introduce fast frequency response. Given that spinning reserve is frequently below 5 MW (~40% of the time) and that PV loss of 6.5 MW drives frequency to 48.83 Hz requiring UFLS, system operations should enforce minimum reserve thresholds that cover the largest credible contingency (including renewable drops) during vulnerable periods. Where thermal/hydro ramping is limited, fast frequency response resources (battery storage, inverter-based response, or local peaking units) should be considered, especially in zones with high renewable contribution.
- Modernise UFLS from “routine containment” to coordinated adaptive protection. UFLS should remain the last line of defence, but settings should be reviewed so that load shedding is triggered proportionally to event severity (e.g., ROCOF- or frequency-gradient sensitive logic), consistent with recent UFLS findings (Kanjelesa et al., 2023). This is important because the study shows UFLS is currently required for PV loss cases under low reserve (2 MW shed to recover from 48.83 Hz to 49.82 Hz).
- Improve redundancy at critical transformer injection points and manage near-limit transformers. Because the Musha transformer operates at 96% and Jabana N-1 leads to 136% overload on the remaining step-up transformer,

reinforcement should focus on transformer redundancy, parallel capacity upgrades, and operational constraints (e.g., limiting transfers during contingency states) to prevent sustained overloads.

- Prioritise topology-risk corridors and islanding preparedness. Since the grid's frequency stability can depend on whether key corridors (e.g., Karongi–Shango) are available, outage planning and maintenance scheduling should consider dynamic security impacts (not just steady-state flows). Where islanding is unavoidable, operating procedures should define minimum generation/reserve requirements for each island, and protection schemes should be reviewed to avoid uncontrolled island collapse.

This study provides a valuable foundation for further research on improving Rwandan grid stability and such areas include:

i. Investigate the impact of higher penetration levels of renewable energy on grid stability, and develop innovative strategies to enhance resilience, such as incorporating battery storage systems and demand response programs.
ii. Investigate the integration of advanced control schemes, such as Wide-Area Monitoring Systems (WAMS), to enhance grid management and stability.

REFERENCES

Abakar. Djibrine, A.A. Abouelsoud1, S.J. Michael and S.Simiyu. Sitati. et al. (2020). Transient Stability Analysis of the multimachine power system using ETAP software. *International Journal of Electrical and Electronics Engineering Studies, 6*(2056-5828), 1-12. Retrieved from https://www.eajournals.org/wp-content/uploads/Transient-Stability-Analysis-of-the-Multimachine-Power-System-Using-ETAP-Software.pdf

Abdourahimoun et al. (2025, March). Stability Study of a Power Grid Integrating a Photovoltaic (PV) Power Plant Using PSS/E. *Journal of Scientific and Engineering Research*, 51-58. Retrieved from https://jsaer.com/download/vol-12-iss-6-2025/JSAER2025-12-6-51-58.pdf

Adeleke. Aderibigbe, A. F. (2022). Impact of Distributed Generations on Power Systems Stability: A Review. *IEEE Nigeria 4th International Conference on Disruptive Technologies for Sustainable Development* (pp. 2-5). Nigeria: IEEE. doi:10.1109/NIGERCON54645.2022.9803062

Aikins and Amuzuv. (2020, June). Power System Stability Improvement of Ghana's Generation and Transmission System Using FACTS Devices. *Journal Electrical and Electronic Engineering, 8*(2), 47. Retrieved from https://www.researchgate.net/publication/342891704_Power_System_Stability_Improvement_of_Ghana's_Generation_and_Transmission_System_Using_FACTS_Devices

Al-Azzawi and Alturk. (2024, June). Frequency stability challenges with renewable energy systems. *International Journal of Applied Sciences and Technology, 6*(2), 42-51. doi:10.47832/2717-8234.19.9

Anderson and Moore. (2013). *Handbook of Electrical Power System Dynamics.* IEEE Press Editorial Board. Retrieved July 2022, from https://www.researchgate.net/profile/Lucian_Toma2/publication/278319669_Handbook_of_Electrical_Power_System_Dynamics_Modeling_Stability_and_Control/links/5f32922aa

6fdcccc43bf50ed/Handbook-of-Electrical-Power-System-Dynamics-Modeling-Stability-and-Control.

Baleboina and Mageshvaran. (2023, November). A survey on voltage stability indices for power system transmission and distribution systems. *Frontiers in Energy Research Front*, 18-23. doi:10.3389/fenrg.2023.1159410

Bayliss and Hardy. (2007). *Transmission and Distribution Electrical Engineering.* Newness. doi:10.1016/B978-0-7506-6673-2.X5000-9

Colorado State University. (2016). *Introduction to PSS/E*. Colorado: Colorado State University. Retrieved March 20, 2019, from https://www.engr.colostate.edu/ECE461/labs/lab1_PSSEIntroduction.pdf

Dondariya and D.K.Sakravdia. (2021, October). A comprehensive investigation on voltage stability indices for distributed generation placement and sizing. *IEEE Journal of Electrical and Electronics Engineering, 16*(5), 34-43. doi:10.9790/1676-1605013443

Glavic and Greene. (2022, September). Voltage Stability in Future Power Systems. *Elsevier*, 209-223. doi:10.1016/B978-0-12-821204-2.00141-0

J. Duncan Glover, Muluktla S. Sarma and Thomas J. Overbye. (2022). *Power System Analysis and Design.* Chris Carson. Retrieved March 12, 2023, from https://web.nit.ac.ir/~shahabi.m/M.Sc%20and%20PhD%20materials/Power%20System%20Transient%20Analysis%20Course/Books/Power%20System%20Analysis%20and%20Design%20by%20Glover%20and%20Sarma_4thed.pdf

Gourav J. Duncan., Muluktla S. Sarma and Thomas J. Overbye. (2020). A Comprehensive Survey on Real-Time Voltage Stability Assessment for Power Systems. *IEEE International Conference on Industrial and Information Systems*. New Delhi: IEEE. Retrieved from https://www.researchgate.net/publication/346143382_A_Comprehensive_Survey_on_Real-Time_Voltage_Stability_Assessment_for_Power_Systems

Hatziargyriou. N, J. V. Milanović and C. Rahmann. (2021, July). Definition and Classification of Power System Stability Revisited & Extended. *IEEE Transactions on Power Systems*, 3271-3281. doi:10.1109/TPWRS.2020. 3041774

Kanjelesa. Fred, Anthony., Chobela. Mumba., Kabwe. Mulenga., Clement. Siame and Pitshou Ntambu Bokoro.. (2023). Improving stability through adaptive Under-Frequency Load Shedding: the Zambian Scenario. *31st Southern African Universities Power Engineering Conference* (pp. 6-8). Pretoria: ZESCO. Retrieved from https://www.researchgate.net/publication/369 108785_ Improving_Stability_Through_Adaptive_Under-Frequency_Load_ Shedding_the_Zambian_Scenario

Kazemi and Ansari. (2022, January). An integrated transmission expansion planning and battery storage systems placement - A security and reliability perspective. *International Journal of Electrical Power & Energy Systems, 134*, 15-23. doi:10.1016/j.ijepes.2021.107329

Kothari and Nagrath. (2022). *Modern Power System Analysis.* New Delhi: Tata McGraw-Hill. Retrieved from https://gcebargur.ac.in/sites/gcebargur .ac.in/files/lectures_desk/MPSA-Sol.pdf

Kroupa, V. F. (2012). *Frequency stability, introduction and applications.* New Jersey: A John Wiley & Sons, Inc. Retrieved from http://www.iqytechnical college.com/BAE%20673-Frequency%20Stability.pdf

Kundur, Prabha. (1994). *Power System Stability and Control.* Newyork: McFraw-Hill, Inc. Retrieved October 2023, from https://dl.poweren.ir/downloads/ PowerEn/Book/2019/Jun/Power%20System%20Stability%20and%20Control %20-%20Prabha%20Kundur%20(PowerEn.ir).pdf

Lindner. Marco, Hans Abele, Christoph. John and Joachim. Lenher. (2022). Suitable Classification of Power System Stability Phenomena. *CIGRE Symposium. 37.*

Trondheim: CIGRE. doi:https://www.researchgate.net/publication/392853208_Suitable_Classification_of_Power_System_Stability_Phenomena

Mengqi Yao, S. R. (2023). Using demand response to improve power system small-signal stability. *Science direct, 36*, 3-7. doi:10.1016/j.segan.2023.101214

Obio and Mutale. (2015). A comparative analysis of energy storage and N-1 network security in transmission expansion planning. *50th International Universities Power Engineering Conference* (pp. 5-9). Stoke UK: IEEE. doi:10.1109/UPEC.2015.7339947

Ojha and Simkhada. (2022, July). Rotor Angle Stability of Synchronous Generator in Power System Network. *Elsevier*, 209-223. doi:10.13140/RG.2.2.32807.83366

Olaogun P. O., Adebisi O. I., Adejumobi I. A. and Adams D. O. (2024, February). Transient Stability Improvement on Power Network using Static Synchronous Compensator: A Case of The Nigerian 330 KV Electricity Grid. *Arid Zone Journal of Basic and Applied Research, 3*(2811-2881), 42-64. Retrieved from https://azjournalbar.com/wp-content/uploads/2024/03/42_64_TRANSIENT-STABILITY-IMPROVEMENT-ON-POWER-NETWORK-USING-STATIC-SYNCHRONOUS-COMPENSATOR-A-CASE-OF-THE-NIGERIAN-330-KV-ELECTRICITY-GRID.pdf

Onyegbadue. A. Ikenna, Stephen N. Ukagu and Dennis O. Okonkwo. (2024, December). Voltage Stability Assessment of Nigeria 330 kV Power Grid: A Critical Bus Perspective. *UNIZIK Journal of Engineering and Applied Sciences*, 1382 - 1401. Retrieved from https://www.researchgate.net/publication/386534406_Voltage_Stability_Assessment_of_Nigeria_330_kV_Power_Grid_A_Critical_Bus_Perspective

Rwanda Energy Group. (2023, March 15). *REG*. Retrieved May 2023, from Rwanda Energy Group: https://www.reg.rw/public-information/reports-plans/

Safdarian. Farnaz, Jessica L. Wert, Dalton Cyr and Thomas J. Overbye. (2024). Power System Resiliency and Reliability Issues from Renewable Resource Droughts. (pp. 1-6). Kansas: IEEE. doi:10.1109/KPEC61529.2024.10676081

Sajadi. Amirhossein, Jo Ann Rañola, M, Rick Wallace Kenyon, Bri-Mathias Hodge and Barry Mather. (2023, January). Dynamics and Stability of Power Systems With High Shares of Grid-Following Inverter-Based Resources: A Tutorial. *IEEE Access*, 1-2. doi:10.1109/ACCESS.2023.3260778

Salami, Y. (2017, October). *Multiple Contingency Analysis of Power Systems.* Retrieved April 15, 2023, from CORE: https://files01.core.ac.uk/ download/pdf/ 154914762.pdf

Saleh. Ahmed. Mohammed , Vokony. István, Muhammad. Waseem and Amgad. Naji. Ali. Ahmed. (2024, October). Power system stability in the Era of energy Transition: Importance, Opportunities, Challenges, and future directions. *Elsevier, 24*(100820), 6-13. doi:10.1016/j.ecmx.2024.100820

Sauer and Pai. (2006). *Power System Dynamics and stability.* Urbana: The University of Illinois at Urbana. Retrieved September 5, 2022, from https://courses.physics.illinois.edu/ece576/sp2018/Sauer%20and%20Pai%20 book%20-%20Jan%202007.pdf

Shahzad, A. (2022, August). A Comprehensive Review on Power System Risk-Based Transient Stability. *Journal of Electrical Engineering, Electronics, Control and Computer Science, 8*(4), 12-17. doi:10.48550/arXiv.2206.05113

Shahzad, U. (2021, November). A Review of Challenges for Security -Constrained Transmission Expansion Planning. *7*(24), 21-30. doi:10.4028/www.scientific. net/ AMM.818.129

Shrestha and Gonzalez-Longatt. (2021, August). Parametric Sensitivity Analysis of Rotor Angle Stability Indicators. *MDPI, 14*(16). doi:10.3390/en14165023

Siemens. (2017). *Siemens Global.* Retrieved February 12, 2018, from Siemens Global: https://assets.new.siemens.com/siemens/assets/api/uuid:480a532bff8def3f8531fff18f7ccf446001e685/siemenspti-software-psse-brochure-2017.pdf

Stevenson, W. D. (1995). *Elements of Power System Analysis.* London: McFraw-Hill, Inc. Retrieved July 20, 2022, from http://103.203.175.90:81/fdScript/RootOfEBooks/E%20Book%20collection%20-%202025%20-%20G/EEE/Power%20System%20by%20William%20D.%20Stevenson,%20Jr..pdf

The World Bank Group. (2024). *Pathways to Sustainable and Inclusive Growth in Rwanda" Country Economic Memorandum.* The world Bank Group. Newyork: The world Bank Group. doi:https://documents1.worldbank.org/curated/en/099112724132525970/pdf/BOSIB-5cce6743-e43b-4f27-8b9e-ad1c61b91a9f.pdf

Transpower Newzealand. (2024, December 14). *Transient Rotor Angle Stability.* Transpower Newzealand. Retrieved February 9, 2025, from Transpower New Zealand: https://static.transpower.co.nz/public/bulk-upload/documents/Transient%20Rotor%20Angle%20Stability%20Study.pdf?VersionId=_Ptqx6VD5.P7GP8QwssrXEGMK1KkcZNu

Ur. Rehman. Atta, Ajmal. Farooq, Imtiaz. Ahmad ,Shafiullah. Khan, Ihteshamul. Haq, Amir. Ayaz, Muhammad. Saad. (2023, August). Contingency analysis & voltage stability on IEEE 39-bus. *International Journal of Advanced Natural Sciences and Engineering Researches, 7*, 78-85. Retrieved from https://as-proceeding.com/index.php/ijanser/article/view/1339/1283

Ur. Rehman. Atta, Ajmal. Farooq, Imtiaz. Ahmad ,Shafiullah. Khan, Ihteshamul. Haq, Amir. Ayaz, Muhammad. Saad. (2023, August). Steady state contigency analysis of IEEE-39 bus system using PSS/E. *International Journal of Advanced Natural Sciences and Engineering Researches, 7*, 78-85. Retrieved from https://scispace.com/pdf/steady-state-contingency-analysis-of-ieee-39-bus-system-12j1wjkn9l.pdf

Valuva. Chandu, Subramani. Chinnamuthu, Tahir. Khurshaid and Ki-Chai Kim. (2023, July). A Comprehensive Review on the Modelling and Significance of Stability Indices in Power System Instability Problems. *MDPI, 16*, 25-32. doi:10.3390/en16186718

Van Cutsem and Vournas. (2008). *Voltage Stability of Electric Power Systems.* Springer Science+Business Media, LLC. Retrieved November 18, 2022, from https://download.e-bookshelf.de/download/0000/0023/25/L-G-0000002325-0002332165.pdf

APPENDICES

Appendix I: Research Approval Letter

JOMO KENYATTA UNIVERSITY
OF
AGRICULTURE AND TECHNOLOGY
DIRECTOR, BOARD OF POSTGRADUATE STUDIES

JKUAT
www.jkuat.ac.ke
P.O. Box 62000-00200, NAIROBI
03 SEP 2019
INSTITUTE OF ENERGY AND ENVIRONMENTAL TECHNOLOGY
RECEIVED

P.O. BOX 62000
NAIROBI – 00200
KENYA
Email: director@bps.jkuat.ac.ke
TEL: 254-067-52711/52181(6114)
FAX: 254-067-52164/52030

REF JKU/2/11/ EET31-C010-5036/2014 **29th August 2019**

SILAS BIZIMUNGU
C/o IEET
JKUAT

Dear Mr. **Bizimungu**

RE: APPROVAL OF RESEARCH PROPOSAL AND SUPERVISORS

Kindly note that your MSc. research proposal entitled "**Analysis of power system network stability in Rwanda**" has been approved. The following are your approved supervisors:-

1. Dr. Francis Njoka
2. Dr. Churchil Saoke

PROF. MATHEW KINYANJUI
DIRECTOR, BOARD OF POSTGRADUATE STUDIES

Copy to: Director IEET

JKUAT is ISO 9001:2015 and ISO 14001:2015 Certified
Setting Trends in Higher Education, Research, Innovation and Entrepreneurship

Appendix II: Journal Article Publication

ASEAN Engineering Journal

Full Paper

ANALYSIS OF RWANDA'S GRID POINT OF STABILITY LOSS

Silas Bizimungu[a*], Francis Njoka[b], Churchill Saoke[a, c], Clement Siame[d]

[a]Institute of Energy and Environmental Technology, Jomo Kenyatta University of Agriculture and Technology. P. O. Box 62000 – 00200, Nairobi, Kenya
[b]Department of Energy Technology, Kenyatta University. P. O. Box 43844 – 00100, Nairobi, Kenya
[c]Department of Physics, Jomo Kenyatta University of Agriculture and Technology. P. O. Box 62000 – 00200, Nairobi, Kenya
[d]Transmission Department, ZESCO. P. O Box 33304, Lusaka, Zambia

*Corresponding author
silasb@ieee.org

Article history
Received
19 April 2022
Received in revised form
01 January 2023
Accepted
04 February 2023
Published online
31 August 2023

Graphical abstract

Abstract

Electricity stability is the key component in ensuring reliable power supply which is a major hurdle in most developing countries. Power angle being part of grid stability pillars, this work sought to theoretically and numerically investigate the maximum power angle variation that the power system in Rwanda could experience while maintaining transient stability at an acceptable range beyond which generators lose synchronism affecting overall system stability. A steady state and dynamic stability assessment of the lightly loaded Rwandan grid is conducted using PSS/E while MATLAB is used to obtain input values for calculating the system stability power angle. This involved collecting actual network parameters, creating an accurate model of the entire Rwandan grid and validating the model simulation results using regularly metered values at various critical busbars of the network. Results from the study show that a sudden drop in load of 11 MW and 6 MVAr leads to a variation of power angle of the largest power plant by 23° triggering transient stability problems leading to loss of synchronism. Both calculated and simulation results show that, a sudden power angle variation of between 23° to 23.5° at the swing bus power plant, causes the monitored generating units to trip triggering a long-term instability. This was done while also interrogating possible mitigation measures based on the developed and validated model. Based on the system status, the study revealed that the grid point of stability can be determined through simulation using software and to further obtain optimum stability, installation of active devices such as shunt reactors helps the grid to counter sudden variation of power angle due to line and load tripping.

Keywords: Power angle, System stability, lightly loaded, Voltage, dynamic simulation.

1.0 INTRODUCTION

In present day times, power systems are operated much closer to their stability limits due to economic and environmental constraints [1]. The operating conditions of a power system should be always stable, meeting the desired operational criteria. It should also be secure in the event of any contingency [2] [3]. The transfer of power through a transmission network and their affiliated transient stability are however, naturally influenced by the power angle variations [4] due to sudden load change, system faults and switching of transmission lines. Under normal operating conditions, the power angle varies in such a way that the grid elements and applicable parameters remain intact, hence system operators do not recognize such small variations [5] [6]. When a system experiences a sudden disturbance, a new point of stability must be attained failure to which triggers loss of synchronism of generators [7].

In the case of Rwanda, the grid operates with almost no reserve margin, most lines are loaded at only about 20% of their capacity. This makes the grid susceptible to transient stability problems especially power angle deviations. This presents a major challenge to the grid operator in ensuring that the

Article link: https://journals.utm.my/index.php/aej (https://doi.org/10.11113/aej.V13.18556)

Appendix III: Power Generated (MW) at Different Power Plants, System Frequency and Spinning Reserve (MW)

MURUKU II	MURUKU I	Mukungwa	Nyabarongo	Mukungwa 2	Gicye 1	Gicye 2	Gisenyi	Gihira	Keya	Rukarara 1	Rukarara 2	Nsoho Solar	Rwaza	Jabana I	Jabana II	Kivuwatt	Frequency (Hz)	Pgen, agg (MW)	Spinning reserve (MW)
8.53	2.78	3.20	9.90	1.67	1.90	2.80	1.25	1.28	1.13	4.20	1.40		1.60		10.60	26.40	50.14	85.53	6.90
10.91	2.68	3.20	9.90	1.77	1.75	1.70	1.40	1.28	1.13	4.20	1.40		1.60		10.40	26.38	50.08	85.68	6.90
13.10	2.88		9.70	1.71	1.75	1.79	1.30	1.28	1.13	3.70	1.40		1.58		10.60	26.40	49.84	84.42	4.50
10.07	3.22		10.10	1.71	1.75	1.80	1.40	1.18	1.11	3.70	1.40		1.38	4.90	10.47	26.38	49.96	86.65	3.90
13.48	3.18		10.00	1.69	1.90	1.88	1.30	1.28	1.10	5.40	1.40	1.13	1.08		10.50	26.40	49.99	86.48	4.00
10.38	3.60		10.00	1.68	1.90	1.99	1.08	1.18		5.20	1.40	1.13	0.90	5.10	11.40	26.40	50.22	93.30	4.00
12.21	1.78	3.50	10.20	1.63	1.90	1.99	1.12	1.78	1.10	5.20	1.30	1.94	0.60	4.50	11.90	26.40	49.70	89.35	6.30
14.09	3.65	3.50	12.80	1.43	1.91	1.98	1.28	1.28	1.10	2.80	1.30	1.95	0.58	3.60	11.60	26.40	49.61	100.35	3.70
14.57	3.70	5.00	12.40		1.88	2.01	1.34	1.28	1.10	2.60	1.30	2.38	0.48	2.50	11.50	26.50	50.08	106.31	2.60
9.64	3.79	5.00	12.40	0.95	1.70	1.79	1.27	1.28	1.10	2.70	1.30	2.08	0.90	3.20	11.32	26.40	50.05	105.31	2.60
3.78	1.32	4.10	10.30	1.20	1.70	1.80	1.30	1.10	1.98	2.80	1.30	0.48	1.10	2.90	10.20	26.50	49.48	91.34	5.60
1.19	1.68	5.60	12.10	1.29	1.70	1.70	1.52	1.88	1.98	2.80	1.30	1.68	1.27	2.40	10.90	26.50	49.40	91.79	4.30
8.09	3.83	4.50	10.30	1.31	2.50	2.40		1.88	2.20	2.80	1.30	1.19	1.34	2.60	11.70	26.40	49.64	97.50	5.20
8.29	3.92	3.10	10.50	1.42	2.30	2.40	1.69	1.80	2.10	2.80	1.30	0.04	1.36	2.20	11.90	26.40	49.87	95.86	6.40
8.72	3.92	3.10	20.40	1.60	2.30	2.50	1.70	1.88	1.80	7.50	1.70		1.38	2.60	10.00	26.40	49.73	107.16	7.50
6.39	3.71	3.10	20.10	1.60	2.10	2.29	1.70	1.60	1.85	4.50	1.80		1.42	3.40	10.40	26.38	50.08	102.43	7.80
9.04	3.19	5.40	10.70	1.60	1.85	2.28	1.69	1.60	1.11	4.20	2.20		1.54	3.38	11.90	26.40	49.98	97.57	3.90
6.24	2.75	4.00		1.67	1.85	2.84	1.60	1.48	1.10	4.30	2.20		1.53	3.28	11.40	26.40	49.90	84.05	2.00
10.32	2.82	4.10		1.67	1.75	2.04	1.35	1.48	1.41	4.40	2.20		1.58	3.50	11.50	26.40	50.13	83.99	3.90
8.38	2.54	3.20		1.77	1.75	1.71	1.45	1.48	1.40	4.50	2.10		1.52	3.38	11.38	26.40	49.98	79.89	2.80
6.94	2.49	3.20		1.73	1.75	1.99	1.45	1.28	1.40	5.30	2.10		1.49	3.60	11.38	26.50	49.93	79.68	2.80
				1.71		0.00			1.40				1.12	0.00				4.34	0.00
4.78	2.75	6.70		1.71		0.00			1.40				0.00	2.28			50.55	19.61	5.50
3.82	2.69	6.10		1.69	1.75	0.29	1.57	1.28	1.20	7.80	2.10		1.38		10.40	26.00	50.46	70.29	8.40
0.57	2.97	2.90	10.10	1.41	1.75	2.08	1.50	1.00	1.20	7.90	2.00	0.01	1.41		0.00	26.38	49.93	70.14	7.00
8.99	3.04		12.30	2.96	1.88	1.89	1.34	1.38	1.20	7.70	1.50	1.32	1.44		0.00	22.98	49.73	77.91	1.70
7.94	2.97		10.40	1.06	1.88	2.09	1.61	1.38	1.20	7.60	1.50	2.10	1.47	2.40	3.40	26.40	49.96	82.66	3.60
7.60	3.04		11.00	0.25	3.04	2.80	1.50	1.38	1.20	7.20	1.70	0.22	1.43	2.98	4.40	26.40	49.67	79.63	3.00
7.11	3.04		11.10	0.47	3.04	3.20	1.50	1.28	2.10	4.70	1.80	1.91	1.25	2.68		26.38	49.61	81.66	2.70
6.74	2.95		10.80	1.50	3.04	2.96	1.52	1.88	2.10	4.90	1.90	0.07	1.09	3.28		26.40	49.78	78.59	3.20
9.05	2.84		10.50	0.77	3.04	3.05	1.70	1.88	2.13	4.80	1.90	0.48	0.67	2.78		26.50	49.64	80.59	3.50
8.91	2.80		13.00	0.93	3.04	3.39	1.70		2.15	5.00		1.68	0.55	4.40		26.50	49.64	83.93	1.00
8.20	2.79		12.40		3.03	3.40			2.14	3.90	1.90	1.19	0.58	3.90	5.60	26.50	49.58	83.95	1.60
3.27	2.98		9.80		3.03	3.32	1.70	1.88	2.12	3.90		0.04	0.93	5.10	10.40	26.50	49.87	79.70	4.20
5.48	3.08		20.50	1.06	1.78	2.60	1.70	1.88	2.12	5.30	1.80		0.90	4.00	10.50	26.50	49.90	93.04	4.50
7.10	4.23	6.10	19.80	1.13	3.00	3.20	1.70	1.88		5.30	1.80		0.86	4.50	11.20	26.50	49.93	117.68	12.50
8.28	3.44	6.10	20.10	1.43	2.60	2.40	1.60	1.88	2.02	5.40	1.80		0.98	4.70	11.20	26.40	49.84	117.51	11.70
5.90	2.87	3.00	20.00	1.53	2.60	2.80	1.53	1.80	1.90	4.70	1.80		1.30		10.10	26.50	50.25	97.38	8.00
8.37	2.72	3.00	10.00	1.57	2.60	2.86	1.55		1.89	4.80	1.80		1.40		11.40	26.40	49.98	85.60	7.00
11.20	2.37	3.50	10.20	1.58	2.22	1.60	1.58	1.80	1.68	4.80	1.90		1.50		5.80	26.40	49.78	81.35	6.30
10.32	2.23		10.20	1.43	2.22	2.40	1.47	1.40	1.84	5.90	1.90		1.30		5.60	26.40	50.02	78.13	3.80
7.90	2.23		10.30	1.53	2.22	2.40	1.48	1.30	1.22	5.40	1.90		1.40		5.60	26.40	50.02	75.08	3.50
7.62	2.21		10.30	1.58	2.22	2.40	1.58	1.30		5.40	1.90		1.40		5.60	26.30	50.02	72.28	3.90
4.80	2.35		9.80	1.55	2.22	2.30	1.17	1.30	1.52	5.30	1.90		1.40		5.20	26.50	49.75	70.58	4.20
1.49	2.50		12.30	1.59	2.20	2.09	1.24	1.30	1.40	6.80	1.90		1.20		5.00	26.40	50.14	71.58	3.70
5.13	2.78	4.00	13.20	1.69	2.30	2.20	1.35	1.40		5.30	1.80		0.95		9.70	26.50	49.84	81.63	2.80
4.88	2.34	3.00	10.40	1.65	2.30	2.49	1.14	1.80	1.37	6.60	1.80	0.76	0.75		10.30	26.40	49.75	82.66	6.60
5.99	2.23	3.00	10.30	1.55	2.12	2.09	1.78	1.50	1.36	6.40	1.80	1.06	0.74		11.80	26.30	50.02	89.18	4.70
4.84	2.50	3.10	10.00	0.95	2.12	2.08	1.78	1.40	1.36	5.20	1.80	1.43	0.94	5.00	9.80	26.40	49.93	90.69	6.90
4.84	2.57	3.10	10.30	0.98	2.11	2.28	1.69	1.40	1.35	5.10	1.60	1.70	1.07	4.90	11.70	26.50	49.97	99.72	6.80
7.07	2.55	3.00	10.20	1.16	2.10	1.97	1.78	1.50	1.31	5.10	1.60	0.97	1.14	4.40	9.90	26.40	49.73	104.15	6.80
5.13	2.74	3.10	10.30	1.17	2.10	2.29	1.70	1.30	1.30	5.00	1.60	1.84	1.17	4.20	11.80	26.30	49.75	102.19	6.60
8.14	2.67	3.10	11.70	1.18	2.10	2.72	1.69	1.40	2.10	5.10	1.50	1.70	1.24	4.20	9.90	26.40	49.98	103.32	5.20
7.76	2.82	4.20	10.00	1.28	2.30	2.19	1.78	1.80	2.12	5.30	2.20	0.97	1.25	4.40	11.60	26.50	49.64	104.53	5.80
3.06	2.82	4.00	13.40	1.10	3.05	2.84	1.78	1.80		7.50	2.20	1.84	1.24	4.20	11.50	26.50	49.81	104.53	4.60
4.86	3.00	4.00	10.10	1.48		1.91		1.70		8.10	2.10	0.04	1.24	3.90	11.20	26.50	50.14	101.98	5.90
6.01	3.32	5.20	12.70				1.68	1.80		8.30	2.10	0.04	1.11	5.00	11.30	26.40	49.93	96.07	2.10
6.62	3.49	5.20	15.40	1.57			1.68	1.80		8.40	2.10		1.02	4.80	11.40	26.50	49.98	109.84	0.00
9.82	4.01	7.20	19.80				1.70	1.80	2.12	8.20	2.10		1.37	5.30	10.90	26.40	49.81	127.96	11.90
10.12	3.71	6.20	20.00	1.48	1.99	3.00	1.70	1.70	2.10	8.10	2.10		1.40	3.80	10.60	26.40	49.75	126.66	11.60
7.63	3.85	3.20	19.80	1.68	2.01	2.70	1.78	0.20	2.12	8.40	2.10		1.43	4.70	10.50	26.50	50.02	107.38	8.00
9.50	2.89	4.00	10.00	1.70	2.40	2.46				7.00	2.10		1.42	4.80	5.30	26.40	49.84	82.82	6.00
5.81	2.83	3.10	10.30	1.71	2.38	2.40	1.69	0.50	1.80	7.10	2.10		1.39	4.60	5.30	26.30	49.87	81.13	6.00
7.45	2.62	3.10	9.80	1.71	2.41	1.60	1.43	1.80	1.74	7.20	2.10		1.37	4.70	5.30	26.30	49.98	82.66	7.00
8.82	2.65	3.10	10.30	1.71	2.28	2.30			1.72	7.20	2.10		1.30	4.60	4.60	26.40	49.93	81.92	6.80
10.84	2.88	3.20	10.20	2.23	2.01	2.30	0.84		1.66	7.20	2.10		1.33	1.60	4.30	26.40	49.67	81.29	6.60
10.06	3.01	3.20	10.20	1.69	2.00	0.60	1.55	1.70	1.66	7.10	2.10		1.12	1.60	5.40	26.60	49.75	83.32	6.60
5.29	3.32	3.10	10.30	1.68	2.02	2.40	1.69	1.70	1.63	8.00	2.10		1.28	4.40	5.40	26.40	50.14	84.14	6.60
6.32	3.65	3.20	10.30	1.64	2.00	1.91	1.69	1.80	1.60	7.90	2.10	0.18	1.20	4.60	4.20	26.50	49.78	83.72	6.50
9.51	3.23	3.96	19.60	1.61	2.04	2.19	1.78			8.10	2.10	0.25	1.18			26.50	49.83	86.17	7.50
5.87	3.50	4.00	22.30	1.69	2.02	2.18	1.70	1.80	1.52	8.00	2.10	0.77	1.20	4.20		26.50	49.90	94.27	4.70
4.82	8.82		20.40	1.58	2.02	2.28			1.50	7.80	2.10	0.81	1.18	1.80	5.30	26.50	49.81	88.03	4.60
4.85	3.59		22.30	1.25	2.00	2.77	1.70	1.60	1.45	5.40	2.10	0.87	1.24	4.50	5.40	26.50	49.98	92.35	2.70
3.91	3.84		21.30	1.31	2.60	2.80	1.70	1.80	1.50	5.60	2.10	0.89	1.28	4.60	5.60	26.50	49.78	93.28	3.90
7.45	3.81		20.10	1.33	2.50	2.70	1.68	1.60	1.53	7.30	2.10	0.66	1.31	2.10	5.60	26.50	49.60	96.43	4.90
7.90	3.79	5.10	20.60	1.36	2.60	2.78	1.70	1.30	1.54	7.20	2.10	0.40	1.35	1.70	5.50	26.40	49.83	100.64	5.30

Appendix IV: Power Plants' Reactive Power and System Voltage

MURURU II	MURURU I	Nyaharuuga	Mukungwa 2	Giciye 1	Giciye 2	Gisouyi	Gihira	Keya	Rukarara 1	Rukarara 2	Nasho Solar	Rwaza	Jabana I	Jabana II	Kivuwatt	Voltage (kV)
0.33	-1.55	-5.70	0.19	0.35	-0.16	0.21	0.30	0.03	0.00	0.00	0.00	0.14	0.00	-4.11	-7.60	120.50
0.78	-1.70	-5.80	0.18	0.29	-0.08	0.20	0.10	0.02	0.00	0.00	0.00	0.14	0.00	-4.11	-7.50	121.00
0.79	-1.64	-5.50	0.20	0.32	-0.13	0.19	0.30	0.03	0.00	0.00	0.00	0.14	0.00	-4.13	-7.60	120.20
-0.15	-1.58	-4.90	0.20	0.35	-0.11	0.25	0.20	0.05	0.00	0.00	0.00	0.14	0.00	-4.13	-7.60	119.50
-0.33	-1.37	-8.10	0.17	0.35	-0.11	0.25	0.20	0.05	0.00	0.00	0.00	0.12	1.00	-4.17	-7.60	121.60
-0.66	-1.34	-7.20	0.19	0.36	-0.15	0.21	0.20	0.05	-0.20	0.00	0.00	0.17	0.00	-4.15	-7.50	122.20
0.00	-0.18	-4.90	0.18	0.36	-0.18	0.21	0.20	0.04	0.00	0.00	-0.35	0.16	0.00	-4.09	-7.10	120.10
0.82	-0.27	0.00	0.16	0.34	-0.14	0.20	0.20	0.00	0.00	0.00	-0.27	0.12	1.10	-4.95	-3.00	114.60
0.50	-0.34	-2.08	0.00	0.34	-0.12	0.21	0.20	0.04	0.00	0.00	-0.79	0.06	0.80	-2.21	3.30	114.60
0.00	-0.16	-2.30	0.00	0.33	-0.11	0.21	0.20	0.04	0.00	0.00	-0.49	0.10	0.70	-2.19	3.20	114.70
1.19	-0.13	-2.90	0.11	0.31	-0.15	0.22	0.20	0.04	0.00	0.00	-0.63	0.14	0.70	-2.34	2.20	115.90
0.55	-0.18	-1.80	0.14	0.33	-0.12	0.20	0.30	0.08	0.00	0.00	-0.15	0.19	1.10	-1.99	-3.10	114.90
-0.99	0.00	0.00	0.15	0.32	-0.11	0.24	0.40	0.08	0.00	0.00	-0.56	0.21	0.90	-2.14	-3.20	114.40
-1.48	-0.11	0.00	0.17	0.40	-0.20	0.25	0.40	0.07	0.00	0.00	-0.01	0.24	1.10	-2.25	-3.20	114.60
-2.42	-2.12	-11.30	0.18	0.40	-0.20	0.27	0.40	0.06	-0.30	0.00	0.00	0.23	0.50	-4.46	-7.30	115.70
-2.66	-2.30	-13.60	0.19	0.24	-0.12	0.28	0.40	0.08	-0.30	0.00	0.00	0.23	0.60	-4.55	-7.30	116.90
-1.95	-2.28	-13.60	0.19	0.37	-0.09	0.30	0.40	0.07	-0.30	0.00	0.00	0.24	0.90	-4.55	-7.30	117.30
-2.48	-2.17	-11.30	0.19	0.37	-0.18	0.27	0.30	0.05	-0.20	0.00	0.00	0.25	0.80	-4.04	-7.30	119.40
-2.54	-1.65	-5.50	0.19	0.34	-0.17	0.26	0.30	0.04	-0.30	0.00	0.00	0.16	0.80	-4.64	-7.20	119.70
-4.37	-1.63	0.00	0.19	0.34	-0.14	0.27	0.30	0.05	-0.30	0.00	0.00	0.18	0.80	-4.55	-7.20	121.60
-1.85	-1.61	0.00	0.19	0.34	-0.17	0.24	0.30	0.06	-0.30	0.00	0.00	0.16	0.30	-4.53	-7.30	122.20
-1.04	-1.54	0.00	0.18	0.30	-0.17	0.21	0.30	0.05	-0.40	0.10	0.00	0.16	0.40	-4.58	-7.20	121.40
-3.58	-1.56	0.00	0.20	0.30	-0.14	0.21	0.30	0.05	-0.60	0.00	0.00	0.15	0.40	-4.62	-7.10	123.10
-3.60	-1.52	0.00	0.20	0.30	-0.15	0.23	0.30	0.06	-0.50	0.00	0.00	0.16	0.30	-4.64	-7.30	123.30
-11.24	-1.08	0.00	0.19	0.00	0.00	0.00	0.00	0.06	0.00	0.00	0.00	0.09	0.70	0.00	0.00	128.30
-3.30	-1.42	0.00	0.18	0.34	-0.01	0.27	0.20	0.06	0.00	0.00	0.00	0.03	0.00	-3.39	-7.10	125.20
-2.01	-1.15	1.90	0.41	0.34	-0.13	0.23	0.20	0.07	0.00	0.10	-0.01	0.03	0.00	0.00	-7.30	112.40
0.00	-1.00	-2.90	0.36	0.37	-0.13	0.23	0.30	0.06	0.00	0.00	-0.50	0.04	0.00	0.00	-6.30	111.30
0.00	-0.91	-4.60	0.12	0.42	-0.15	0.25	0.30	0.06	-0.10	0.00	-0.68	0.04	0.60	-2.14	-4.80	113.90
-0.55	-0.77	0.00	0.16	0.67	-0.13	0.12	0.30	0.06	0.00	0.00	-0.01	0.03	0.60	-1.74	-4.70	114.10
-1.60	-0.75	-1.70	0.17	0.67	-0.28	0.24	0.20	0.06	0.00	0.00	-0.64	0.03	0.60	0.00	-1.80	114.90
-0.58	-0.77	-2.90	0.16	0.67	-0.24	0.25	0.40	0.14	0.00	0.00	-0.25	0.03	1.00	0.00	-7.40	115.30
-0.81	-0.72	-2.40	0.09	0.67	-0.16	0.24	0.40	0.14	0.00	0.00	-0.15	0.01	1.00	0.00	-7.20	114.40
0.00	-0.77	0.00	0.00	0.63	-0.10	0.00	0.00	0.14	0.00	0.00	-0.40	0.03	1.00	-0.46	-7.20	113.20
-1.65	-0.72	-3.40	0.00	0.53	-0.11	0.22	0.40	0.12	0.00	0.00	-0.01	0.02	1.20	-2.46	-3.10	115.90
-1.51	-1.13	-7.30	0.30	0.34	-0.09	0.27	0.40	0.13	0.00	0.00	0.00	0.03	0.90	-2.37	-5.10	117.10
-3.65	-2.90	-11.30	0.13	0.51	-0.08	0.27	0.40	0.00	-0.20	0.00	0.00	0.03	1.40	-4.22	-7.30	119.10
-0.53	-2.87	-9.90	0.14	0.51	-0.10	0.26	0.40	0.11	-0.20	0.00	0.00	0.03	0.80	-4.22	-7.30	117.40
-0.58	-2.28	-8.20	0.15	0.43	0.02	0.26	0.40	0.12	-0.20	0.00	0.00	0.03	0.80	-4.24	-7.30	116.40
0.34	-1.86	-11.30	0.16	0.47	0.01	0.24	0.40	0.08	-0.20	0.00	0.00	0.02	0.00	-3.86	-7.30	118.90
0.29	-1.82	-5.00	0.15	0.47	0.01	0.22	0.00	0.11	-0.20	0.00	0.00	0.01	0.00	-4.49	-7.30	118.80
0.40	-1.72	-4.20	0.14	0.40	0.01	0.22	0.40	0.09	-0.20	0.00	0.00	0.14	0.00	-2.21	-7.30	118.00
2.25	-1.69	-4.70	0.15	0.38	0.03	0.16	0.30	0.10	-0.30	0.00	0.00	0.14	0.00	-2.21	-7.30	118.60
1.37	-1.76	-5.30	0.14	0.38	0.05	0.18	0.40	0.06	-0.30	0.00	0.00	0.14	0.00	-2.12	-7.20	119.00
0.54	-1.67	-5.90	0.14	0.38	0.02	0.18	0.30	0.00	-0.30	0.00	0.00	0.14	0.00	-1.96	-7.20	120.30
1.20	-1.51	-4.10	0.15	0.37	0.07	0.16	0.20	0.14	-0.20	0.00	0.00	0.13	0.00	-1.99	-7.30	118.90
1.69	-1.48	-8.10	0.16	0.37	0.11	0.15	0.40	0.08	-0.30	-0.20	0.00	0.15	0.00	-0.11	-7.30	122.50
2.20	-1.82	-5.00	0.18	0.40	0.04	0.21	0.30	0.00	-0.20	-0.20	0.00	0.15	0.00	-3.64	-7.50	121.50
1.94	-1.34	-4.70	0.18	0.40	-0.21	0.18	0.30	0.06	-0.20	0.00	-0.23	0.11	0.00	-3.97	-1.30	118.70
1.28	-0.97	-4.40	0.18	0.39	-0.15	0.20	0.30	0.04	0.00	-0.10	-0.39	0.12	0.00	-4.73	-4.20	119.10
-0.08	-0.77	-5.00	0.11	0.37	-0.14	0.29	0.10	0.05	0.00	0.00	-0.50	0.18	1.20	-2.25	2.30	118.40
0.96	-0.66	-3.40	0.11	0.38	-0.17	0.26	0.30	0.04	0.00	0.00	-0.55	0.18	1.00	1.16	2.30	116.60
0.20	-0.66	-1.60	0.14	0.38	-0.15	0.27	0.30	0.04	0.00	0.00	-0.31	0.19	1.40	0.00	2.30	114.10
-1.27	-0.44	0.00	0.13	0.38	-0.18	0.29	0.30	0.05	0.00	0.00	-0.66	0.20	1.40	0.00	2.30	114.10
-0.49	-0.53	-2.70	0.14	0.41	-0.22	0.27	0.30	0.08	0.00	0.00	-0.55	0.23	0.90	0.16	2.20	115.20
0.00	-0.40	0.00	0.14	0.41	-0.16	0.26	0.40	0.10	0.10	0.00	-0.31	0.21	1.10	0.00	1.20	115.30
0.30	-0.35	0.00	0.17	0.52	-0.23	0.29	0.40	0.00	0.00	0.00	-0.60	0.21	0.90	0.18	1.20	113.90
0.72	-0.37	-2.30	0.17	0.00	-0.11	0.00	0.40	0.00	0.00	0.00	-0.01	0.21	0.30	0.13	1.20	114.10
-1.19	-0.29	0.00	0.00	0.00	0.00	0.28	0.40	0.00	0.00	0.00	-0.01	0.20	0.80	0.16	-1.10	114.70
-0.69	-0.64	-3.40	0.18	0.00	0.00	0.29	0.40	0.00	0.00	0.00	0.00	0.03	1.30	-2.57	-4.20	114.80
-2.52	-1.91	-8.20	0.00	0.00	0.00	0.22	0.40	0.11	0.00	0.00	0.00	0.03	0.90	-4.24	-7.30	117.50
-2.93	-2.21	-12.40	0.00	0.48	0.00	0.23	0.30	0.11	-0.20	0.00	0.00	0.04	1.00	-4.04	-7.30	118.90
-3.11	-2.09	-11.40	0.29	0.41	-0.14	0.26	0.40	0.10	-0.20	0.00	0.00	0.04	1.00	-4.02	-7.30	118.50
-2.01	-1.70	-12.00	0.10	0.43	-0.12	0.24	0.00	0.10	-0.90	0.00	0.00	0.04	0.80	-4.04	-7.30	119.10
-0.53	-1.74	-5.50	0.24	0.43	-0.10	0.26	0.40	0.11	-0.90	0.00	0.00	0.13	1.20	-1.96	-7.20	118.90
-0.76	-1.58	5.80	0.24	0.46	-0.11	0.00	0.00	0.00	-0.80	0.00	0.00	0.14	1.60	-2.01	-7.30	118.30
-0.57	-1.55	-3.90	0.23	0.41	-0.14	0.29	0.10	0.70	-0.80	0.00	0.00	0.13	1.20	-2.03	-7.20	118.00
0.51	-1.70	-3.80	0.13	0.43	-0.09	0.23	0.40	0.06	-0.80	0.00	0.00	0.14	1.20	-2.01	-7.20	118.10
0.00	-1.53	-4.70	0.12	0.43	-0.13	0.00	0.00	0.06	-0.80	0.00	0.00	0.13	1.30	-1.79	-7.20	119.00
0.00	-1.35	-3.90	0.21	0.40	-0.12	0.11	0.00	0.06	-0.80	0.00	0.00	0.05	0.80	-1.81	-7.30	117.90
0.51	-1.41	-3.60	0.14	0.40	-0.02	0.23	0.30	0.06	-0.40	0.00	0.00	0.04	0.40	-2.08	-7.30	117.40
1.52	-1.56	-6.30	0.14	0.38	-0.15	0.24	0.30	0.05	-0.40	0.00	0.00	0.04	0.20	-2.10	-7.20	119.30
0.80	-1.30	-4.20	0.11	0.41	-0.13	0.27	0.40	0.06	-0.40	0.00	-0.62	0.03	1.00	-1.62	-7.30	117.50
0.00	-0.77	-8.70	0.12	0.37	-0.14	0.25	0.00	0.00	0.00	0.00	-0.83	0.04	0.00	0.00	-7.30	117.90
0.30	-0.53	-6.60	0.13	0.37	-0.16	0.27	0.40	0.06	0.10	0.00	-0.25	0.03	1.00	0.00	-7.30	116.40